Hsp72 overexpression protects from APAP and MCD induced liver injury via attenuation of JNK signalling

Von der Fakultät für Mathematik, Informatik und Naturwissenschaften
der RWTH Aachen University
zur Erlangung des akademischen Grades
einer Doktorin der Naturwissenschaften
genehmigte Dissertation

vorgelegt von

Spezialist, Biologin

Kateryna Levada

aus Donezk (Ukraine)

2016

Berichter:

Universitätsprofessor Dr. rer. nat. Andreas Ludwig

Privatdozent Dr. med. Pavel Strnad

Universitätsprofessor Dr. phil. nat., Gabriele Pradel

Tag der mündlichen Prüfung: 24.10.2016

TABLE OF CONTENTS

ABBREVIATIONS

ALD: Alcoholic liver disease

ALF: Acute liver failure

ALS: Amyotrophic lateral sclerosis

ALT: Alanine aminotransferase

AP-1: Activator protein 1

Apaf-1: Apoptosis protease-activating factor 1

APAP: Acetaminophen

APS: Ammonium persulfate

ASH: Alcoholic steatohepatitis

ASK1: Apoptosis signal-regulating kinase 1

AST: Aspartate aminotransferase

ATP: Adenosine triphosphate

b-HB: beta-Hydroxybutyric acid

bp: Base pair

BSA: Bovine serum albumin

CD31: Cluster of differentiation 31

CD45: Cluster of differentiation 45

cDNA: Complementary DNA

CHIP: C-terminus of HSC70-interacting protein

CTRL: Control/Untreated sample

Cyp1a2: Cytochrome P450, Family 1, Subfamily A, polypeptide 2

Cyp2b10: Cytochrome P450, family 2, subfamily b, polypeptide 10

Cyp2e1: Cytochrome P450, Family 2, Subfamily E, polypeptide 1

Cyp3a11: Cytochrome P450, family 3, subfamily a, polypeptide 11

DEPC: Diethylpyrocarbonate water

DMEM: Dulbecco's Modified Eagle's Medium

DMSO: Dimethylsulphoxide

DNA: Deoxyribonucleic acid

dNTP: Deoxynucleotide Set

DOX: Doxycycline

DTT: 1, 4- Dithiothreitol

ECL: Enhanced chemiluminescence

EDTA : Ethylenediaminetetraacetic acid

EndoG: Endonuclease G

ERK: Extracellular signal-regulated kinase

EtOH: Ethanol

F: Forward

FCS: Fetal calf serum

GFAP: Glial fibrillary acidic protein

GSH: Glutathion

GSSG: Oxidized glutathion

Gst1: Glutathione S-transferase

H&E: Hematoxylin & eosin staining

h: Hour

H2O2: Hydrogen peroxide

HBV: Hepatitis B

HCC: Hepatocellular carcinoma

HCV: Hepatitis C

Hep: Hepatocytes

HRP: Horseradish peroxidase

HSC: Hepatic stellate cells

Hsc70: Heat shock cognate 71 kDa protein

HSF: Heat Shock Factor

Hsp: Heat shock protein

Hsp27: Heat shock protein 27 kDa protein

Hsp60: Heat shock protein 60 kDa protein

Hsp72: Heat shock 70 kDa protein 1

Hsp90: Heat shock protein 90 kDa protein

HSR: Heat shock response

IL1: Interleukin 1

IL-6: Interleukin 6

JNK : c-Jun amino-terminal kinase

KC: Kupffer cells

L7: Ribosomal protein L7

Lap: Liver activator protein

LSEC: Liver sinusoidal endothelial cells

MAPK: Mitogen-activated protein kinase

MCD: Methionine and choline deficient

min: Minute

mL: Mililiter

MLKL: Mixed lineage kinase domain-like protein

mRNA: Messenger RNA

NAFLD: Non-alcoholic fatty liver disease

NAPQI: N-acetyl-p-benzoquinone imine

NASH: Non-alcoholic steatohepatitis

NF-κB: Nuclear factor “kappa-light-chain-enhancer” of activated B-cells

nm: Nanometer

p c-JUN: Phosphorylated c-JUN

p38MAPK: p38 mitogen-activated protein kinases

PBS: Phosphate buffered saline

PC: Phosphatidylcholine

PE: Phosphatidylethanolamine

pJNK: Phospho-SAPK/JNK

PMSF: Phenylmethane sulfonyl fluoride

PMSF: Phenylmethanesulfonyl fluoride

PVDF : Polyvinylidene fluoride

qRT-PCR: Quantitative real-time polymerase chain reaction

R: Reverse

RIP1: Receptor-interacting protein 1

RIP3: Receptor-interacting protein 3

RLU: Relative luciferase units

RNA: Ribonucleic acid

RNS: Reactive nitrogen species

ROS: Reactive oxygen species

RPLPO: Large ribosomal protein

RPM: Rounds per minute

RPMI: Roswell Park Memorial Institute medium

RT: Room temperature

RT-PCR : Reverse transcription PCR

SAM: S-adenosylmethionine

SDS-PAGE: Sodium dodecyl sulphate polyacrylamide gel electrophoresis

SEM: Standard error of the mean

STAT-1: Signal transducer and activator of transcription 1

Sult1a1: Sulfotransferase family 1A member 1

TAE: Tris-acetate-EDTA

TBS: Tris-buffered saline

TEMED: Tetramethylethylenediamine

TG: Transgenic

TLC: Thin-layer chromatography

tTA: Tetracycline-responsive transactivator

Ugt1a1: UDP glucuronosyltransferase 1 family, polypeptide A1

Ugt1a6: UDP glucuronosyltransfe-rase 1 family, polypeptide A6

VLDL: Very-low-density lipoprotein

WT: Wild type

µg: Microgram

µl: Microliter

µm: Micrometer

1. Introduction

1.1. The biological importance of chaperones

After the synthesis, proteins need to obtain a proper 3D structure that enables them to function properly. This process includes the correct folding of the polypeptide chain. During their life-time, the correct 3D structure may become impaired due to various stresses such as exposition to reactive oxygen species that induce protein misfolding. The molecular chaperones are a large group of proteins that assist in the noncovalent folding, unfolding and the assembly and disassembly of protein complexes [1, 2]. Important function of chaperones is to avoid newly synthesized polypeptides and assembled subunits to form nonfunctional aggregates [3]. Chaperones are also involved in protein quality control and may direct irreversibly damaged proteins to undergo degradation [4].

1.2. Classification and function of Heat Shock Proteins (Hsp)

An appropriate temperature range is important for an optimal growth of cells [5] and this range varies between different types of cells and organisms. Consequently, changes in temperature affect structure and function of cells. In particular, a too high temperature leads to increased oxidative stress and protein misfolding. The characteristic adaptation mechanism for this stress situation is termed the heat shock response (HSR) [6]. The HSR is a universal and conserved genetic system existing in every cell and organism [5-7]. The HSR activates expression of cytoprotective genes known as heat-shock proteins (Hsps). In line with that, many Hsps are expressed at low levels under basal physiological conditions [8, 9], but their synthesis increased in response to enhanced temperature due to the HSR.

The cell contains several different classes of chaperones and a subgroup of chaperones are the Hsps [3]. The latter constitute a large family of evolutionary conserved proteins which are classified according to their molecular weight [9]. Different Hsps are found in different types of organisms [10, 11] and different cell compartments (Table 1.1).

Chaperone family	Organism	Typical family members	Subcellular compartment	Function
Hsp 100	E.coli	ClpA,B,C	Cytosol	Tolerance of extreme temperatures
	S.cerevisiae	Hsp104	Cytosol	
Hsp 90	E.coli	HtpG	Cytosol	Assist with protein folding, stabilize proteins, required for tumor growth
	S.cerevisiae	Hsp83	Cytosol	
	Mammals	Hsp90	Cytosol	
		Grp94	Endoplasmatic reticulum (ER)	
Hsp70	E.coli	DnaK	Cytosol	Expressed in different cellular compartments, assist with protein folding and unfolding, provide thermotolerance
	S.cerevisiae	Ssa 1-4	Cytosol	
		Ssb 1,2	Cytosol	
		Kar2	ER	
		Ssc1	Mitochondria	
	Mammals	Hsc70	Cytosol/nucleus	
		Hsp70	Cytosol/nucleus	
		Bip	ER	
		mHsp70	Mitochondria	
Hsp60	E.coli	groEL	Cytosol	Involved in protein folding in the mitochondria/chloroplast
	S.cerevisiae	Hsp60	Mitochondria	
	Plants	Cpn60	Chloroplasts	
	Mammals	Hsp60	Mitochondria	
Hsp40	E.coli	DnaJ	Cytosol	Co-factor of Hsp70
	S.cerevisiae	Ydj1	Cytosol/nucleus	
	Mammals	Hsp40	Cytosol/nucleus	
Small Hsps	E.coli	IbpA and B	Cytosol	Provide thermotolerance, cytoprotection, and support cell survival under stress conditions. Participate in mitochondrial protein folding, important in pregnancy, cancer and immune tolerance
	S.cerevisiae	Hsp27	Cytosol	
	Mammals	αA and αB-crystallin	Cytosol	
		Hsp27, Hsp10	Cytosol	

Table 1.1. Nomenclature and subcellular localization of Hsps in different organisms (Modified from [11]).

While Hsps are often used as a synonym for stress-inducible proteins, some of them are also expressed constitutively. These are involved in folding of newly synthesized polypeptide chains, while refolding of stress-denatured proteins is often accomplished by inducible Hsp family members. Hsps also facilitate trafficking, quality control and degradation of proteins [1, 4]. Hsps are typically induced during multiple stress situations in order to help cells survive otherwise lethal stresses [6, 12]. These [6, 7] result in the un/misfolding of individual proteins [13-15] and lead to translocation of heat shock factor (HSF) into the nucleus thereby eliciting the HSR. Under basal condition, HSF is a monomer. Upon exposure to stress factors, it trimerizes, translocates to the nucleus and binds to DNA to activate the transcription of Hsp genes (Figure 1.1) [16].

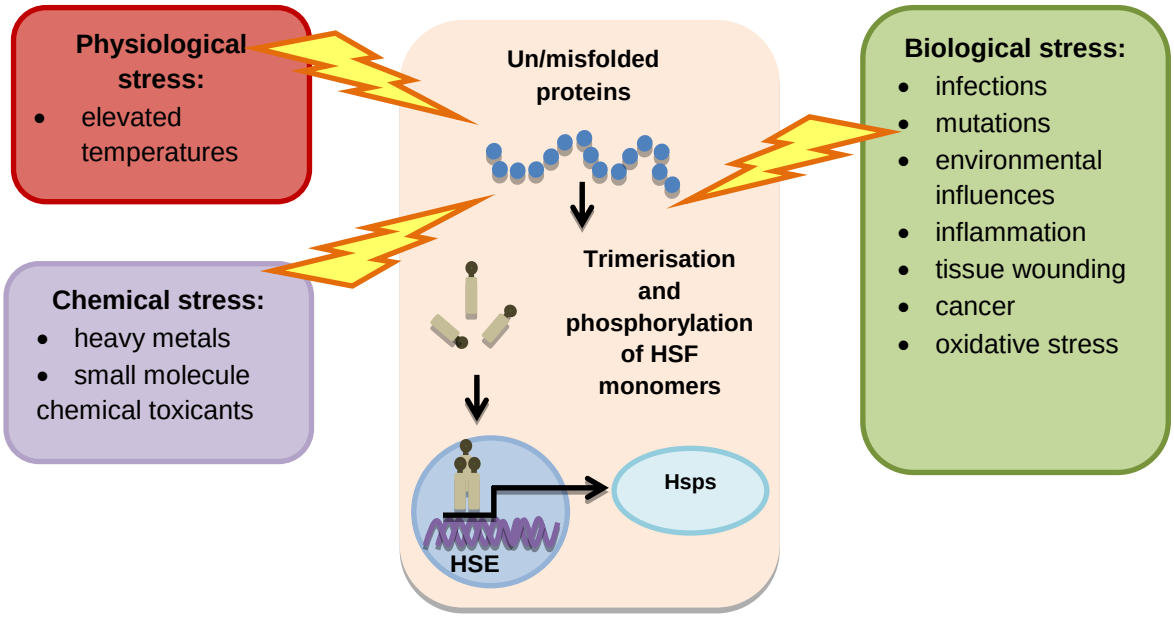

Figure 1.1. Schematic view of activation of transcription of Hsps genes. Under basal condition, Heat Shock Factor (HSF), the master regulator of heat shock protein expression, is an inactive monomer. Different stress situations lead to misfolding of individual proteins. Un/misfolded proteins activate the trimerization and phosphorylation of HSF monomers. HSF trimers bind to DNA sequence elements called heat shock elements (HSE) and activate the transcription of Hsp genes.

Protein quality control and prevention of protein missfolding are crucial for cellular and organismal health. Accordingly, Hsps serve as cytoprotective proteins for different diseases including infections [17, 18], neurodegenerative, cardiovascular [19, 20] disorders or diabetes [21, 22]. Of note, Hsps have also been shown to mediate protection from inflammation [23, 24].

1.3. Classification of Hsp70 family

The Hsp70s are the largest subfamily of chaperones. They are central components of protein folding process and are expressed in virtually all types of organisms. However, the amount of produced Hsp70s varies among different organisms. For example, E. coli has only 3 Hsp70 family members, mice harbor – 7 proteins while human genome contains 13 functional Hsp70s genes [9]. This variety leads to functional diversity and specificity [9]. Since the discovery of human Hsps, their nomenclature underwent multiple changes and often one and the same gene have a different name (Table 1.2).

Name of gene	Name of protein	Alternative names	Homology to HspA1A, %	Reference
HSPA1A	HSPA1A	HSP70-1; HSP72; HSPA1	100	[25]
HSPA1B	HSPA1B	HSP70-2	99	[25]
HSPA1L	HSPA1L	hum70t; hum70t; Hsp-hom	91	[26]
HSPA2	HSPA2	Hsp70-3, HspA2	84	[27]
HSPA5	HSPA5	BIP; GRP78; MIF2	64	[28]
HSPA6	HSPA6	HSP70B′	85	[29]
HSPA7[a]	HSPA7	Heat shock 70kD protein 7	77	[30]
HSPA8	HSPA8	HSC70; HSC71; HSP71; HSP73	86	[31]
HSPA9	HSPA9	GRP75; HSPA9B; MOT; MOT2; PBP74; mot-2	52	[32, 33]
HSPA12A	HSPA12A	FLJ13874; KIAA0417	38	[34]
HSPA12B	HSPA12B	RP23-32L15.1; 2700081N06Rik	44	[34]
HSPA13b	HSPA13	Stch		
HSPA14	HSPA14	HSP70-4;HSP70L1; MGC131990		

Table1.2. The human Hsp70 family (modified from Kampinga [9, 35]).[a] annotated as pseudogene, but possibly a true gene, [b] Under consultation with HGNC and the scientific community.

The structure of Hsps genes is highly conserved and Hsp70 proteins from prokaryotic organisms are identical to approximately 50% in their amino acid composition with eukaryotic Hsp70s [35]. Therefore, it was suggested that proteins of Hsp70 family play an important role for the cell metabolism. The human Hsp70 family members have both redundant and specific functions. Most Hsp70s are cytoplasmic proteins. Among them, the Hsc70 (also known as Hsp73 and HSPA8) is constitutively expressed in cytoplasm and is crucial for folding of newly synthesized proteins [4]. Bip (also known as Hsp70-5 or Grp78) and mtHsp70 (or Hsp70-9 or Grp75) are found in the lumen of the ER and in the mitochondrial matrix, respectively [9, 14]. Of note, the HSPA1A and HSPA1B genes are more than 99% identical and differ only by two amino acids [35]. Because of their stress-protective properties, they are among the most studied genes of the Hsp70 family.

1.4. Structure and function of Heat shock protein 72 (Hsp72)

The HSP1A1 is a stress-inducible and intronless gene coding for Hsp72 protein. The basal level of Hsp72 expression is dependent on the cell type and in the phase of cell cycle, given that it accumulates in G1- and S-phase [35, 36].

Hsp72 as other members of Hsp70 superfamily has a typical highly conserved domain structure consisting of a N-terminal ATPase domain, a C-terminal peptide recognition/binding site and a short linking sequence (EEVD) [3, 37]. The C-terminus is responsible for interaction with different co-chaperones or binding partners [38]. However, regulation of the substrate binding activity is accomplished through the ATP binding domain [37, 39]. Of note, members of the co-chaperone family HSP40 interact with this domain and stimulate the ATPase-activity [40, 41]. The ultimate C-terminal part of Hsp72 proteins, the EEVD (amino acid designations) motif, gives possibility to interact with tetratricopeptide repeat domain containing-proteins such as HOP (adapter protein which mediates interaction of Hsp72 with Hsp90) or CHIP (inhibits the HSP40-stimulated ATPase activity of HSP72) [39, 42].

It was shown before that Hsp72 has house-keeping and stress-inducible properties [35]. The house-keeping functions of Hsp72 are transport of proteins between cellular compartments, prevention of aggregation, folding the proteins to

their native state and degradation of misfolded proteins [15, 43, 44]. Different researcher groups demonstrated that under conditions of stress Hsp72 possesses the capacity to assembly or disassembly polypeptide complexes and prevents the harmful aggregation of denatured proteins [43, 44].

Upon a variety of stresses, Hsp72 plays crucial role in the cell metabolism. Hsp72 also protects from different forms of cell death. To this end, Hsp72 is involved in inhibiting programmed cell death through different mechanisms. It can protect cells from apoptosis in caspase-dependent or caspase-independent manner. During activation of caspase-dependent apoptosis, Hsp72 can bind directly to apoptosis protease-activating factor 1 (Apaf-1) and block association with procaspase 9, thereby inhibiting the formation of the mitochondrial apoptosome [45, 46]. Additionally, Hsp72 can inhibit the activation of caspase-3 [47] or prevent activation of apoptosis signal-regulating kinase 1 (ASK1) [48]. With regard to caspase-independent pathway, Hsp72 was found to prevent release of cytochrome c from mitochondria [47, 49] or to interact with the mitochondrial apoptosis-inducing factor (AIF) and to protect from the AIF-induced chromatin condensation [50].

Last but not least, overexpression of Hsp72 protects against activation of apoptosis-mediated agents as tumor necrosis factor-a (TNFα), interleukin 1 (IL1), interleukin 6 (IL6) [51, 52].

In the situation of stress, mitogen-activated protein kinase/extracellular signal-regulated kinase (MAPK/ERK) and c-Jun N-terminal kinase (JNK) signaling pathways lead to overexpression of Hsp72 via activation of HSFs [53, 54]. Several studies showed that Hsp72 directly interacts with the ASK1, JNK and p38 mitogen-activated protein kinases (p38MAPK), thereby decreasing their phosphorylation and inhibiting cell death [38, 48, 55, 56]. Moreover, it was also found that Hsp72 may indirectly via co-chaperone C-terminus of HSC70-interacting protein (CHIP) promote the proteasomal degradation of ASK1 as well as inhibit TNF-induced apoptosis [57].

1.5. The role of Hsp72 in the in different human diseases

As Hsp72 plays a crucial role for cellular and organismal health, this protein is also instrumental in prevention of different human diseases. Transgenic animals overexpressing Hsp72 are protected from various stress situations (Table 1.3). On the other hand, Hsp72 knockout mice exhibit the opposite phenotype [58].

Tissue	Hsp72 overexpressing mice	Reference
Neural tissue	Decrease in harmful protein aggregation (Parkinson's disease, Alzheimer's disease)	[58, 59]
Skeletal muscle tissue	Reduction of fat mass	[55, 60, 61]
	Intact glucose and insulin tolerance	
	Increase of palmitate oxidation	
	Decrease in intramuscular lipid accumulation	
	Increased number of mitochondria	
Cardiac muscle tissue	Protection from myocardial damage	[62]

Table 1.3. Phenotype of Hsp72 overexpressing mice in different tissue.
Modified from [63, 64].

Previous studies showed that Hsp72 is important for protection of terminally differentiated and non-dividing cells, such as neurons and muscles [64, 65]. Misfolded or aggregated proteins cause the cell death in a variety of degenerative disorders of neural tissue such as polyglutamine disease (Huntington's disease [65]), Alzheimer's disease [66, 67], familial amyotrophic lateral sclerosis (ALS) [68] and Parkinson's disease [69, 70]. Several investigations showed that Hsp72 inhibits the apoptosis induced by mutant proteins, which would otherwise aggregate in neural degenerative disease [58, 71, 72].

Hsp72 overexpression in the skeletal muscles increases lipid oxidation, facilitates muscle function [73], protects against injury [74] and improves structural and functional recovery after inactivity-induced atrophy [75].

Furthermore, it was shown before, that human obesity and insulin resistance are associated with decreased expression of HSP72 [55, 76]. On the other hand, transgenic animals overexpressing Hsp72 are protected against diet- or obesity glucose and insulin resistance [55].

Different research groups studied the effect of overexpression of Hsp72 on ischemic injury in animal models [64]. Accordingly, it was reported that overexpression of Hsp72 protects from ischemia-induced tissue injury in the brain [77, 78], heart [79, 80] and liver [81].

Overexpression of Hsp72 was also shown to have an important anti-inflammatory effect. For example, recent studies showed that it effectively inhibits HMGB1 release and the resulting proinflammatory reaction in macrophages [82] and prevents the development of inflammatory processes in the large intestinal mucosa [83]. As another explanation of its anti-inflammatory properties, overexpression of Hsp72 interrupts the phosphorylation of IκB, JNK and p38 and inhibits the DNA binding of the related transcription factors (NF-κB, AP-1 and STAT-1) [84, 85].

1.6. Liver and experimental models of liver injury

1.6.1. Liver, cell types and function

The liver is an organ that is indispensable to life of higher vertebrates. Its major functions are production of plasma proteins, detoxification and production of bile as well as involvement in lipid, glucose and protein metabolism.

Histologically, the liver consists of two types of cells: parenchymal and non-parenchymal cells. More than 70% of liver mass constitutes of parenchymal hepatocytes. They are involved in protein synthesis and storage, modification and detoxification of different exo- and endogenous substances, synthesis of cholesterol, bile salts and phospholipids. They also produce primary bile and plasma proteins. Among the many proteins, hepatocytes produce also enzymes aspartate (AST) and alanine aminotransferase (ALT). They are both released into the blood stream when the liver cells are damaged. Because of that, serum levels of ALT and AST are sensitive markers of hepatocellular injury. Of note, hepatocytes have a remarkable capacity for proliferation and therefore liver can regenerate well from acute injuries or surgical procedures [86].

The liver sinusoids represent the smallest vessels in the liver connecting the portal venules with central veins. They contain two types of cells: liver sinusoidal endothelial cells (LSEC) and Kupffer cells (KC), the latter being the resident liver macrophages. On the other hand, hepatic stellate cells (HSC, non-parenchymal cells) are localized in the perisinusoidal space, between a sinusoid and the hepatocytes [87].

1.6.2. Mechanism of acetaminophen-induced injury

Acute liver failure (ALF) is characterized as rapid development of hepatocellular dysfunction and can be caused by different agents, including drugs, autoimmune insult or viral hepatitis. Acetaminophen (APAP, N-acetyl-p-aminophenol) is an analgesic and antipyretic drug used worldwide. At therapeutic doses, the use of APAP is safe; however overdose of APAP is the most common cause for ALF in USA and Great Britain [88].

At normal therapeutic doses, APAP is degraded by glucuronidation and sulfation [89]. Glucuronidation pathway is catalyzed by different types of enzymes of UDP glucuronosyltransferases family such as UDP glucuronosyltransferase family 1 member A1 (Ugt1a1) and UDP glucuronosyltransferase family 1 member A6 (Ugt1a6). These enzymes increase solubility of acetaminophen in the water [90]. Sulfotransferase family 1A member 1 (SULT1A1) catalyzes sulfation of acetaminophen that makes acetaminophen more polar [91]. These non-toxic, inactive metabolites are subsequently eliminated by the kidney.

In the case of APAP overdose, APAP becomes metabolized by enzymes from cytochrome P450 family. Cytochrome P450 2E1 (CYP2E1) and cytochrome P450 1A2 (CYP1A2) catalyze the transformation of acetaminophen to reactive metabolite N-acetyl-p-benzoquinoneimine (NAPQI). Normally, conjugation with glutathione (GSH) is able to detoxify NAPQI. However, after overdose of APAP, glutathione (GSH) becomes depleted and NAPQI forms hepatotoxic covalent protein adducts [92, 93], thereby leading to damage of hepatocytes and formation of reactive oxygen and nitrogen species (ROS/RNS). Previously, it was shown that APAP-induced cell death is caused mainly by necrosis and other non-apoptotic pathways [94-96]. Formation of ROS activates phosphorylation of JNK1/2 and translocation of phosphorylated form of JNK1/2 into mitochondria that leads to damage of mitochondria and release of AIF and endonuclease G (EndoG). Translocation of EndoG into nuclei activates DNA fragmentation and promotes the development of necrosis [95, 97](Figure 1.2).

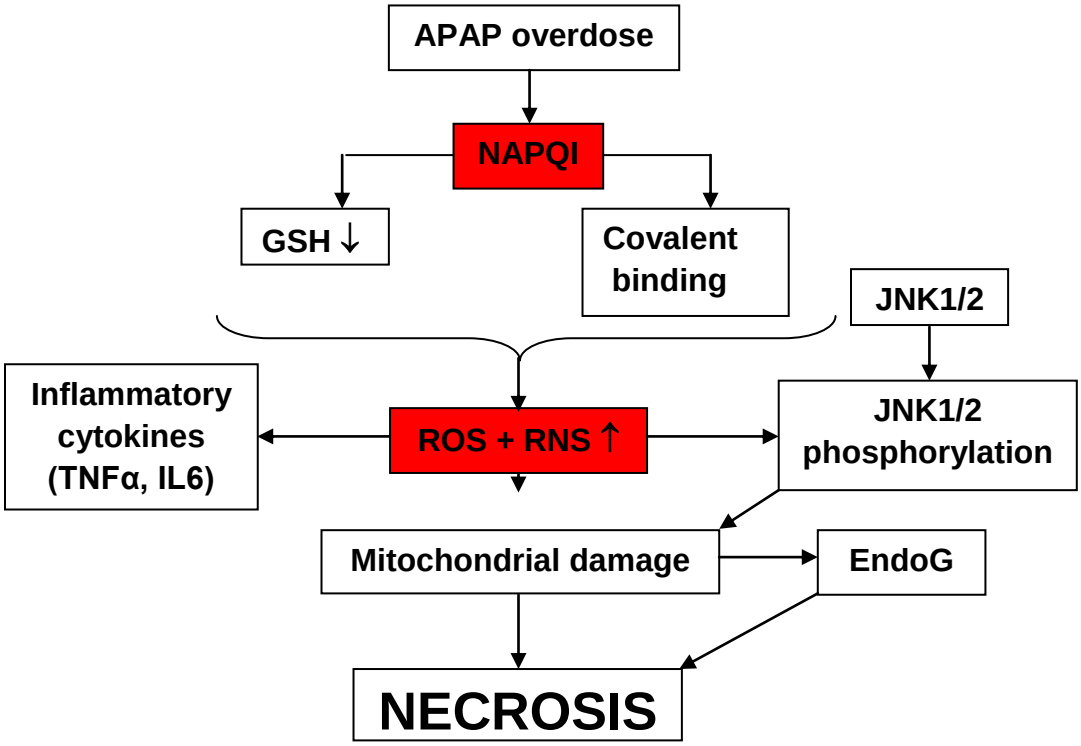

Figure 1.2. Schema of the mechanistic determinants of acetaminophen-induced hepatic necrosis (modified from [98]).

APAP – acetaminophen, NAPQI – N-acetyl-p-benzoquinone imine, GSH – glutathione, JNK1/2 – c-Jun N-terminal kinase1/2, TNFα – tumor necrosis factor-α, IL6 - interleukin 6, ROS – reactive oxygen species, RNS - reactive nitrogen species, EndoG - endonuclease G

APAP-induced liver injury results in activation of KC and release of inflammatory cytokines (TNF-α, IL-6,) and chemokines that play an important role in toxicity and regeneration of hepatocytes [98]. Masubuchi and coworkers have demonstrated that IL-6 knockout mice are more susceptible to APAP-induced hepatotoxicity than non-transgenic littermates and displayed reduced expression of Hsp72 [99].

Several studies suggested that cytoprotective function of Hsp72 may ameliorate APAP-induced cell-death. For example, in study of Salminen at al., induction of Hsp72 expression in liver hepatoma cell line (HepG2) via pretreatment by thermal shock protected the cells from harmful effect of different hepatotoxicants (bromobenzene, cadmium, cyclophosphamide or diethylnitrosamine) [100]. Another

group demonstrated that silencing of Hsp72 expression in HepG2 cell line made the cells susceptible to oxidative stress induced by hydrogen peroxide (H2O2) [101].

APAP-induced hepatotoxicity has been found to activate the Hsp72 expression in mice [102-104]. Tolson and coworkers have reported that Hsp72-knockout animals are more susceptible to APAP-hepatotoxicity and demonstrated elevated ALT levels in the serum, that were consistent with morphological findings showing a more pronounced liver injury [105]. On the other hand, induction of Hsp72 expression with geranylgeranylacetone (GGA) protected the animals from APAP-induced injury, decreased their ALT levels, but did not affect the key parameters of APAP metabolism, as Cyp2E1 expression or GSH amount [103].

1.6.3. Mechanism of development of hepatic steatosis

Nonalcoholic fatty liver disease (NAFLD) is the most common chronic metabolic liver disorder in the Western society [106-108]. A subset of patients with NAFLD develops the more severe form termed as nonalcoholic steatohepatitis (NASH) that is characterized by infiltration of macrophages and hepatocellular ballooning [109]. The NASH patients are at risk to develop liver cirrhosis and hepatocellular carcinoma (HCC) [106, 109].

However, the mechanisms leading to emergence of NASH are still largely unknown and controversial [110, 111]. A key event is the lipotoxicity of the accumulated fat species that results in formation of reactive oxygen species (ROS) and apoptosis [111-113]. While the exact fat species responsible for this process are not unequivocally specified, free fatty acids and cholesterol are among the major suspects since they were shown to cause TNF-α-mediated liver damage and generation of ROS [113]. The resulting inflammation may further contribute to ROS generation thereby starting a vicious cycle [111].

Several animal models have been used to investigate the mechanisms underlying the development of human NASH [112]. Among them, methionine and choline deficient (MCD) diet belongs to the most extensively characterized models [107]. Methionine and choline cannot be de novo synthesized by cells and are normally provided by the diet. Methionine is important for formation of S-adenosylmethionine (SAM), which is involved in the synthesis of cysteine, lecithin, phosphatidylcholine and many other macromolecules. Choline is a part of phospholipids that are important for structure of cellular membranes. It is also a key

precursor for acetylcholine, an important antioxidant [107]. Moreover, sufficient methionine/choline supply is essential for hepatic β-oxidation in mitochondria and production of very-low-density lipoproteins (VLDLs) that export lipids from liver to the bloodstream [114].

The MCD diet results in accumulation of triglycerides in the liver, mitochondrial damage, development of oxidative stress, inflammation and hepatocellular injury including cell death via apoptosis [114, 115]. In comparison to most other dietary mouse NASH models, MCD diet-induced insult is more severe and results in more reliable fibrogenesis [116].

Oxidative stress and the consecutive ROS-generation activate different signaling pathways leading to hepatic inflammation and damage of hepatocytes. Among them, activation of JNK-signaling pathway is associated with inflammation and insulin resistance. In a human study, activation of JNK was observed in NASH, but not in NAFLD-patients [117]. In hepatic cell culture lines (HepG2, Huh7) as well as in primary mouse hepatocytes, inhibition of JNK protected the cells from lipotoxicity induced by saturated fatty acids [118]. Schattenberg and coworkers have demonstrated that deletion of JNK1 and JNK2 in hepatocytes protects from MCD-induced inflammation and insulin resistance. The protection is mainly mediated by JNK1, since JNK2 knockout mice did not show any obvious phenotype when compared to non-transgenic animals on the same diet [119, 120].

The lipotoxic injury results in different types of cell death, including apoptosis, necrosis and necroptosis [119, 121, 122]. Necroptosis is an alternative form of cell-death mediated by receptor-interacting protein (RIP) 1 and RIP3 kinases [123, 124]. The latter enzyme induces phosphorylation of mixed lineage kinase domain-like protein (MLKL) [125] thereby triggering the cell death pathway. Of note, NASH patients have an elevated level of Rip3 in the liver [126, 127]. Additionally, it was shown that JNK may be considered as a mediator of Rip3-dependent liver injury in the MCD fed animals [126]. To support the biological relevance of Rip3 kinase, Afonso and coworkers have demonstrated that deletion of Rip3 kinase attenuated MCD-induced liver injury, inflammation, steatosis and oxidative stress [127].

Interestingly, NAFLD and obesity increase expression of Hsp72 in the liver and adipose tissue of nondiabetic subjects [128]. In an animal study, Chung at al. demonstrated that skeletal/cardiac muscle-specific Hsp72 overexpression in mice protects against diet- or obesity induced hyperglycemia, hyperinsulinemia, glucose

intolerance, and insulin resistance [55]. Additionally, they showed that overexpression of Hsp72 prevents high-fat-feeding-induced phosphorylation of JNK in the skeletal muscles, thereby blocking inflammation and preventing insulin resistance [55].

Aims of study

Hsp72 is a classic, stress-inducible heat shock protein. It has been shown before that Hsp72 protects the organism from variety of diseases and stress situations. However its hepatic function remains largely unknown due to a lack of a suitable transgenic model [55].

The aim of the present study was to elucidate the importance of Hsp72 in the mouse liver. To directly address this issue, a new transgenic mouse model with inducible, liver specific Hsp72 overexpression was generated.

In my thesis I focused on following questions:

1) What are the effects of Hsp72 overexpression in the liver under basal condition?
2) Does Hsp72 overexpression affect liver injury under different stress conditions and if yes, what are the underlying mechanisms?
3) Is the hepatic function of Hsp72 of a potential relevance to patients with liver disease?

2. MATERIALS AND METHODS

2.1. Materials

2.1.1. Chemicals and reagents

Name of product	Company
2-vinylpyridine	Sigma
Acetaminophen (powder)	Fagron
Acetic Acid 100%	AppliChem
Acrylamide 30%	Roth
Agarose	Invitrogen
Ammonium persulfate (APS)	Sigma
Bovine serum albumin (BSA)	Serva
Bovine serum albumin (BSA) fatty acid free	Sigma
Bromophenol Blue sodium salt	Sigma
Coomassie Brilliant Blue (R250)	BioRad
Desoxynucleotides-Set (dNTP)	ThermoScintific
Diethylpyrocarbonate (DEPC) water	Invitrogen
Dimethylsulphoxide (DMSO)	Sigma
Direct PCR Tail	Peqlab
Direct Red 80	Sigma
DL-Dithiothreitol – DTT	Sigma
D-Luciferin, potassium salt	PerkinElmer
DNA ladder/Gene ruler (50 bp and 1 kb)	Thermo Scientific
DNA Loading Dye (6x)	Thermo Scientific
ECL Plus Western Blotting Detection Reagents	GE Healthcare
ECL Western Blotting Detection Reagents	GE Healthcare
Entellan	Merck
Eosin G 0.5 %	Roth
Ethanol	Sigma
Ethylenediaminetetraacetic acid (EDTA)- disodium salt	Sigma
Fetal calf serum (FCS)	Pan Biotech
Formalin 4%	Fischer
Glycerol	Sigma
Goat-Serum	Invitrogen
Hematoxylin	Roth
HepatoZyme	Life Technologies
Hydrogen peroxide 30 % (H2O2)	Merck
Isoflurane (Forane)	Abbvie
Isopropanol	VWR Chemicals
Kaiser's glycerol gelatine	Merck
L-Glutamine	Sigma
Magnesium chloride	Sigma
Metaphosphoric acid	Sigma
Methanol	Sigma
Methionine choline-deficient (MCD) diet	MP Biomedicals
Sodium chloride (NaCl)	AppliChem

Sodium hydroxide (NaOH)	AppliChem
Non-fat dry Milk	AppliChem
Oil Red O	Sigma
Oligo dT Primer	Promega
Page ruler plus	ThermoScientific
Palmitic acid	Sigma
Pefablock SC	Roth
Penicillin/Streptomycin (P/S)	Pan Biotech
PeqGreen Dye	PeqLab
Percoll	GE Healthcare
Phenylmethane sulfonyl fluoride (PMSF)	Sigma
pHMeter-calibration solutions (pH 4,7, 9)	Merck
Phosphate Buffered Saline Solution (PBS) 1x, 10x	PAN Biotech
PhosSTOP tablets	Roche
Ponceau S	BioRad
Protease Inhibitor Cocktail	Sigma
RNAlater® RNA Stabilization Buffer	Qiagen
Saline (NaCL 0,9%)	Braun
Sodium dodecyl Sulfate (SDS)	Roth
Standart diet (Specialdiäten GMBH)	Ssniff
Sucrose	Sigma
Tetramethyl ethylene diamine (TEMED)	Sigma
TissueTek Compound	Sakura
Triethanolamine	Sigma
Tris Base	AppliChem
Tris Cl	AppliChem
Triton X-100	Sigma
Trypan blue stain (0.4%)	Gibco
Tween 20	Roth
Williams E Medium	Sigma
Williams E Medium (without Phenol red)	Pan Biotech
Xylol	Roth
β- Mercaptoethanol	Sigma

2.1.2. Equipment and instruments

Name of product	**Company**
7300 Fast Real-Time-PCR System	Applied Biosystems
Agarose gel chamber	Bio-Rad
Balances	Satorius
BioDocAnalyze Transiluminator	Biometra
Block thermostate	Biostep
Blotting Trans-BlotTM Cell	BioRad
Cell culture Incubator	Heraeus
Centrifuge 5418	Eppendorf
Cooling centrifuge 5417R	Eppendorf
Deep freezer Heraeus,	Kendro Lab products

Ice machine	Ziegra
ImageQuant LAS 4000	GE Healthcare
Infinite 200	Tecan
IVIS Lumina XR	Caliper
Luminometer	Berthold
Magnetic stirrer MR 3001	Heidolph
Microscope (DM550B)	Leica microsystem
Microwave oven MW800	Continent
Mini Trans Blot® cell	BioRad
Mini-Protean® Tetra cell	BioRad
NanoDrop 2000c	Thermo Scientific
pH-Meter (Seven Easy pH S20-K)	Mettler
Pipettes	Eppendorf/VWR
Power supplies	BioRad
Reax Top Vortex Mixer	Heidolph
Shaker Rocker 25	Labnet International Inc
TissueLyser II	Quiagen
TProfessional TRIO Thermocycler	Biometra
Tube rotator	VWR
Ultracentrifuge OptimaL80 XP	Beckmann Coulter
Waterbath VWB18	VWR

2.1.3. Consumables

Name of product	**Company**
96-well plate PCR Plate, Semi-Skirted	VWR
Biocoat collagen 60 mm dishes	BD Falcon
Cell scraper	SPL Life Sciences
Coverslips	Roth
Cryo tubes	Thermo Scientific
Disposable Scalpels sterile	Feather
Falcon 2059 polypropylene tube	BD Falcon
Injection needles	Braun
Micro tube 1.1ml Z-Gel	Sarstedt
MicroAmp Optical Adhesive Film	Applied Biosystems
Nunclon Delta Surface (96-well plate)	Thermo Scientific
PCR-tubes	B2B
Poly-D-Lysine Cellware 4-well cultureSlide,	BD BioCoat
Polyvinylidene fluoride (PVDF) Membran (0,4 µm pore size)	Millipore
Safe –Lock Eppendorf plastic tubes (0.5, 1.5 und 2 ml)	Eppendorf
Stainless steel beads	Qiagen
Sterile syringe filter 0.2 µm	VWR
SuperFrost microscope slides T	Thermo Scientific
Syringe	Braun
Tissue-Tek Cryomold	Sakura

Ultracentrifuge tubes	Beckmann Coulter
Whatman filters	Whatman

2.1.4. Reaction Kits and Enzymes

Name of product	**Company**
ABC kit PK-6100	Vector
Avidin/Biotin blocking Kit	Vector
Direct PCR-Tail	Peqlab
DNase Set (RNase-Free)	Qiagen
dNTP-Mix RT PCR	Peqlab
Free fatty acid Quantification Kit	Abcam
GSH/GSSG assay kit	Cayman
Interleukin 6 kit assay	R&D systems
Luciferase assay system	Promega
M-MLV Reverse Transcriptase	Promega
M-MLV RT 5x Buffer	Promega
My Budget PCR MasterMix	Bio Budget
Nova Red substrate kit (for peroxidase)	Vector
Proteinase K	Peqlab
Random Primer	Thermo Scientific
RNAqueous micro Kit	Ambion
RNeasy Mini Kit	Qiagen
Stripping Buffer (Restore Western Blot Stripping Buffer)	Thermo
Super Script II reverse Transcriptase	Invitrogen
SYBR® Green qPCR SuperMix	Applied Biosystem
TNF-a kit assay	R&D systems
β-Hydroxybutyrate (Ketone Body) colometric Assay Kit	Cayman

2.1.5. Construct and vector list

Name of the product	**Company**	**Catalog number**
human Hsp72 construct pcDNA5/FRT/TO V5 HSPA1A	Addgene	Plasmid 19456
pBI-L Tet Vector	Clontech Laboratories	GenBank AccessionNo.:U89934.

2.1.6. Antibodies

2.1.6.1. Primary antibodies for Western Blot (WB) and Immunohistochemistry (IHC) staining

Name of the product	Origine	Catalog number	Company
Cytochrome P450 2E1	rat	9140	Abcam
Hsc70 Ab (Hsp73)	rabbit	SPA-819	Stressgen
Hsp 27 (M-20)	goat	sc-1049	Santa Cruz
Hsp60	rabbit	ADI-SPA-805	Enzo
HSP70/HSP72	rabbit	ADI-SPA-812	Enzo
Hsp90	rabbit	4877	Cell Signaling
JNK1 (2C6)	mouse	3708	Cell Signaling
JNK2 (N-18)	rabbit	sc-827	Santa Cruz
Phospho-c-Jun (Ser73)	rabbit	9164S	Cell Signaling
Phospho-SAPK/JNK (Thr183/Tyr185)	rabbit	9251S	Cell Signaling
Phospho-SAPK/JNK (Thr183/Tyr185) (81E11)	rabbit	4668S	Cell signaling
Rip3	rabbit	2283	ProSci
β-Actin (monoclonal)	mouse	A-1978	Sigma

2.1.6.2. Secondary antibodies

Name of the product	Catalog number	Company
Goat anti-mouse IgG (H+L), HRP conjugated	G21040	Invitrogen
Goat anti-rabbit IgG (H+L), biotinylated	BA-1000	Vector
Goat anti-rabbit IgG (H+L), HRP conjugated	G21234	Invitrogen
Goat anti-rat IgG (H+L), HRP conjugated	A10549	Invitrogen
Rabbit anti-goat IgG (H+L)	R21459	Invitrogen

2.1.6.3. Primary antibodies for flow cytometry

Name of the product	Origine	Catalog number	Company
Anti-Mouse CD45	Rat	557659	BD Pharmingen
Anti-Mouse Ly-6G	Rat	561236	BD Pharmingen
Anti-Mouse F4/80	Rat	25-4801	BioScience
Anti-Mouse CD11b	Rat	17-0112	BioScience

2.1.7. Oligonucleotides (Primers)

All primers were synthesized either by Biomers, the Serco Industrial Park West in Ulm/Donau, Germany or by Eurofins genomics, Germany. Primers were designed using the program "Primer3 Input (version 0.4.0)" and the data available at http://www.ncbi.nlm.nih.gov. Alternatively, previously published primers were used.

2.1.7.1. Primers for genotyping

Genotyping primers	5'- Sequence -3'	Product length (bp)
HspA1A (Hsp72)	F: CTGTACCAGGGTGCCGGTGGT R: GTCCCCAAACTCACCCTGAAGTTCT	150
Lap-tTA	F: GCTAGGTGTAGAGCAGCCTACATTG R: GTCCAGATCGAAATCGTCTAGCGCG	800

2.1.7.2. Primers for qRT-PCR

Gen	Abbreviation	Species	5'- Sequence -3'	Accession
Albumin	mAlb	Mouse	F: CAGCGGAGCAACTGAAGACT R: GGTTTGGACCCTCAGTCGAG	NM_009654.4
Cluster of differentiation 31	mCD31	Mouse	F: GGAAGTGTCCTCCCTTGAGC R: CTTCTCGGGACATGGACGAC	NC_000077.6
Cytochrome P450, family 1, subfamily a, polypeptide 2	mCyp1a2	Mouse	F: TCTGCCAGTCTCCAGCCCCT R: AGATGGCAGTGGCCAGTAGCA	NM_009993.3
Cytochrome P450, family 2, subfamily b, polypeptide 10	mCyp2b10	Mouse	F: CAATGTTTAGTGGAGGAACTGCG R: CACTGGAAGAGGAACGTGGG	NM_009999.3
Cytochrome P450, family 2, subfamily e, polypeptide 1	mCyp2e1	Mouse	F: CTGGCCGAGGGGACATTCCTGT R: AGGGAAAACCTCCGCACGTCCT	NM_021282.2
Cytochrome P450, family 3, subfamily a, polypeptide 11	mCyp3a11	Mouse	F: TGCTGTCACAGACCCAGAGACG R: ACTCATTATCCCCACTGGGCCA	NM_007818.3
Glial fibrillary acidic protein	mGFAP	Mouse	F: GGA GAG GGA CAA CTT TGC AC R: ATA CGC AGC CAG GTT GTT CT	NM_001131020.1
Glutathione S-transferase	mGst	Mouse	F: GGGCCAGAGCTGGAAGGAGGA R: CCTCAAACTTGGGGAGCTGCCC	NC_003070.9
Heat shock protein family	(m+h) HSP72	Mouse + human	F: ACGGGCGCGACCTGAACAAG R: ATCAGGATGGCCGCCTGCAC	NM_005345.5 NM_010479.2

A (Hsp70) member 1A				
Heat shock protein family A (Hsp70) member 1A	hHsp72	Human	F: GCCAACAAGATCACCATCAC R: TTTGTACTTCTCCGCCTCCT	NM_005345.5
Interleukin 6	mIL6	Mouse	F: ACAAAGCCAGAGTCCTTCAGAGAGA R: TGGTCTTGGTCCTTAGCCACTCC	NM_031168.1
Large Ribosomal Protein	RPLPO	Human	F: GCAATGTTGCCAGTGTCTGT R: GCCTTGACCTTTTCAGCAAG	NM_001002.3
Protein tyrosine phosphatase, receptor type C	mCD45	Mouse	F: GCT CAA ACT TCT GGC CTT TG R: AGG GCA TTC TCT GTT GTG CT	NM_001111316.2
Ribosomal protein L7	L7	Mouse	F: GAAAGGCAAGGAGGAAGCTCATCT R: AATCTCAGTGCGGTACATCTGCCT	AK017074.1
Sulfotransferase family 1A member 1	mSult1a1	Mouse	F: TGCAAAGGATGTGGTTGTCT R: GACCCATAGGACACTTTCCC	NM_133670.1
UDP glucuronosyl-transferase 1 family, polypeptide A1	mUgt1a1	Mouse	F: ATGATCTGCTTGGTCATCCA R: CATCATCACCATCGGAACTC	NM_201645.2
UDP glucuronosyl-transferase 1 family, polypeptide A6	mUgt1a1	Mouse	F: TATCTGACAGGATGGCTTGC R: CCTAGAACTGAGGCCCAAAG	NM_145079.3

2.1.8. Animal list

Mouse lines	Company/Reference
C57BL/6N	Charles River
hHsp72	Generated and characterized in my thesis
Lap-tTA	Sunami et al., 2012 [129]

2.1.9. Buffers

Buffers	Composition of buffers
10% Formalin (pH=7.3) (1L)	100g Paraformaldehyde (PFA) 900 ml 1xPBS
Anticoagulation rinsing buffer (for hepatocyte isolation)	1m M EDTA in Basic rinsing buffer
APS (Ammonium persulphate) 10%	1ml: 0,1g ammonium persulphate 1000µl distilled water
Basic perfusion buffer (1L)	8 g NaCl

(for HSC isolation, pH 7.3–7.4)	400mg KCl 78 mg NaH2PO4 × H2O 151mg NaHPO4 × 2 H2O 2380mg HEPES 350mg NaHCO3 190mg EGTA 900mg glucose 6mg phenol red, in distilled water
Basic rinsing buffer 1 (1L) **(for hepatocyte isolation, pH 7.4)**	9 g NaCl 420 mg KCl 990 mg glucose 4.8 g HEPES 2.1 g NaHCO3 in distilled water
Basic rinsing buffer 2 **(for hepatocyte isolation, pH 7.4)**	50 ml Basic rinsing buffer 2 mM of CaCl2 30 mg type 2 collagenase 30 mg type 2-S Trypsin inhibitor
Blocking Buffer	2% (v/v) normal goat serum, 2.5 % (v/v) BSA in 1x PBS
Coomassie Brillant Blue Staining solution (1L)	0.5 g of coomassie R250 250 mL of Methanol 100 mL of acetic acid 650 mL of dH2O
Coomassie de-staining solution (1L)	95 mL of Methanol 95 mL of acetic acid 810 mL dH2O
1 mM Ethylenediaminetetraacetic acid (EDTA, pH = 8.0)	0.37g EDTA Distilled Water (MilliQ) – 1000 mL
FACS washing buffer	HBSS without calcium and magnesium 0.06% of bovine serum albumin (BSA) 0.3 mM EDTA 10 mM HEPES
Gey's buffered salt solution (1L) **(GBSS, pH 7.3–7.4)**	370mg KCl 10mg MgCl2 × 6 H2O 70mg MgSO4 × 7 H2O 75mg Na2HPO4 × 2 H2O 30mg KH2PO4 991mg glucose 227mg NaHCO3 225mg CaCl2 × H2O 8000 mg NaCl

	6mg phenol red in distilled water
Hank's complete (pH 7.3–7.4)	HBSS without calcium or magnesium 10mM HEPES 0.06%bovine serum albumin (BSA), 0.3mM EDTA
HBSS (1L) **(Hank's buffered salt solution)**	8000 mg NaCl, 400 mg KCl, 140 mg CaCl2, 100 mg MgSO4•7H2O, 100 mg MgCl2.6H2O, 60 mg Na2HPO4.2H2O, 60 mg KH2PO4, 1000 mg glucose, 350 mg NaHCO3, in distilled water
Homogenization buffer	0.187 M Tris-HCl (pH 6.8) 3% SDS 5 mM EDTA in distilled water
Laemmli Buffer (4X Reducing)	125 mM Tris-HCl (pH 6.8) 4% SDS 20% Glycerol 4% β-Mercaptoethanol 0.01% Bromophenol blue in distilled water
Laemmli Buffer (non-reducing)	125 mM Tris-HCl (pH 6.8) 4% SDS 20% Glycerol 0.01% Bromophenol blue in distilled water
Oil Red O stock dye	Oil Red O: 0.5g Isopropanol: 100 ml
Oil Red O working solution	30 ml Oil Red O stock dye 20 ml distilled water
PBS -EDTA buffer (pH=8) **(Phosphate buffered saline-EDTA)**	5 mM EDTA in 1x PBS
Perfusion buffer 2 **(for HSC isolation, pH 7.3–7.4)**	Basic perfusion buffer 0.5mg/mL pronase E
Perfusion buffer 3	Basic perfusion buffer

(for HSC isolation, pH 7.3–7.4)	0.4mg/mL pronase E 1.5U/mL collagenase P 0.02mg/mL DNase I
Resolving Gel Buffer	1.5 M Tris-HCl/H2O (pH 8.8)
SDS Gel Running buffer (10X) (L)	SDS 12.5g Tris Base 37.5g Glycine 180g
SDS Gel Running buffer (1X) (L)	100 ml 10X running buffer 900 ml distilled water
SDS **(Sodium dodecyl sulphate)10%**	SDS 10g 100 ml distilled water
Sucrose buffer (0.25 M) (100ml)	25 ml 1M Sucrose Stock Solution 5 ml 1M Tris, pH 7.4 1ml 0,5M $MgCl_2$ 68ml distilled water 100 µl DTT 1ml PMSF
1M Sucrose Stock Solution (10 ml)	3.42g Sucrose 10ml distilled water
TAE (Tris acetate-EDTA) buffer (10X)	48.5g Tris 11.4 ml glacial acetic acid 48.720 ml 0.5M EDTA (pH 8.0) in distilled water
TAE (Tris acetate-EDTA) buffer (1X) (1L)	100 ml 10X TAE buffer 900 ml distilled water
TBS (Tris-buffered saline) (10X) (1L) pH=7,6	24,2g Tris 80g NaCl 1L distilled water
TBST (1X) (1L)	100 ml 10X TBS 900 ml distilled water 0.2 % Tween 20
Transfer buffer (10X) (1L)	Tris base 3.16g Glycine 7.21g Methanol 200 ml 1L distilled water
Transfer buffer (1X) (1L)	100 ml 10X Transfer buffer 900 ml distilled water
1M Tris, pH 7.4 (100ml)	12.11g Tris 100ml distilled water

0.5M $MgCl_2$ (magnesium chloride) (50ml)	2.38g MgCl2 50ml distilled water

2.1.10. Softwares

Software	Company	Source
Adobe Photoshop CS2	Adobe	University Hospitals Aachen, Germany
Adobe Illustrator CS2	Adobe	
Living Image® Version 4.3.1	Caliper	
Excel, Word, Powerpoint	Microsoft	
KC4	BioTek Instruments, Inc.	
Axio Vision Rel.4.8	Zeiss	
7300 Sequenz-Detektion-Software	Applied Biosystems	
ImageQuant LAS 400	GE Healthcare	
i-control	Tecan	
GraphPad Prism 5	GraphPad	http://www.graphpad.com/
Endnote X7.1	Thomson Reuters	RWTH Aachen, Germany
Image J	Wayne Rasband	http://rsbweb.nih.gov/ij/
Primer3 Input (version 0.4.0)		http://frodo.wi.mit.edu/
The gene bank data		http://www.ncbi.nlm.nih.gov

2.2. Methods

2.2.1. Human subjects

To analyze expression of Hsp72 in various human diseases we examined liver biopsies from healthy subjects as well as from patients with NASH (non-alcoholic steatohepatitis), ALD (alcoholic liver diseases) and HCV (chronic hepatitis C infection; Table 2.1.). Samples were acquired from the Universities of Ulm and Bondy Liver Unit and were collected in years 2006 – 2010. All samples were divided into two parts: one part was formaldehyde-fixed and used for histological staining, the other part was frozen for RNA isolation. To confirm the diagnosis, HCV RNA amount in blood was quantified with the Cobas TaqMan/Amplicor systems (Roche, Switzerland). Diagnosis of ALD/NASH, was based on medical history (i.e. presence/absence of significant alcohol consumption) and histological analysis of H&E-stained liver biopsy. Samples were provided by Dr. Nurdan Guldiken [130].

To study the impact of inflammation/fibrosis on expression of Hsp72, samples were subdivided into groups with minimal/mild/moderate fibrosis stage/inflammatory grade (Table 2.1).

Samples	Number of samples, M/F	Age	Inflammation grade	Fibrosis stage
Control group	**3/3**	**42 (±10)**	**0 (±0)**	**0,1 (±0,09)**
NASH	**6/4**	**49 (±16)**	**1,5 (±0.11)**	**2,2 (±0,2)**
ALD	**12/3**	**49 (±9)**	**1,2 (±0,19)**	**2,5 (±0,17)**
HCV	**9/4**	**40 (±12)**	**1,4 (±0,14)**	**1,3 (±0,23)**

Results are expressed as mean ± SEM and list inflammation grades/fibrosis stages according to Kleiner scoring systems (ALD, NASH) and the METAVIR scoring system (HCV, controls).

ALD - alcoholic liver diseases, HCV - chronic hepatitis C infection, NASH - non-alcoholic steatohepatitis.

Table 2.1. Patient's characteristic.

2.2.2. Animal studies

To study the importance of Hsp72 in the liver, we generated new transgenic mouse lines overexpressing human Hsp72 (see Chapter 3.1.1, Figure 3. 1.for details) Mice were generated in the transgenic facility of university Tübingen by microinjection of an Hsp72 construct into the pronuclei of fertilized zygotes of the C57BL/6N inbred strain. The presence of the transgene was verified by genotyping (see chapter 2.2.4 for details).

For this study we used hemizygot the previously described single transgenic Lap-tTA [131], the newly generated Hsp72 or non-transgenic and double transgenic (i.e. containing both Lap-tTA and Hsp72) Hsp72 overexpressing mice on C57BL/6 background. Animals were housed in plastic cages and kept at a room temperature (22°C) in Animal Facilty of the Ulm University (Ulm, Germany) or University Hospitals in Aachen (Aachen, Germany). Both water and chow were given ad libitum. The breeding room was kept at a 12 hour day-night cycle. All treatments have been made in accordance with the German guidelines for animal research and animal welfare.

2.2.2.1 Tissue samples

For all experiments, the blood and tissue samples were collected from double transgenic mice and their non-transgenic littermates. At a given time, animals were sacrificed via overdose of isoflurane (Abbvie). The blood of the mice was collected from the vena cava inferior into the micro tube 1.1ml Z-Gel (Sarstedt, REF 41.1500.005, Germany) for separation of serum. Samples were centrifuged at 10000 G for 5 min (20°C) and the supernatant was collected. Serum parameters and concentrations of acetaminophen in the serum were measured in Clinical Chemistry Department of University Hospital Ulm and Aachen unless mentioned otherwise.

The bile ducts were carefully removed, washed with 1xPBS (Gibco) and stored in RNA-Later (Qiagen) at -20°C for future RNA-isolation (see below).

The liver tissue of the mice was removed and cut into pieces that were used for the following purposes:

1) isolation of RNA – parts of liver tissue were placed into tubes with RNAlater (Qiagen), that immediately stabilized RNA. The samples were stored at -20°C.
2) for protein isolation – samples were immediately snap-frozen in liquid nitrogen and then stored at -80°C.

3) for histological/immunohistochemical (IHC) analysis - samples were fixed in 10 % formalin overnight
4) for Oil-red O staining – samples were placed into Tissue-Tek Cryomold (REF: 4557, Sakura, Germany) and were covered with Tissue-Tek Compound (Sakura, Germany) providing a specimen matrix for cryostat sectioning. To guarantee a quick freezing process, the Cryomolds were placed into methylbutane that was pre-cooled over liquid nitrogen. Frozen samples were stored at -80°C.

2.2.2.2. Acetaminophen-induced liver injury

To test whether Hsp72 overexpression may affect acetaminophen-induced liver toxicity, 2 months old mice were fasted for 12 h, weighed and intraperitoneally injected with 800 mg/kg acetaminophen (APAP) (powder, Fagron GmbH & Co KG, Germany). To that end, 0.16 g of APAP was dissolved in a mixture of 0.5 mL DMSO (Sigma) and 0.5 ml of 0.9% NaCl (Braun) solution. 4 hours (h) and 18h after the injection the mice were sacrificed via overdose of isoflurane (Abbvie) (Figure 2.1). Livers were removed, weighed and cut into pieces for analyses and histological staining respectively (for details on storage and handling, see chapter 2.2.2.1).

The blood of the mice was collected from the vena cava inferior. Serum parameters and concentrations of acetaminophen in the serum were measured in Clinical Chemistry Department of University Hospital Ulm and Aachen (for details see chapter 2.2.2.1).

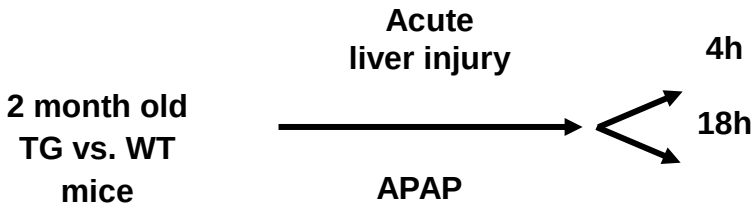

Figure 2.1. Schematic view of acetaminophen treatment.

2.2.2.3. MCD-induced liver injury

To test whether Hsp72 overexpression protects from development of lipotoxic injury, two months old double transgenic animals and their non-transgenic littermates were fed with methionine choline-deficient (MCD) diet ad libitum (Cat. No: 960439, MP Biomedicals, USA) for 8 weeks (Figure 2.2). The diet was pre-mixed and ordered as pellets (MP Biomicals). Mice fed standard diet (Specialdiäten GMBH, D-59494,

Soest, Ssniff, Germany) were used as controls. 8 weeks after beginning of the feeding, animals were sacrificed with an overdose of isoflurane (Abbvie). Livers were removed and processed as described above (for details, see chapter 2.2.2.1). Serum parameters were measured in the Clinical Chemistry Department of University Hospital Ulm and Aachen.

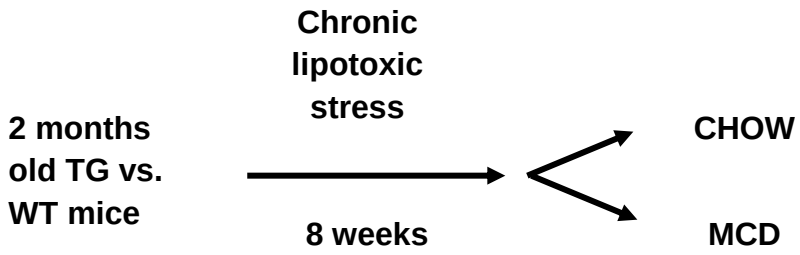

Figure 2.2. Schematic view of methionine choline-deficient (MCD) diet.

2.2.3. Cell culture experiments

2.2.3.1. Isolation of primary hepatocytes

Primary mouse hepatocytes from double transgenic Hsp72 overexpressing mice and their non-transgenic littermates were isolated by standard two-step liver perfusion method by Q3-Plattform (University Hospitals, Aachen, Germany) as described previously [132]. Briefly, mice were anaesthetized using 7 mg/kg body weight Xylazine and 105 mg/kg body weight of Ketamine. In the first step of perfusion, the liver was perfused with 20 mL of the anticoagulation rinsing buffer and subsequently with basic rinsing buffer 2 (for composition, see chapter 2.1.9) at a flow rate of 7.5 mL/minute.

After perfusion, the liver was removed and put into a petri dish including a 4°C cold washing buffer consisting of DMEM cell medium (Gibco) supplemented with 4.5 g/L glucose, 25 mM HEPES, antibiotics for cell culture, 4 mM glutamine, and 10% fetal bovine serum. The liver was gently dissected and the hepatocytes were removed by shaking.

The cell suspension was then filtered through a cloth and diluted into 50 mL of washing buffer (4°C). To remove non-parenchymal cells (NPCs), the cell suspension was centrifuged for 4 minutes at 4 °C and 18 rcf. The supernatant containing NPCs was collected and the hepatocytes (pellet) were re-suspended in 20 mL of washing

buffer by gently shaking the falcon tube. The centrifugation step was repeated two times.

To obtain only the viable cells, a percoll gradient centrifugation was performed. To that end, the hepatocytes were suspended in 10 ml of hepatocyte culture medium (Hepatozym, Life Technologies, #17705-021, Germany) and 10 ml of percoll (GE Healthcare, Cat.No: 17-0891-02) and 3 ml of 10xPBS (PAN Biotech) was added. The suspension was mixed by gentle pipetting and the centrifugation was performed at 50g (4°C) for 10 min. The pellet was re-suspended in 10 ml of ice cold hepatocyte culture medium supplemented with 1% penicillin-streptomycin (Gibco) and L-Glutamine (Gibco). Cell viability was examined by the Trypan blue exclusion test (Gibco, 15250-061). The cells were counted and seeded at commercially available, 60-mm collagen-coated culture dishes (BD Falcon Biocoat collagen 6-well plates, Lot: 0319961) at a density of $7{,}5 \times 10^5$ cells/2 ml. Alternatively, the cells were placed on poly-D-Lysine 4-well culture slides at a density of 7.5×10^4 cells (BD BioCoat, cat.: 354577). Cells were grown in a humidified incubator at 37°C and 5% CO_2. 4 hours after the isolation, the cells were briefly washed twice with 1xPBS (PanBiotech) and the medium was replaced. In addition, medium was replaced for a second time after overnight culture.

2.2.3.2. Stimulation of primary hepatocyte culture with 0.5 mM palmitic acid

To induce an acute lipotoxic injury, hepatocytes were subjected to treatment with 0.5mM palmitic acid (PA) for 24 hours. Untreated cells or cells treated with control solution were used as controls. Treatment solution was prepared according to the method of [133] with some modifications. Briefly, 100 ml of 5mM stock solution was prepared by dissolving 128.2 mg palmitic acid (Sigma, P0500-106) in 25 ml of 0.01M NaOH and heating the suspension to 70°C for 30 minutes. To increase the uptake of treatment solution by hepatocytes, PA mixture was conjugated with 18 ml of 24% fatty acid free BSA (Sigma, A7030). For that purpose, PA solution was first cooled down to 40°C, 24%BSA solution was added and stirred until it dissolved. Finally 10 ml of 1xPBS was added and filled up with distilled water to 100 ml. Control solution was prepared the same way without adding of PA. 5mM stock or control solution were diluted 1:100 in Williams E Medium (Sigma, #W4128) supplemented with 1% fetal bovine serum (FCS, Gibco), penicillin-streptomycin and L-Glutamine. Williams E medium without any supplements was used for untreated hepatocytes.

After the isolation, primary hepatocytes were kept in culture overnight before the start of the experiment. Afterwards, they were briefly washed twice with 1xPBS and one of the solutions depicted in Figure 2.3 were added. Cells were treated for 24 hours and subsequently were collected for future analysis. Level of alanine transaminase (ALT) and lactate dehydrogenase (LDH) in the cell culture supernatant were measured in the Clinical Chemistry Department of University Hospital Aachen (Aachen, Germany). Cells were then washed with 1xPBS and collected by scraping for future analysis.

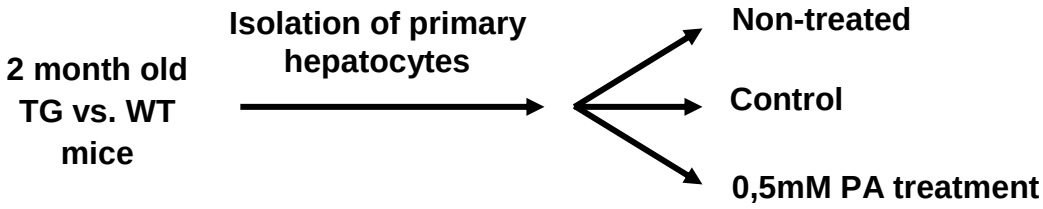

Figure 2.3. Schematic view of 0.5 mM palmitic acid treatment.

2.2.3.3. Isolation of different liver cell types

Kupffer cells, hepatic stellate cells and liver sinusoidal endothelial cells were isolated by Q3-Plattform as described below (University Hospitals, Aachen, Germany). After the first part of the isolation described in chapter 2.2.3.3.1. and 2.2.3.3.2., pellet that contains the cells was diluted in FACS-Buffer (composition of the buffers is listed in chapter 2.1.9) and filtered. Cell-mixture was incubated with the appropriate fluorescent FACS-antibodies (see Chapter 2.1.6.1 for antibody informations) for 30 min at room temperature. After that, the mixture was washed with FACS-Buffer and centrifuged for 10 min at 4°C (500G) to pellet the cells. Next, cell sorting was done using a BD FACS Aria II SORP Cell Sorter (BD Biosciences, Franklin Lakes, NJ, USA) and cells were sorted according to Table 2.2. After FACS-cell sorting, cells were washed twice with 1xPBS and RNA isolation was performed immediately after that (see Chapter 2.2.6.1).

Cell type	FACS-signal	
	Negative:	**Positive:**
LSEC	CD45, CD146	CD31
HSC	CD45, Ly6G, F4/80	Indo-1
KC	Ly6G, Indo-1	CD45dim, CD11bdim+F4/80

Table 2.2. Specific FACS signal for different liver cell types.

2.2.3.3.1. Isolation of hepatic stellate cells (HSC)

Isolation of hepatic stellate cells was done as described previously [134]. Briefly, mice were anaesthetized and liver was perfused via the Vena portae (see chapter 2.2.3.1 for details) with basic perfusion buffer 1, perfusion buffer 2 and perfusion buffer 3 (composition of the buffers is listed in chapter 2.1.9). Each perfusion step lasted 4.5 minutes and a flow rate of 6.5 mL/minute was used. After that, the liver was gently removed and cell suspension was collected. The mixture of liver cells was digested for 20 minutes in a 37°C warm water bath with perfusion buffer 2. Cells were filtered using a 70 μm nylon gaze, rinsed briefly with a perfusion buffer 2 and centrifuged for 10 min at 4°C and 600 g. The pellet was washed with 4°C cold Gey's buffered salt solution (GBSS) (composition is listed in chapter 2.1.9). Cells were then centrifuged for 10 min at 4°C and 600 g and suspended in GBSS buffer (without NaCl that was supplemented with iohexol (Nycodenz, Axis-Shield,Dundee, Scotland) to a final concentration of 18%. Subsequently, the mixture was pipetted to the bottom of a falcon tube containing GBSS and centrifuged at 4°C and 1500g for 22 min. This centrifugation step led to an isolation of HSCs at the interphase between the GBSS and iohexol layer. The suspension at the interphase was removed and washed with a 4°C cold GBSS (cell culture grade) or 4°C Hank's complete medium (for composition see chapter 2.1.9). Finally, the cells were centrifuged for 10 min at 600 g and the supernatant was discarded. Cells were dissolved in FACS buffer (composition of the buffers is listed in chapter 2.1.9) for following staining and FACS-sorting steps (for details, see chapter 2.2.3.3).

2.2.3.3.2. Isolation of liver sinusoidal endothelial cells (LSEC) and Kupffer cells (KC)

Isolation of liver sinusoidal endothelial cells (LSEC) and Kupffer cells (KC) was done as described previously [135]. Briefly, mice were anesthetized and the liver was perfused with 37°C warm solutions at a flow rate of 8 mL/min (see chapter 2.2.3.1 for details). First, HBSS solution without calcium and magnesium (PAA, Piscataway, NJ, USA) was applied for 10 min. After that, GBSS (Sigma-Aldrich, St. Louis, MO, USA) was used for three minutes. The perfused liver was removed and the liver pieces were digested for 10 min at 37°C with GBSS buffer. During the digestion, the suspension was gently stirred. Afterwards, the cells were filtered through nylon gaze (100 µm pores) and washed via centrifugation at 100 g at 21°C for 2 min without brake. The supernatant containing the target cells (LSEC and KC) was removed and centrifuged at 800 g at 21 °C without brake for 10 min. By this procedure, the cells were peletted and the supernatant was discarded. The pellet was dissolved in 10 mL RPMI1640 including L-Glutamine and the antibiotics 1% penicillin-streptomycin (all from Invitrogen, Carlsbad, CA, USA). Subsequently, the cell suspension was under-layered with 25% Percoll (GE Healthcare, Little Chalfont, UK) dissolved in phosphate-buffered saline (PBS). Finally, the bottom layer was under-layered with 50% Percoll in PBS. Centrifugation was performed for 30 min at 800 g and 21 °C without brake. This led to the concentration of the LSECs and KCs at the interphase between both Percoll layers. This interphase solution was gently transferred into a fresh tube, mixed with a 5x FACS washing buffer, and centrifuged for 10 min at 800 g and 4 °C and the supernatant was discarded. Cells were dissolved in FACS buffer (composition of the buffers is listed in chapter 2.1.9) for following staining and FACS-sorting steps (for details, see chapter 2.2.3.3).

2.2.4. Mouse genotyping

2.2.4.1. DNA isolation

Deoxyribonucleic acid (DNA) was isolated from 2-3 mm long mouse tail tips. Briefly, the tail tips were digested in a mixture of 180 µl Direct PCR-Tail Buffer (Peqlab) and 20 µl Proteinase K (Peqlab) at 55°C overnight and then heated at 85 °C for 45 min to inactivate Proteinase K. The supernatant that contains the DNA was collected after short centrifugation (1000 rpm) and stored at 4°C.

2.2.4.2. Polymerase chain reaction (PCR)

For genotyping of double transgenic and non-transgenic animals, a polymerase chain reaction (PCR) was performed. PCR-mixture was prepared as highlighted below and 25µl was used for every reaction (Table 2.3). The protocol started with an initial denaturation of double strand DNA at 95°C. After that, the mixture was cooled down to allow the denatured primers (for sequence information see chapter 2.1.7.1.) to attach to the single-stranded DNA template (annealing). The subsequent extension step allows the Taq DNA polymerase to synthesize a complementary DNA template and thereby to form a new double strand. After that, a new denaturation step separates the synthesized strands thereby setting the stage for a subsequent DNA amplification. Because of that, PCR reaction leads to an exponential increase in the DNA amount.

Given that PCR program needs to be adjusted to the specific primers and the length of the amplified DNA fragment, modified protocols were used for the genotyping of the Hsp72 and Lap-tTA constructs (Table 2.4, 2.5). The PCR was performed on the Professional TRIO Thermocycler (Biometra, Germany).

Reagents	**Volume, µl**
My Biobudget Mastermix (5x)	5
Forward Primer (10 µM)	1.4
Reverse Primer (10 µM)	1.4
DEPC H_2O	16.2
DNA (10 pg -1 µg)	1
Total volume:	25 µl

Table 2.3. PCR-mixture for amplification of Hsp72/Lap-tTA

Temperature (°C)	**Time**	**Number of cycles**	**Phase**
95	2 min	1	Initial denaturation
95	30 sec	35	Denaturation
58	30 sec		Annealing
72	30 sec		Elongation
72	5 min	1	Final elongation

Table 2.4. PCR-program for amplification of Hsp72

Temperature (°C)	Time	Number of cycles	Phase
94	3 min	1	Initial denaturation
94	40 sec	32	Denaturation
62	40 sec		Annealing
72	70 sec		Elongation
72	2 min	1	Final elongation

Table 2.5. PCR-program for amplification of Lap-tTA

2.2.4.3. Gel Electrophoresis

To estimate the size of the obtained PCR-products we used agarose gel electrophoresis that separates the DNA based on its length. 1% agarose gels supplemented with 0.05µl/ml PeqGreen DNA/RNA Dye (PeqLab) were prepared in 1x TAE buffer (Chapter 2.1.9). PeqGreen is a dye, which exhibit an intense fluorescence by the excitation with ultraviolet light after intercalation between double-stranded DNA. The gel electrophoresis yielded a ~ 150 bp fragment for the Hsp72 construct and a 800 bp fragment for the Lap-tTA amplicon.

2.2.5 Luciferase activity assay

To analyze the activity of luciferase that was introduced into the transgenic animals as a reporter construct, I performed an *in vivo* and *in vitro* luciferase activity assay. Firefly luciferase is an enzyme that catalyzes oxidation of luciferin thereby leading to a light emission.

2.2.5.1. Luciferase activity assay *in vivo*

The analysis of luciferase activity *in vivo* was performed using IVIS LUMINA XR system (Caliper) as a detector. First, a stock solution of D-Luciferin (PerkinElmer) was dissolved at 15mg/mL in 1xPBS and subsequently, sterile filtered through a 0.2 µm pore syringe filter (Cat.No: 28145-477, VWR, Germany). Mice were injected intraperitoneally with 200 µl (10 µL/g of body weight) of D-Luciferin solution, anesthetized with isoflurane (Abbvie) and placed in the imaging chamber of machine. Activity of luciferase was measured at 550 – 620 nm wavelengths; fluorescence was constant for at least 1 minute. The fluorescence signal was converted into an image with the help of Living Image software and was used for further quantification. After the measurement, animals were put back to plastic cages and kept for future experiments.

2.2.5.2. Luciferase activity assay *in vitro*

The analysis of luciferase activity *in vitro* was performed by Lumat LB 9501 as a detector (Berthold) using the Luciferase assay system (Promega) according to manufactures protocol. 20 mg of tissue specimen (liver/brain/pancreas/kidney/ intestine/lung/heart/spleen/colon) was homogenized with 500 µl of 1x Passive Lysis Buffer (PLB) (Promega). The tissue lysates were centrifuged at maximal speed for 30 sec at 4°C. 20µl of supernatant was mixed with 100µl of Luciferase Assay Reagent (Promega) that contains the luciferin. The fluorescence was measured by luminometer. 1x PLB buffer without any added sample was used as a negative control.

2.2.6. Isolation and quantification of Ribonucleic acid (RNA)

2.2.6.1. Isolation of total RNA from liver tissue/cells

After harvesting, liver samples were immediately placed to tubes containing RNAlater® RNA Stabilization Buffer (Qiagen) in order to prevent RNA degradation (see Chapter 2.2.2.1 for details). RNA was isolated with the help of the RNeasy Mini Kit (Qiagen GmbH, Germany) according to the manual. Briefly, small piece of liver tissue (no more than 30 mg) was homogenized in 600 µl of RLT Buffer supplemented with 1% β- Mercaptoethanol. Homogenization of the tissue was achieved by grinding with stainless steel beads in a TissueLyser II (Qiagen). In the next step, the RNA from the homogenate was bound to silica-gel membrane of the provided columns. To do so, the tissue lysates were transferred into RNeasy mini spin columns and centrifuged. To get rid of the unwanted DNA that precipitates together with RNA and binds to silica-gel membrane as well, I performed incubation with DNaseI (RNase-Free DNase Set (Qiagen) for 15 min at room temperature. To purify the bound RNA, the columns were washed with washing buffers (RW1 and RPE buffers) via short centrifugation steps. At the end, RNA was eluted with RNase-free water.

To obtain the RNA from the different liver cell types that were isolated by the Q3-Plattform (University Hospital Aachen, Germany) (for details see Chapter 2.2.3.1 and Chapter 2.2.3.3), the samples were first diluted in 10 ml of cell culture medium. The cell suspension was centrifuged at 750g (4°C) for 10 min and supernatant was discarded. The cell-containing pellet was immediately homogenized with 350 µl of RLT Buffer supplemented with 1% β-Mercaptoethanol. The subsequent isolation of RNA was performed as described above.

2.2.6.2. Purification of total RNA from common bile ducts

For isolation of total RNA from small amount of tissue (<10 mg) as like bile duct, the RNAqueous-Micro kit (Ambion) was used following the manual to obtain maximally concentrated RNA. After harvesting, the bile duct samples were immediately placed into tubes with RNAlater and stored at -20°C till usage. The isolation started with a homogenization of samples in 100 µl of Lysis solution containing guanidinium thiocyanate, a strong agent that disrupts cell membranes and inactivates ribonucleases. Homogenization of bile duct samples was achieved by grinding with beads and TissueLyser II (Quiagen). The tissue lysate was mixed with 50µl of ethanol and transferred to the Micro Filter Cartridge and centrifuged for 10 sec at maximal speed. During this process, the RNA bound to silica-based filters. To purify the RNA, filters were washed twice with different types of washing buffers. Finally RNA was eluted with 15 µl of pre-heated (75°C) Elution solution by centrifugation at maximum speed. To optimize RNA-quality and to remove contaminating DNA, the samples were treated with DNase I and a subsequent DNase inactivation was performed as recommended by the manufacturer.

2.2.6.3. Determination of RNA concentration and purity

To determine the RNA purity and concentration, NanoDrop 2000c (Thermo Scientific) was used. The concentration of RNA was detected by measuring of absorbance at 260nm. Protein contamination was assessed by measuring the ratio of absorbance at 260/280 nm. Ratio between 1.8-2.0 indicates highly pure RNA.

2.2.6.4. Reverse transcription PCR (cDNA synthesis) from isolated RNA

To translate the RNA into cDNA I used the M-MLV-Reverse-Transcriptase Kit (Promega). 1 µg of RNA was mixed with RNAse-free DEPC water (Invitrogen) and 0.2µg/µl Oligo dT primer (Promega) was added. This mixture was gently mixed and incubated for 5 min at 70°C. The Oligo dT primer binds to the complementary poly-A tail of mRNA and creates initiation point for translation of complementary (c)DNA strand. In this way, only the mRNA becomes transcribed into cDNA. After the addition of the primer, samples were kept on ice while the Master Mix for the reverse transcriptase was prepared (for composition see Table 2.6). Finally, 10µl of Master Mix was added per sample and the transcription was carried out for 1h at 37°C. Finally, cDNA samples were diluted 1:10 with DEPC water and stored at -20°C.

Reagents	Volume	Incubation temperature, °C	Incubation time, min
RNA	12,5 µl (1µg of RNA)	70	5
OligodT primer	2,5 µl (final concentration in mixture 0,2 µg/µl)		
Total volume:	**15µl**		
Master mix:	Add 10 µl of Master Mix		
MLV 5X buffer	5 µl	37	60
dNTPs set (10mM)	1,25 µl		
MLV RT enzyme	1 µl		
H_20	2,75 µl		
Total volume of PCR product:	**25 µl**		

Table 2.6. Master Mix and PCR-program for cDNA synthesis

2.2.6.5. Quantitative real time PCR (qRT-PCR)

To determine mRNA expression of specific genes, quantitative real time PCR (qRT-PCR) was performed using the 7300 Fast Real Time PCR system (AppliedBiosystems). To quantify the amount of the DNA during the amplification, qRT-PCR-mixture was used that contains fluorescent dye SYBR Green (Applied Biosystems). SYBR Green is a dye that intercalates with cDNA and emits a fluorescence signal after binding. The relative amount of the gene of interest, i.e. amount compared to the quantity of a house-keeping gene of interest, was determined by the ΔΔCt method [136]. This method is based on so called Ct values for both genes, i.e. values where the DNA concentration reached a certain threshold. More abundant genes reach this threshold earlier and because of that, ratio between the Ct values reveals the relative amount of the gene of interest.

The PCR-mixture was prepared according to Table 2.7 and pipetted into 96-well plate PCR Plates (Order No: I1402-9700, VWR, Germany). The samples were analyzed in duplicates. Mouse ribosomal protein (L7) and human Large Ribosomal Protein (RPLPO) were used as internal controls (see Chapter 2.1.7.2 for primer informations). The plate was sealed with MicroAmp Optical Adhesive Film (Applied Biosystems) to prevent evaporation of the samples. Samples were collected to the bottom of the plate via a centrifugation at 2000 g for 3 minutes. Given that the master mix contains a Hot Start Taq DNA polymerase, an extended initial denaturation step

was needed (i.e. 95°C for 10 min) to release the polymerase from its wrap. After that, 45 amplification cycles were carried out, each containing a denaturation step (10 sec, 95°C) and a combination of annealing and elongation steps (1 min, 60°C) (Table 2.8).

The results were evaluated with the help of 7300 Sequence Detection Software (AppliedBiosystems) Version 1.3.1. The results were expressed as mean ± SEM.

Reagent	**Volume, µl**
SYBR® GreenER qPCR SuperMix	5
DEPC treated water	3
Forward primer (100 pmol/µl)	0.5
Reverse primer (100 pmol/µl)	0.5
c-DNA template (1 µg/µl)	1
Final volume	**10**

Table 2.7. qRT-PCR-mixture.

Phase	**Temperature, °C**	**Time**	**Number of cycles**
Activation	95	10 min	1
Denaturation	95	10 sec	45
Annealing and elongation	60	1 min	

Table 2.8. qRT-PCR program

2.2.7. Protein extraction and western blotting

2.2.7.1. Total protein extraction from liver tissue

To analyze the concentration of the proteins of interest, total protein extraction was performed. Approximately 25 mg of liver tissues was homogenized in 600 µl of Homogenization Buffer that contains 3% of sodium dodecyl sulphate (SDS, Roth) (for composition see chapter 2.1.9). This buffer efficiently denatures proteins and protects thereby the samples from degradation. Disruption of tissue was done by grinding with stainless steel beads in the TissueLyser II (Qiagen). Afterwards, the samples were heated at 95°C for 5 minutes to further denature of proteins. Subsequently, the lysates were sonicated for 5 min at 4°C to further disrupt the genomic DNA. Finally, samples were centrifuged at 14000 rpm for 3 min. Supernatant that contains the total proteins was collected, diluted 1:1 with 4x Laemmli Buffer (for composition see chapter 2.1.9) and heated to 98°C for 5 min and kept at -80°C.

2.2.7.2. Total protein extraction from primary hepatocyte culture

The dishes with primary hepatocytes were placed on ice and washed twice with ice-cold PBS. Then 500 ml ice-cold Homogenization buffer (for composition see chapter 2.1.9) per one 60 mm dish (BD Falcon) was added. Cells were scraped using a Cell scraper (SKU: 90020, SPL Life Sciences). Cell suspension was placed to plastic tubes and shaked for 30 min at 4°C by tube rotator (VWR, Germany). Then cell lysates were centrifuge for 20 min (12,000 rpm) at 4°C. Finally, supernatant that contains the total proteins was collected, diluted 1:1 with 4x Laemmli Buffer (for composition see chapter 2.1.9) and heated to 98°C for 5 min and kept at -80°C.

2.2.7.3. Separation of proteins by SDS-PAGE

To analyze the amount of specific proteins in tissue/cell lysates, a western blotting was performed. First of all, proteins were separated according to their molecular weight by polyacrylamide gel electrophoresis (PAGE). According to the size of the protein of interest, 8% or 10% acrylamide-containing gels were employed. If proteins of interest were bigger than 50kDa, separation was performed with 8% gel, for proteins with size between 30-50kDa, a 10% gel was used. The gels consisted of two parts: a stacking and a resolving gel. Gel mixtures were prepared according to Tables 2.9; 2.10. The resolving gel was poured to the bottom of the assembly and let to polymerize for at least 30 minutes before pouring the stacking gel. At the end, 10% ammonium persulphate (for details see chapter 2.1.9) and tetramethyl ethylene diamine (TEMED) were added to the mixture since they start the polymerization reaction.

Reagents	Resolving gel, 8%	Resolving gel, 10%
H_2O,ml	2,05	2,35
Trenngel Buffer,ml	1,3	1,3
30% Acrylamide,ml	1,65	1,32
10% SDS,µl	50	50
10%APS,µl	25	25
TEMED,µl	7,5	7,5

Table 2.9. Gel composition and preparation of resolving gel

Reagents	Stacking gel
H_2O,ml	1,5
Trenngel Buffer,ml	0,65
30% Acrylamide,ml	375
10% SDS,µl	25
10%APS,µl	12,5
TEMED,µl	2,5

Table 2.10. Gel composition and preparation of stacking gel

Prior to the electrophoresis, the isolated proteins were denatured and mixed with 4x Laemmli Buffer that contains β-mercaptoethanol and SDS (see chapters 2.2.7.1 and 2.2.7.2) which result in disulfide bonds disruption and formation of negatively charged proteins, respectively. The proteins were loaded into polyacrylamide gels, where they migrated first into the stacking gel. It has bigger pores that resolving gels and leads to concentration of the proteins into a this layer at the interphase between resolving and stacking gels. In the resolving gel, proteins become separated according to their molecular weight. Given that they are negatively charged, they move from the negative to the positive electrode. The electrophoresis was performed with 70V for 30 min (migration thorough stacking gel) and continued with 110V for 1h 10 min (migration through resolving gel). A BioRad Western Blot system (BioRad, Germany) was used. To determine the molecular weight of proteins, Page Ruler Prestained Protein Ladder (Thermo Electron GmbH, Germany) was included in each gel.

2.2.7.4. Staining of proteins in acrylamide gels with Coomassie brilliant blue

To visualize the proteins in the polyacrylamide gel, I used 0.05% Coomassie Brillant Blue Staining solution (for composition see chapter 2.1.9). The staining was perfomed for 1h at room temperature. After that, the gel was de-stained with Coomassie de-staining solution (for composition see chapter 2.1.9) until the protein bands were clearly visible.

2.2.7.5. Western blotting

To determine the amount of specific proteins, Western blotting was performed. Separated proteins were transferred from polyacrylamide gel to polyvinylidene fluoride (PVDF) membrane (0.4 µm pore size, Millipore) by blotting in 1x Transfer buffer (composition according to chapter 2.1.9). Transfer of proteins was done with a wet blot-system (Bio-Rad, Germany) using constant current of 0.2 A (Ampere) for 80 minutes.

To analyze the efficiency of blotting of proteins onto PVDF membrane Ponceau S staining was performed. PVDF membrane was soaked for 20 min into the Ponceau S Staining solution (composition according to chapter 2.1.9). After that, the stained membrane was washed with Tris Buffered Saline containing 0.1% Tween (1xTBST) solution, (for composition see chapter 2.1.9) until the protein bands were clearly visible.

To reduce the unspecific binding of antibodies to the membrane, the PVDF membrane with separated proteins was blocked for 1h at room temperature in blocking solution. The 5% blocking solution was prepared by adding either 5% (w/v) non-fat dry milk (AppliChem) or 5% (w/v) bovine serum albumin (BSA, Serva) to the in 1xTBST. The choice of milk vs. BSA was made based on the recommendation of the manufacturer of the antibody. After blocking, the membrane was incubated with the primary antibody of interest (see Chapter 2.1.6.1 for antibody informations) overnight at 4°C. Primary antibody was diluted in blocking buffer (see above for details). To remove unbound primary antibody, the membrane was washed 3 times with 1xTBST (10 minutes each) and incubated for 1h at room temperature (RT) with secondary antibody that is conjugated with horseradish peroxidase (HRP) (see Chapter 2.1.6.2 for antibody information). Secondary antibody was diluted 1:10000 in the appropriate blocking buffer. Finally, to visualize the protein of interest, membrane was covered with ECL luminol reagent (GE Healthcare). This reagent contains substrate for HRP that is bound to the secondary antibody. HRP catalyzes the oxidation of luminol that leads to a chemiluminescent reaction. The generated light emission was detected by a luminescent image analyzer LAS-4000 Mini detection system (Fujifilm) or ImageQuant LAS4000 (GE Healthcare, UK).

2.2.8. Histological stainings

After harvesting, liver samples were immediately placed in 10% buffered formalin and kept overnight at room temperature (see chapter 2.2.2.1 for details). The tissue samples were dehydrated in a graded ethanol series and embedded in paraffin. Finally, they were sectioned (2 µm) and stained with Haematoxylin and Eosin (H&E) or were used for immunohistochemistry (IHC) staining.

2.2.8.1. Hematoxylin and eosin (H&E) Staining

To analyze the extent of liver injury and inflammation a hematoxylin and eosin (H&E) staining was used. The liver tissue sections were deparaffinized in Xylol (Roth) and hydrated with serial dilution of Ethanol (Sigma) according to Table 2.11.

Deparrafinization step		**Hydration step**			
Xylol I	Xylol II	100% EtOH I	100% EtOH II	97% EtOH	70% EtOH
10 min	10 min	4 min	4 min	4 min	4 min

Table 2.11. Deparaffinization and hydration steps for histological stainings

At the end, samples were washed with deionized water for 2 min at room temperature. Afterwards, samples were soaked into a commercially available Hematoxylin solution (Roth, Germany) for 5 min. This solution stains the nuclei and other basophilic structures blue. Next, samples were washed with tap water for 5 minutes. The cytoplasm and eosinophilic/acidophilic structures were colored in pink, red or orange with Eosin G 0.5 % (Roth, Germany) for 1 min. The samples were again washed to remove stain for 2 min (room temperature) in running deionized water. Afterwards, for dehydration of stained tissue, slides were shortly incubated in a serial dilution of Ethanol (70%, 97%, 100%, 100%) for 2 minutes each. After final dehydration step in Xylol for 10 min, the sections were covered with Coverslips (Roth, Germany) and entellan as the mounting medium (Merck, Germany).

The morphological quantification was done by an experienced pathologist (Assoz. Prof. Johannes Haybäck, Institute of Pathology, Medical University Graz,

Austria) according to a score summarized in Table 2.12. To quantify the inflammation grade, a 20x lens was used and 6 fields were analyzed per sample.

Lobular inflammation (at least in one area):		
Score	# of inflam-matory cells	Description
Score 0	none	no
Score 1	<2/20x	minimal
Score 2	2-4/20x	mild
Score 3	>4/20x	moderate

Table 2.12. The morphometrical quantification of lobular inflammation.

2.2.8.2. Immunohistochemistry staining

To investigate the exact localization of Hsp72 overexpression within the liver tissue, immunohistochemistry staining (IHC) was performed. First, paraffin sections were deparaffinized in Xylol (Roth) for 10 min and shortly hydrated with a serial dilution of ethanols from 100% to 70% followed by washing steps with water and 1xPBS (5min each).

Because formalin fixation crosslinks proteins and thereby often masks the antigen, an antigen unmasking was performed using EDTA buffer (pH = 8, for composition see chapter 2.1.9). The EDTA buffer was preheated in microwave for 10 min at 630 W and samples were placed and boiled for 30 min at 200W. After that, slides were cooled down in the buffer for 30 min and washed with 1xPBS 3 times (5 min for each step).

To reduce an unspecific background, a blocking of endogenous peroxidase and biotin was performed. To that end, slides were treated with 1% hydrogen peroxide (H_2O_2) in methanol for 10 min at room temperature. In addition, avidin as a biotin blocking reagent was used prior to the incubation with an biotinylated antibody. To that end, samples were incubated for 20 min at room temperature with a blocking buffer (see chapter 2.1.9 for details) containing avidin (4 drops per 1 ml of buffer). Afterwards, sections were exposed with primary antibody anti-Hsp72 (SPA812, Stressgen) overnight. Antibody was diluted 1:100 in blocking buffer that contains 4 drops avidin and 4 drops biotin per 1 ml.

Next, slides were washed with 1xPBS and incubated with biotinylated secondary anti-rabbit antibody (dilution: 1:200 in blocking buffer, Vector, BA-1000) for 30 min at room temperature. Afterwards, samples were washed 3 times with 1xPBS

(5 min, at room temperature). Specific signal was detected with a chromogenic reporter - AB enzyme reagent prepared according to the manufacturer´s instructions (Vector Laboratories). As a substrate for visualizing the specific signal, Vector Nova Red (Vector Laboratories, INC) was used. It reacts with AB enzyme and gives a red-brown color thereby visualizing the localization of the specific antigen.

At the end, samples were washed 3 times with 1xPBS. For counterstaining of nuclei and other basophilic structures, Haematoxylin staining (1:10 diluted with water, Roth, Germany) was performed for 30 sec at room temperature. Finally, slides were washed for 10 min with running tap water, dehydrated in serial dilution of Ethanol (70%, 97%, 100%, 100%) and for 2 min in Xylol and covered with coverslips (Roth, Germany) and entellan as a mounting medium (Merck, Germany). The slides were analyzed by a light microscope (Axio imager.Z1, Zeiss).

2.2.8.3. Oil-Red O staining

For histological visualization of neutral triglycerides and lipids in the liver tissue, I used an Oil Red O staining. Stock solution of Oil Red O was prepared in Methanol (Sigma) (composition according to chapter 2.1.9). After that, fresh Oil Red O working solution was diluted from stock solution with water (see chapter 2.1.9), incubated for 10 min at RT, filtered and kept protected from light.

Oil Red O staining was done using frozen liver sections or, alternatively, in primary mouse hepatocyte cell culture. Primary mouse hepatocytes were grown inside culture slides covered with Poly-D-Lysine (BD BioCoat, Germany) which is used to enhance the cell attachment to the bottom of the dish (see chapter 2.2.3.1 for details). Prior to the staining, cells were washed twice with 1xPBS and fixed in 10% Formalin (composition according to chapter 2.1.9) for 10 min. Next, samples were briefly washed with running tap water for 5 min and rinsed with 60% Isopropanol (Sigma, Germany). For frozen liver sections the same fixation and washing steps were used.

At the end, staining was done with fresh Oil Red O working solution for 15 min at RT. Slides were rinsed with 60% Isopropanol (Sigma, Germany). For counterstaining of nuclei and other basophilic structures Haematoxylin (Roth, Germany) diluted 1:1 with water was used for 1,5 min. Finally, slides were washed with distilled water and mounted with aqueous Kaiser's glycerol gelatine (Merck, Germany).

2.2.9. Subcellular Fractionation

To determine the exact location of transgenic Hsp72 in the cell compartments a subcellular fractionation was performed as it was described previously by Wattiaux et al. [137] with minor modifications. Briefly, cell fractions were divided according to density and size to different cellular fractions (nuclear, cytoplasmic, mitochondrial, lysosomal fractions and fractions that contains autophagosome (heavy and light)) via Nycodenz gradient centrifugation.

The Nycodenz gradient was prepared 2 h in advance as detailed in Figure 2.4. (see below), loaded into ultracentrifugation tube (Beckmann Coulter, Germany) (Figure 2.1) and stored at 4°C until usage.

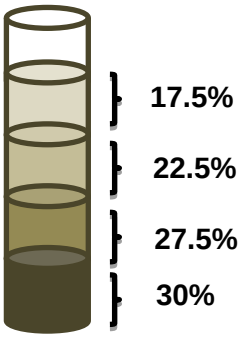

For one sample		
Percentage, %	**Nycodenz, ml**	**H_20, ml**
17,5	2.1	9.9
22,5	2.7	9.3
27,5	3.3	8.7
30	7.2	16.8

Figure 2.4. Preparation of Nycodenz gradient solution and its loading into ultracentrifugation tube

For this method I used a freshly harvested liver tissue. Livers were washed with 1xPBS and with 0.25M Sucrose buffer (for composition see chapter 2.1.9). Then 1g of liver tissue was homogenized in 3 ml 0.25M Sucrose buffer and filtered through a double gauze. Tissue lysates were centrifuged at 2.000G for 5 min at 4°C. Supernatant 1 was collected; pellet 1 was re-suspended into 1.5 ml of 0.25M Sucrose buffer and centrifuged again with the same procedure. Supernatant 2 was collected; pellet 2 was mixed gently by pipetting with 90 µl of 1xPBS and kept as nuclear fraction in -80°C. Supernatants 1 and 2 were mixed together and centrifuged at 17.000G for 12 min at 4°C. The resulting supernatant 3 was collected and kept as cytoplasmic fraction in -80°C. Pellet 3 was used for isolation of the remaining cellular organelles. To that end, it was resuspended in 1.5 ml of 0.25M Sucrose buffer and centrifuged at 17.000G for 12 min at 4°C. Afterwards, pellet 4 was solved in 885µl 0.25M Sucrose buffer and 1.26 ml of 85,6% Nycodenz (Progen, #1002424, Germany) in water (pH=7.2).

To isolate mitochondria, lysosome and autophagosome (heavy and light) I used a Nycodenz gradient centrifugation method. Dissolved pellet 4 was gently loaded into ultracentrifugation tube on top of a Nycodenz gradient (see Figure 2.1. for details). Samples were centrifuged in Ultracentrifuge OptimaL80 XP (Beckmann Coulter) with SW41 rotor at 25000 rpm for 3 hours at 4°C.

Finally, different layers corresponding to mitochondria, lysosomes, and autophagosomes (heavy and light) were collected (see Figure 2.5) into different tubes and centrifuged at 14000 rpm for 10 min at 4°C to obtain the pellet with the remaining fractions.

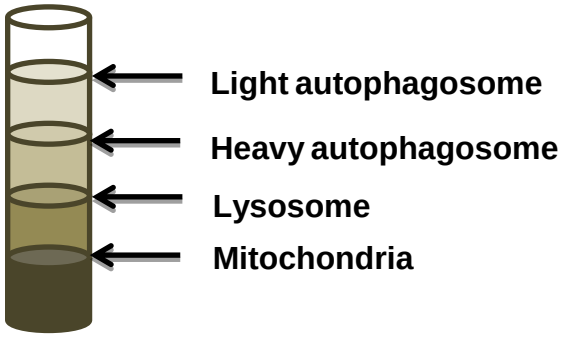

Figure 2.5. Schematic view of localization of subcellular fractions after Nycodenz gradient centrifugation

After centrifugation, individual pellets were kept at -80°C. Before the analysis, the pellets of mitochondrial, lysosomal and autophagosomal fractions were solved in water (200µl for mitochondrial or 100µl for lysosomal and autophagosomal fractions). Before using samples for Western blot, 100µl of Homogenization buffer (composition according to chapter 2.1.9) was added and samples were diluted 1:1 with 4x reducing Laemmli Buffer (composition according to chapter 2.1.9), denatured at 98°C for 5 min and kept at -80°C.

2.2.10. Total and Oxidized Glutathione (GSH/GSSG) assay

Glutathione (GSH) is major endogenous antioxidant in mammalian cells. It protects cellular structures from damage during oxidative stress caused by different sources. Glutathione exists in both a reduced (GSH) and an oxidized (GSSG) state. In the case of APAP overdose, APAP becomes metabolized by enzymes from cytochrome P450 family such as CYP2E1 and CYP1A2 to give rise to reactive metabolite N-acetyl-p-benzoquinone imine (NAPQI). Normally, conjugation with glutathione (GSH) detoxifies NAPQI. However, after overdose of APAP, glutathione

(GSH) becomes depleted and NAPQI forms hepatotoxic covalent protein adducts [92, 93]. The ratio between reduced and oxidized glutathione (GSSG) determines the remaining protective capacity of the cells to resist oxidative stress and APAP toxicity.

To determine the amount of total (GSH) and oxidized (GSSG) forms of glutathione in liver tissue, I performed a spectrophotometric assay according to the instructions of the manufacturer of the Glutathione assay kit (#703002, Cayman). Briefly, 100mg of liver tissue were homogenized with 1ml 1xMES Buffer (#703002, Cayman). Then, tissue lysates were centrifuged at 14.000 rpm at 4°C for 15 min. The supernatants were removed to new tubes and stored on ice. Subsequently, samples were deproteinated to prevent interferences with the assay and mixed 1:1 with MPA reagent (5g of metaphosphoric acid (Sigma-Aldrich, 239275) in 50 ml water). Probes were incubated for 5 min at room temperature and centrifuged for 2 min at 5.000 rpm (4°C). Afterwards, 50µl of 4M TEAM reagent was added to 1ml of supernatant. The solution was vortexed briefly and diluted 1:1 with 1x MES buffer. For preparation of 4M TEAM reagent, 531µl of triethanolamine (Sigma-Aldrich, T58300) was dissolved into 469 µl of water. Finally, kinetic absorbances of samples were measured at 405 nm by microplate reader Infinite 200 (Tecan). Quantification of GSSG level was done after derivatization of GSH with 2-vinylpyridine. To that end, 100 µl of the supernatant was mixed with 2 µl of 1M 2-vinylpyridine (Sigma-Aldrich, 13929-2) solution and 6 µl of triethanolamine (Sigma) and incubated for 1h at RT. Finally, kinetic absorbance values were measured at 405 nm using microplate reader Infinite 200 (Tecan). The results were normalized to the tissue weight.

2.2.11. Determination of Acetaminophen-Protein Adducts

The quantification of amount of Acetaminophen-Protein Adducts was done in Prof. Laura James Lab. (Pediatric Pharmacology and Toxicology, AR-USA) as described previously [93, 138]. Briefly, 100 mg of liver tissue was homogenized in 1 ml of ice cold 1x PBS, pH 7.2 and digested with protease. Afterwards, small molecules were removed by gel-filtration on centrifugal desalting columns equilibrated with PBS, pH 7.2 (exclusion volume > 6,000 daltons). For measurement of APAP-protein adducts the high-performance liquid chromatography with electrochemical detection (HPLC-ECD) method was performed. The results were normalized to total protein concentration and showed in units of nmol APAP-CYS adducts/mg protein.

2.2.12. Measurement of cytokines TNF- α and IL-6

The concentration of TNF-α and IL-6 in the plasma was detected by enzyme-linked immunosorbent assay (ELISA) according to the manufacturer (R&D, M6000B and MTA00B). A quantitative sandwich enzyme immunoassay technique was used. Briefly, monoclonal antibodies specific to mouse TNF- α or IL-6 were pre-coated onto a microplate by the supplier. 50µl of plasma samples (1:1 diluted in water) were pipetted into the wells for binding to immobilized antibodies. Standards and controls samples were used for construction of standard curve and calibration, respectively. Plates were incubated with the samples 2h at RT. To remove unbound substances, plates were briefly washed 4 times with 400 µl of washing buffer for each step. Subsequently, 100 µl (per well) of enzyme-linked polyclonal detection antibodies specific for mouse TNF-α/IL-6 were added. Plates were incubated for 2h and washed again to remove unbound enzyme-linked antibody. At the end, 100µl (per well) of substrate solution was added. Plates were protected from light and incubated for 30 min at RT. The addition of substrate led to an enzymatic reaction that turned the initially blue reagent yellow. Enzymatic reaction was stopped by adding of 100µl of Stop solution to each well. The amount of TNF-α or IL-6 was quantified by measuring of samples optical density at 450nm with a microplate reader. The final results were calculated according to the standard curve.

2.2.13. Determination of basic parameters of lipid metabolism

The amount of triglycerides, free fatty acids, ceramides, phosphatidylcholine and phosphatidylethanolamine in the liver was quantified via thin-layer chromatography (TLC) method in Prof. A. K. Kiemer Lab by Dr. Sonja M. Keßler (Department of Pharmacy, Pharmaceutical Biology, Saarland University, Saarbrücken, Germany) as described previously [139, 140].

Briefly, liver samples were lyophilized. Afterwards, 15 mg of the freeze-dried tissue was dissolved in 18 volumes of a mixture of hexane/2-propanol (3:2) and the mixture was centrifuged at 4°C and 10000 g for 10 min. The supernatant was collected, dried and re-dissolved in an appropriate volume of chloroform/methanol (1:1) and added in equal amounts onto the TLC plates. Finally, TLC was performed using a two solvent system. Results were expressed as means ± SEM.

2.2.14. Measurement of β-Hydroxybutyrate (Ketone Body) in the serum

The term of "Ketone body" include three substances: acetoacetate, β-hydroxybutyrate (β-HB) and acetone. β-Hydroxybutyrate is being produced by the liver, mainly by oxidation of fatty acids and exported to other tissues as a source of energy. Generally, amount of β-HB constitutes approximately 75% of the ketone bodies in serum.

To quantify the amount of β-Hydroxybutyrate in the serum, a colorimetric assay was performed according to manufacturer recommendations (#700190, Cayman). This method is based on detection of oxidation of β-Hydroxybutyrate to acetoacetate. During this process, the cofactor NAD^+ is reduced to NADH that reacts with colorimetric detector and produced a formazan dye.

Briefly, 50µl of standards or serum samples (diluted 1:1 with Assay Buffer) were pipetted into 96-well plate (Thermo Scientific, Germany). Afterwards, 50µl of the developer solution (Cayman) was added and plate was incubated in the dark at 25°C for 30 min. Finally, the absorbance of the formazan dye was detected at 450 nm using microplate reader Infinite 200 (Tecan). The final results were calculated according to the standard curve.

2.2.15. Statistical analysis

All data were expressed as mean ± standard error of the mean (SEM) unless mentioned otherwise. Normality of distribution was tested with the Kolmogorov-Smirnoff-test. Statistical analysis of quantitative variables was performed using the parametrical paired two-tailed Student's t-test for normally distributed samples or the non-parametrical Mann-Whitney U-test for samples without normal distribution. The Newman-Keuls Multiple Comparison Test was used for multi-group comparisons. For statistical analyses was used the software GraphPad Prism 5.

3. Results

3.1. Double transgenic human Hsp72 overexpressing mice display no obvious phenotype under basal condition

3.1.1. Generation of double transgenic human Hsp72 overexpressing mouse

To investigate importance of Hsp72 in the liver, we generated new double transgenic mice overexpressing human Hsp72 in a tissue-specific and inducible manner. A human Hsp72 construct (pcDNA5/FRT/TO V5 HSPA1A, Addgene, Plasmid 19456) was modified by three point mutations to match with the Hsp72 reference sequence (Homo sapiens heat shock protein family A (Hsp70) member 1A (HSPA1A), NM_005345.5). Additionally, a Kozak consensus sequence was added to increase the transcription efficiency (Figure 3.1 C). The modified construct was cloned into the multiple cloning site (Figure 3.1 A) of a commercially available pBI-L vector (GenBank Accession #: U89934), containing a bidirectional tet-responsive promoter (Figure 3.1 B). This tet-responsible promoter allows simultaneous expression of human Hsp72 (target gene) and firefly luciferase (reporter gene) in a doxycycline-dependent manner [129].

The vector was linearized and a portion containing amplicillin resistance and other parts not needed in the mice were cut off with XbaI. To generate transgenic human Hsp72 expressing mice, a pronuclear injection of the construct was performed. The ovi were implanted into pseudopregnant C57BL/6 females. After screening of the offsprings, two Hsp72 founder lines were obtained which displayed germline transmission of the construct. Transgenic Hsp72 overexpressing mice were crossbred with animals carrying tetracycline-responsive transactivator (tTA) under the control of the rat liver activator protein (LAP) promoter. This promotor has been shown previously to enable hepatocyte-specific expression of the target sequences [131].

To prevent the activation of Hsp72/ luciferase gene expression in embryonic and early age stage, mice received 0.1 g/L doxycycline (DOX) in drinking water during pregnancy and for 20 days after birth [129].

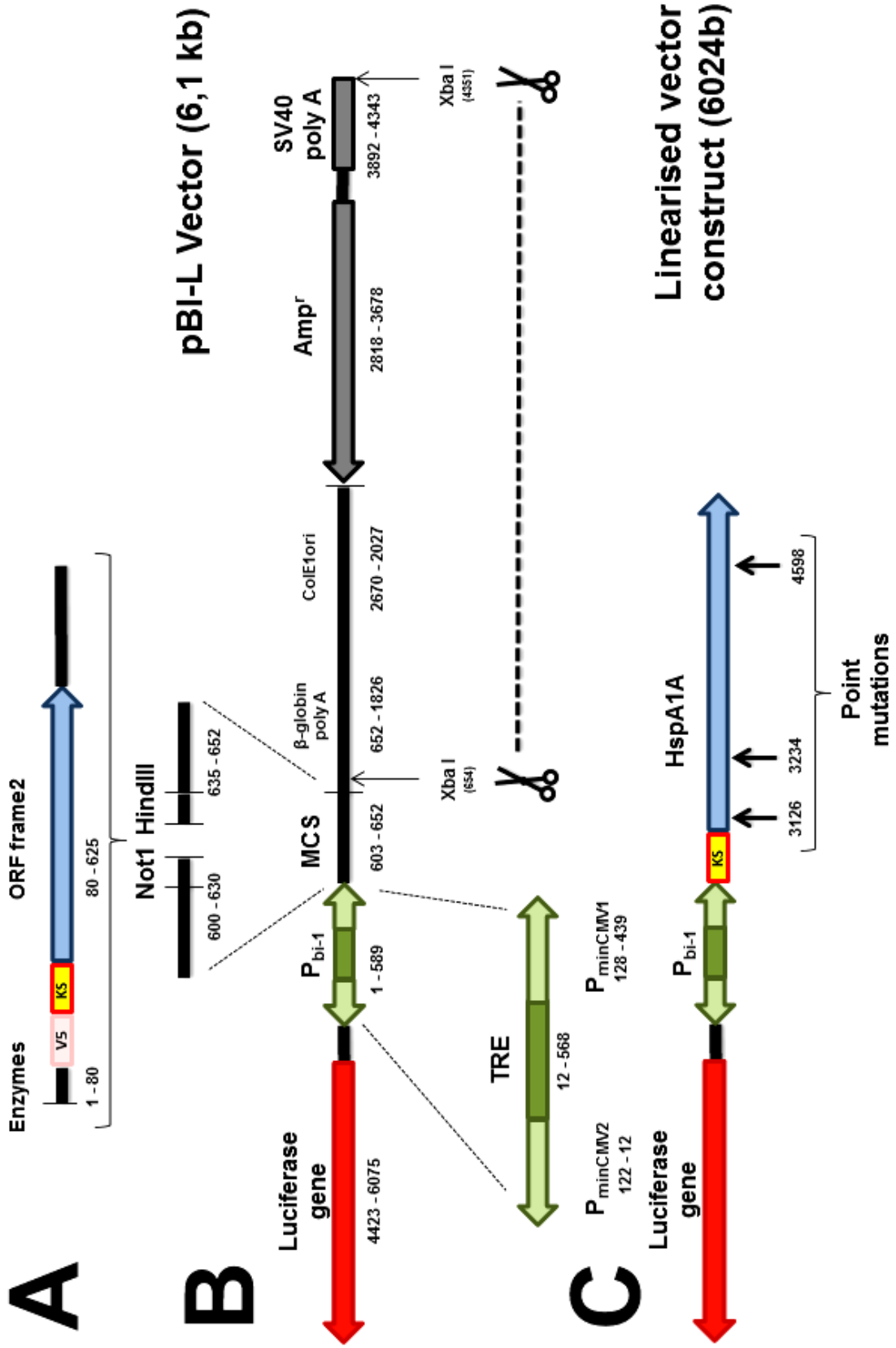
A
pcDNA5/FRT/TO V5 HSPA1A (723 bp)
Enzymes
ORF frame2
V5
KS
1 - 80
80 - 625
B
pBI-L Vector (6,1 kb)
Not1 HindIII
635 - 652
600 - 630
MCS
β-globin poly A
ColE1ori
SV40 poly A
Amp^r
603 - 652
652 - 1826
2670 - 2027
2818 - 3678
3892 - 4343
Xba I (654)
Xba I (4351)
P bi-1
1 - 589
Luciferase gene
4423 - 6075
TRE
12 - 568
P minCMV1 128 - 439
P minCMV2 122 - 12
C
Linearised vector construct (6024b)
HspA1A
KS
3126
3234
4598
Point mutations
P bi-1
Luciferase gene

Figure 3.1. Schematic presentation of constructs used for generation of double transgenic Hsp72 overexpressing mouse. To generate mice overexpressing human Hsp72, I took advantage of the following commercially available Hsp72 construct pcDNA5/FRT/TO V5 HSPA1A (Addgene, Plasmid 19456). To match it to the Hsp72 reference sequence (Homo sapiens heat shock protein family A (Hsp70) member 1A (HSPA1A), NM_005345.5), three point mutations were produced. To improve the transcription efficiency, a Kozak consensus sequence (KS) was added. The modified human HspA1A was cloned into the multiple cloning site (A) of commercial pBI-L plasmid (B). The plasmid contains a bi-directional tet-responsive promoter Pbi-1 that consists of two parts: PminCMV-2 drives the expression of a luciferase gene that serves as a reporter construct (Clontech Laboratories, GenBank AccessionNo.:U89934). PminCMV-1 regulates the production of the introduced hHsp72 construct. V5 - epitope tag for efficient detection of recombinant proteins, ORF frame2 - open reading frame, TRE, Tet-responsive element, MCS, Multiple cloning site, Col E1, origin of replication.

3.1.2. Characterization of phenotype of double transgenic Hsp72 overexpressing mice

3.1.2.1. Genotyping of transgenic mice and analysis of activity of reporter gene – luciferase in vivo and vitro

Presence of human Hsp72 or Lap-tTA genes was detected in double transgenic mice or non-transgenic animals via genotyping PCR (Figure 3. 2, A). RT-PCR demonstrated a massive overexpression of Hsp72 in double-transgenic animals kept in absence of doxycycline. Note that addition of doxycycline prevented Hsp72 overexpression and as expected, no overexpression was seen in single transgenic and non-transgenic animals (Figure 3. 2, B).

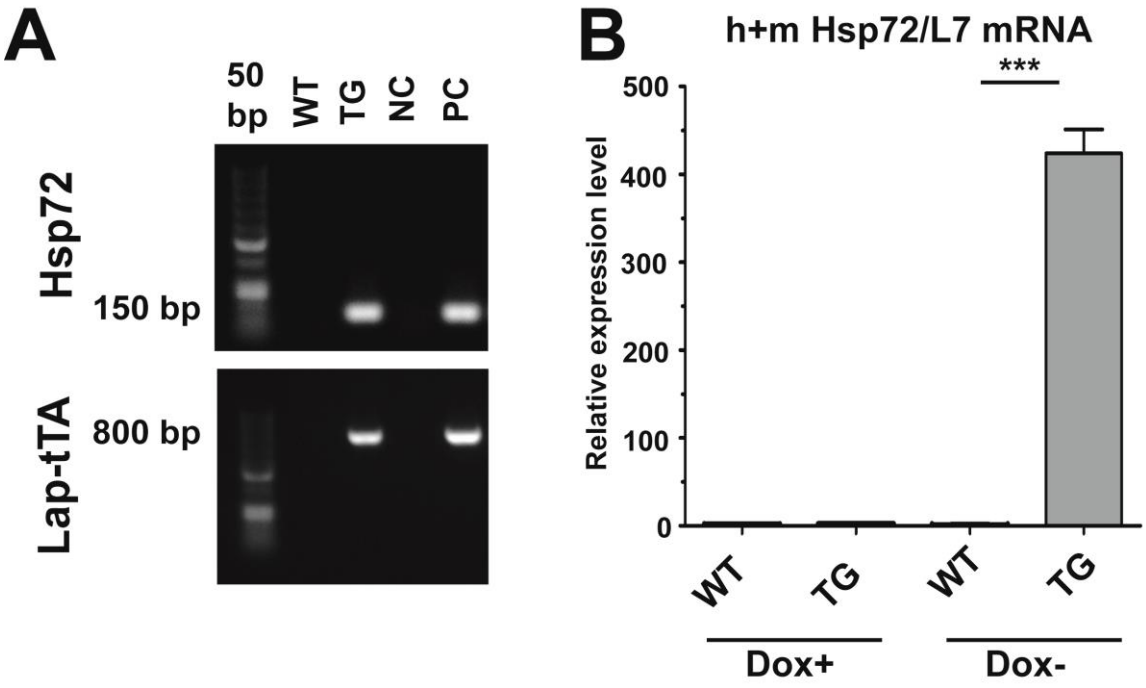

Figure 3.2. Genotyping and quantification of Hsp72 expression in hHsp72-Lap-tTA transgenic mice. Genotyping of mice via PCR (A) with primers for hHsp72 and Lap-tTA (WT – non-transgenic mouse, TG – double transgenic mouse containing both hHsp72 and Lap-tTA constructs, NC – negative control, PC – positive control). Quantification of Hsp72 expression via qRT-PCR (B) using primers that recognize both mouse (i.e. endogenous) and human (i..e. transgenic) Hsp72. L7 (mouse ribosomal protein) was used as an internal control for qRT-PCR. Result are expressed as mean ± SEM (n = 5). (+DOX) and (-DOX) describes whether or not the animals received doxycycline. Triple asterisk indicates $p < 0.005$.

A strong in vivo luciferase activity was detected in double transgenic Hsp72 overexpressing mice in absence of doxycycline, but not in another groups of the animals. The former animals showed a robust liver specific signal. On the other hand, a transgenic animal substituted with doxycycline did not show luciferase activity (Figure 3.3, A).

To analyze activity of the luciferase in vitro, we measured the luciferase activity in liver lysates from the same groups of mice (Figure 3.3, B). The data confirmed previous results in that significant activity of luciferase was observed just in double transgenic Hsp72 overexpressing mice kept without doxycycline, but not in another groups.

To confirm the observed tissue-specificity, a luciferase assay was performed on lysates from different tissues. The data showed that the transgene is

overexpressed only in the liver and not in the other tissues. Luciferase signal in liver of double transgenic animals kept without doxycycline was at least 100 times stronger than values obtained from the other tissue lysates (Figure 3.3, C).

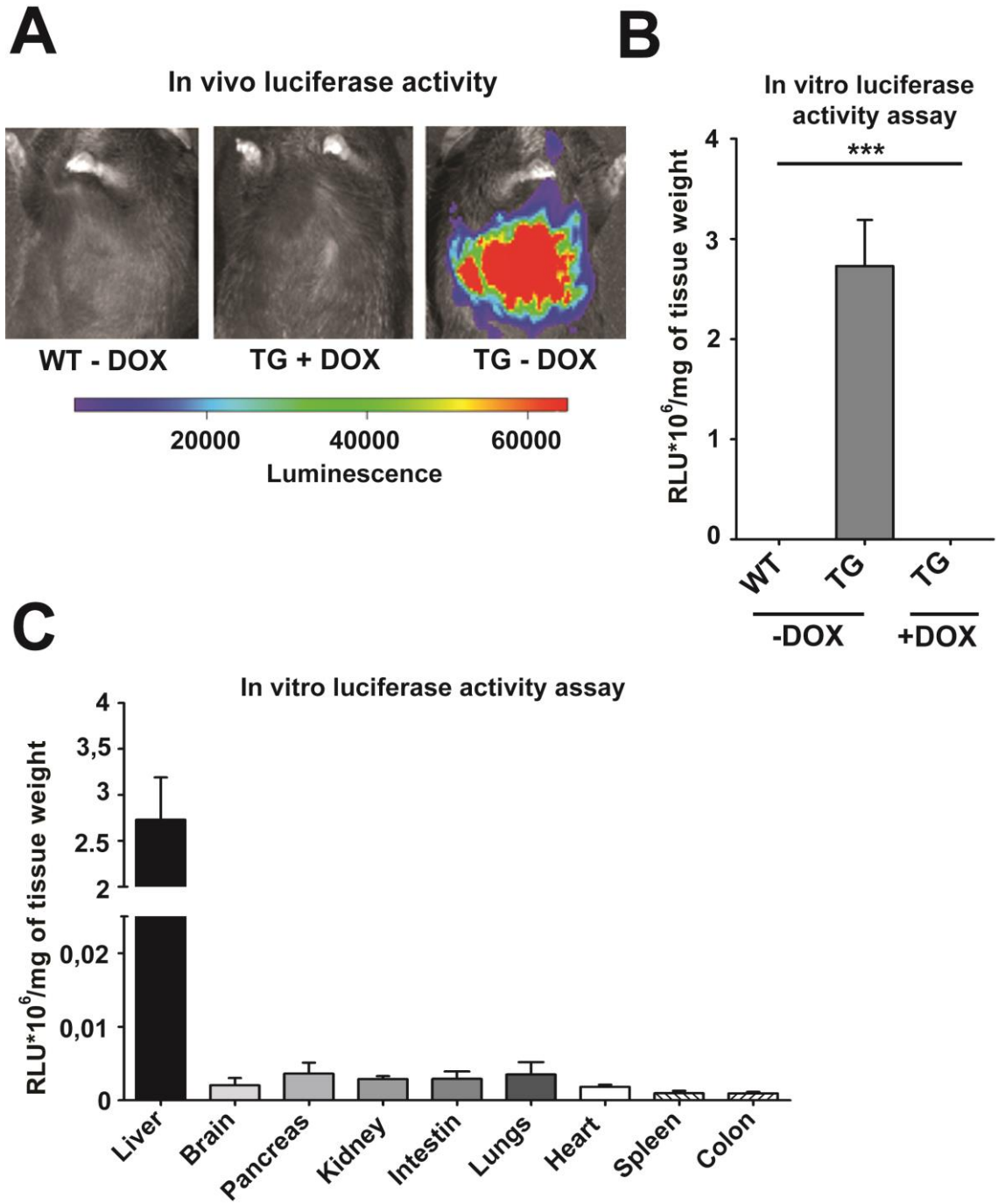

Figure 3.3. Analysis of luciferase activity in vivo (A) and in vitro (B, C). To analyze the activity of luciferase, that was introduced into the transgenic animals as a reporter construct, mice were injected with 200 uL of D-Luciferin and the resulting signal was measured via IVIS Lumina XR (Caliper). Alternatively, a luciferase assay was performed on lysates from depicted tissues. WT and TG refers to non-transgenic animals and double transgenic mice containing both hHsp72 and Lap-tTA constructs, respectively. (+DOX) and (-DOX) illustrates whether or not the animals received doxycycline. In panel C, all animals

were kept without doxycycline. Activity of luciferase was normalized to tissue weight and is given in Relative Luciferase Units (RLU). Results are expressed as mean ± SEM (n = 3). Triple asterisk indicates $p < 0.005$.

3.1.2.2. Impact of Hsp72 overexpression on other Hsp family members

To study whether the overexpression of Hsp72 may affect other Hsp family members, immunoblotting of total lysates of liver tissue was performed (Figure 3.4, A). The transgenic animals overexpressing Hsp72 showed somewhat increased Hsp90 protein levels (Figure 3.4, A, B; $p \leq 0.05$), whereas no differences in other proteins were noted. Hsp72 was detected mainly in cytoplasmic fraction, while nuclear fraction contained substantially lower, but still significant amounts (Figure 3.4, C, for details see appendix 7.4).

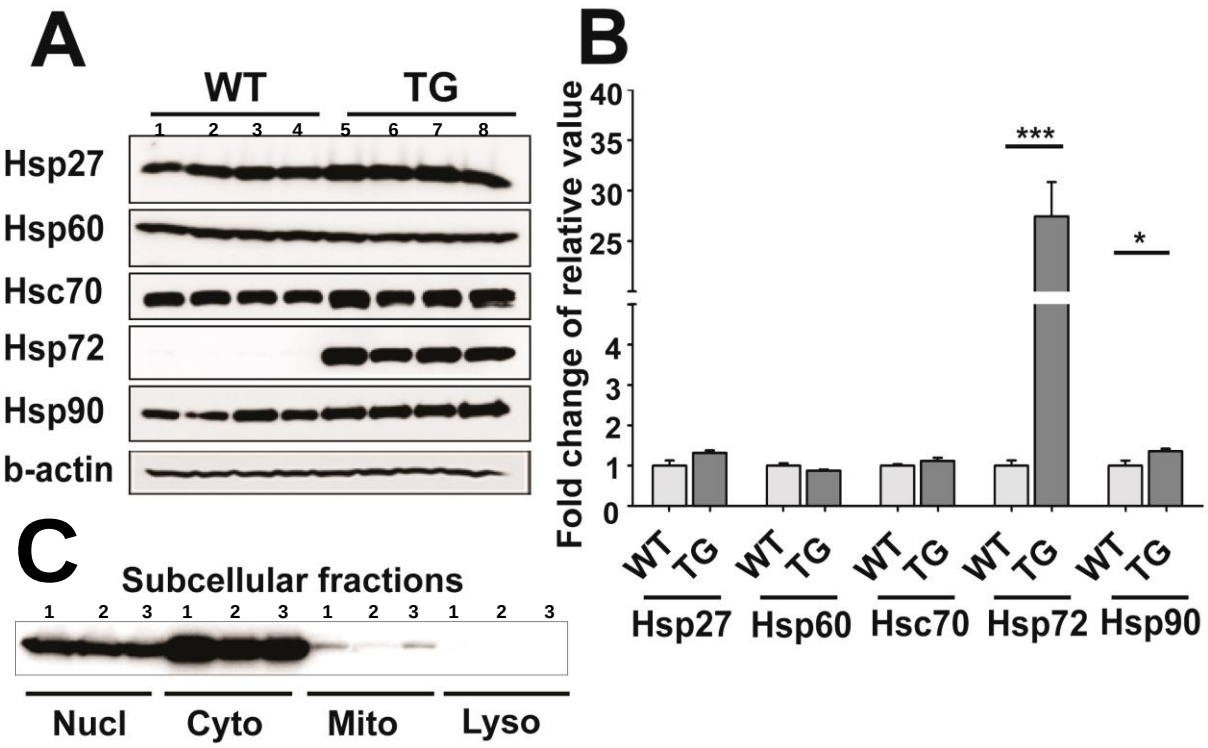

Figure 3.4. Impact of Hsp72 overexpression on other Hsp family members and amount of hHsp72 in different subcellular fractions of double transgenic animals. Amount of the highlighted Hsp family members was determined by immunoblotting (A), b-actin was used as loading control (for details of original western blot, see appendix 7.3). WT and TG refers to non-transgenic animals and double transgenic mice containing both hHsp72 and Lap-tTA constructs, respectively. The numbers 1–4 – number of non-transgenic animals, 5–8 – number of double transgenic mice. Band intensity relative to b-

actin was determined via ImageJ (B). The average protein amount in non-transgenic animals was arbitrarily set as 1 and the amounts in double transgenic mice represent a ratio. Nuclear (Nucl), cytoplasmic (Cyto), mitochondrial (Mito) and lysosomal (Lyso) extracts were obtained from liver tissues and used for quantification of hHsp72 levels in different subcompartments (1–3 – number of double transgenic mice). Asterisk and triple asterisk highlight $p < 0.05$ and $p < 0.01$, respectively.

3.1.2.3. Transgenic mice display hepatocyte-specific hHsp72 overexpression

To investigate the exact location of Hsp72 overexpression within the liver tissue, immunohistochemistry staining was performed. The results demonstrated that double transgenic animals exhibit overexpression of Hsp72 in the hepatocytes. Note that cholangiocytes, i.e. the epithelial cells lining the bile ducts, do not exhibit an increased Hsp72 signal in the double transgenic Hsp72 animals (Figure 3.5, A). The lack of cholangiocellular Hsp72 production was confirmed by qRT-PCR samples (Figure 3.5, B). Of note, mRNA expression of Hsp72 in the liver samples of double transgenic mice was approximately 400 times higher than in WT mice or TG bile duct samples ($p \leq 0.0001$).

As another method to quantify Hsp72 expression in specific cell populations, different liver cell types (Kupffer cells, hepatic stellate cells, liver sinusoidal endothelial cells and hepatocytes; Figure 3.5, C) were used. qRT-PCR showed revealed expression of Hsp72 mRNA in the hepatocytes of double transgenic animals, but not other another liver cell types ($p < 0.005$). To confirm the purity of the isolated liver cell types, qRT-PCR for cell-specifically expressed genes, i.e. mouse CD45 for Kupffer cells (Figure 3.6, A), mouse GFAP for hepatic stellate cells (Figure 3.6, B), mouse CD31 for liver sinusoidal endothelial cells (Figure 3.6, C) and mouse albumin for hepatocytes (Figure 3.6, D) was carried out.

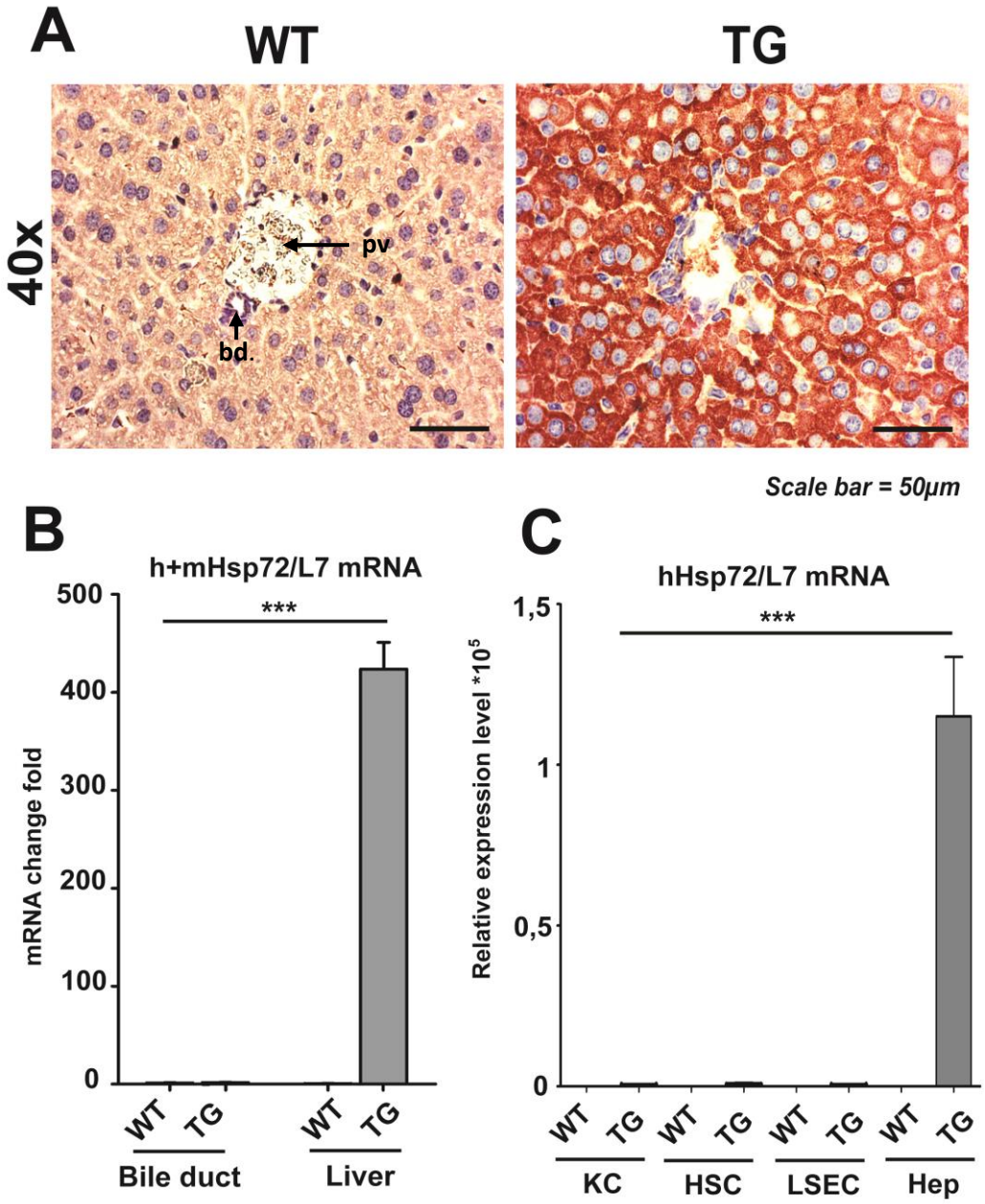

Figure 3.5. Transgenic mice display hepatocyte-specific hHsp72 overexpression. To determine the location of Hsp72 overexpression within the liver tissue, livers from non-transgenic animals (WT) and double transgenic mice containing both hHsp72 and Lap-tTA constructs (TG) were stained with mouse/human Hsp72 (SPA 812)-specific antibody (A). Transgenic mice displayed overexpression of hHsp72 in the hepatocytes, but not in the cholangiocytes, i.e. the epithelial cells lining the bile duct. To confirm the immunohistochemistry finding, a qRT-PCR was done using specific primers h+mHsp72 that recognize both mouse (i.e. endogenous) and human (i..e. transgenic) Hsp72 (B, pv – portal vein, bd – bile duct). Expression of the transgenic hHsp72 in different liver cell types (Kupffer cells (KC), hepatic stellate cells (HSC), liver sinusoidal endothelial cells (LSEC) and hepatocytes (Hep) was quantified via a qRT-PCR using human Hsp72-specific

primer. Transgenic mice demonstrated robust overexpression of hHsp72 in hepatocytes, but not other liver cell types. Results are expressed as mean ± SEM (n = 6). L7 (mouse ribosomal protein) was used as an internal control for all qRT-PCRs. Triple asterisk indicates $p < 0.005$.

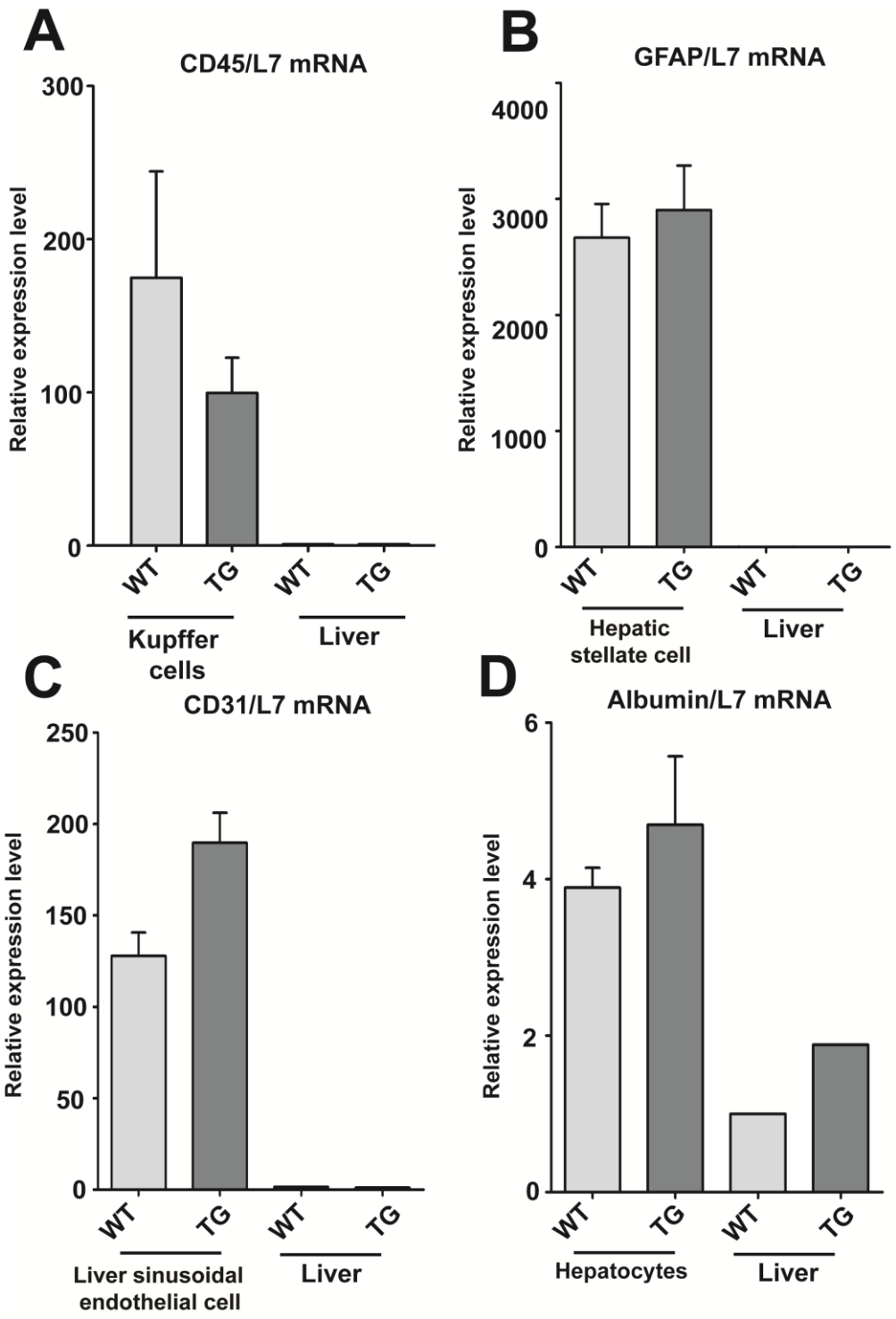

Figure 3.6. Determination of the purity of the isolated liver cell types. To confirm the purity of isolated cell types, qRT-PCR was performed with primers recognizing cell-

specifically expressed genes, i.e. mouse CD45 for Kupffer cells (A), mouse GFAP for hepatic stellate cells (B), mouse CD31 for liver sinusoidal endothelial cells (C), mouse albumin for hepatocytes (D). Results are expressed as mean ± SEM (n = 6). L7 (mouse ribosomal protein) was used as an internal control for all qRT-PCRs. Expression levels in selected cell populations was compared to the expression in whole liver extracts (liver).

3.2. Hsp72 expression is increased in patients with chronic hepatitis C and non-alcoholic steatosis

Since previous studies indicated Hsp72 overexpression in various human diseases [55, 73, 74], we analyzed Hsp72 levels in liver healthy subjects as well as in patients with NASH, ALD and HCV. NASH patients displayed an increase in the hepatocellular, cytoplasmic Hsp72 signal. H&E staining revealed an accumulation of lipid droplets and mild inflammation, whereas a mild liver fibrosis was detected by SR staining (Figure 3.7, A). qRT-PCR showed significantly increased Hsp72 levels in samples from subjects with NASH and chronic hepatitis C infection (HCV) compared to controls ($p < 0.01$, Figure 3.7, B), while alcoholic liver disease (ALD) patients did not have significantly elevated Hsp72.

To investigate the impact of hepatic inflammation/fibrosis on Hsp72 expression, mRNA levels were compared in patients with minimal, mild and moderate inflammation (Figure 3.7, C) or with minimal, mild, moderate and advanced fibrosis (Figure 3.7, D). Hsp72 mRNA expression was significantly higher in samples with moderate versus minimal or mild inflammation grade ($p < 0.01$) whereas no obvious changes were seen between mild and moderate inflammation grade. Moreover, no significant difference was detected in samples with different stage of fibrosis.

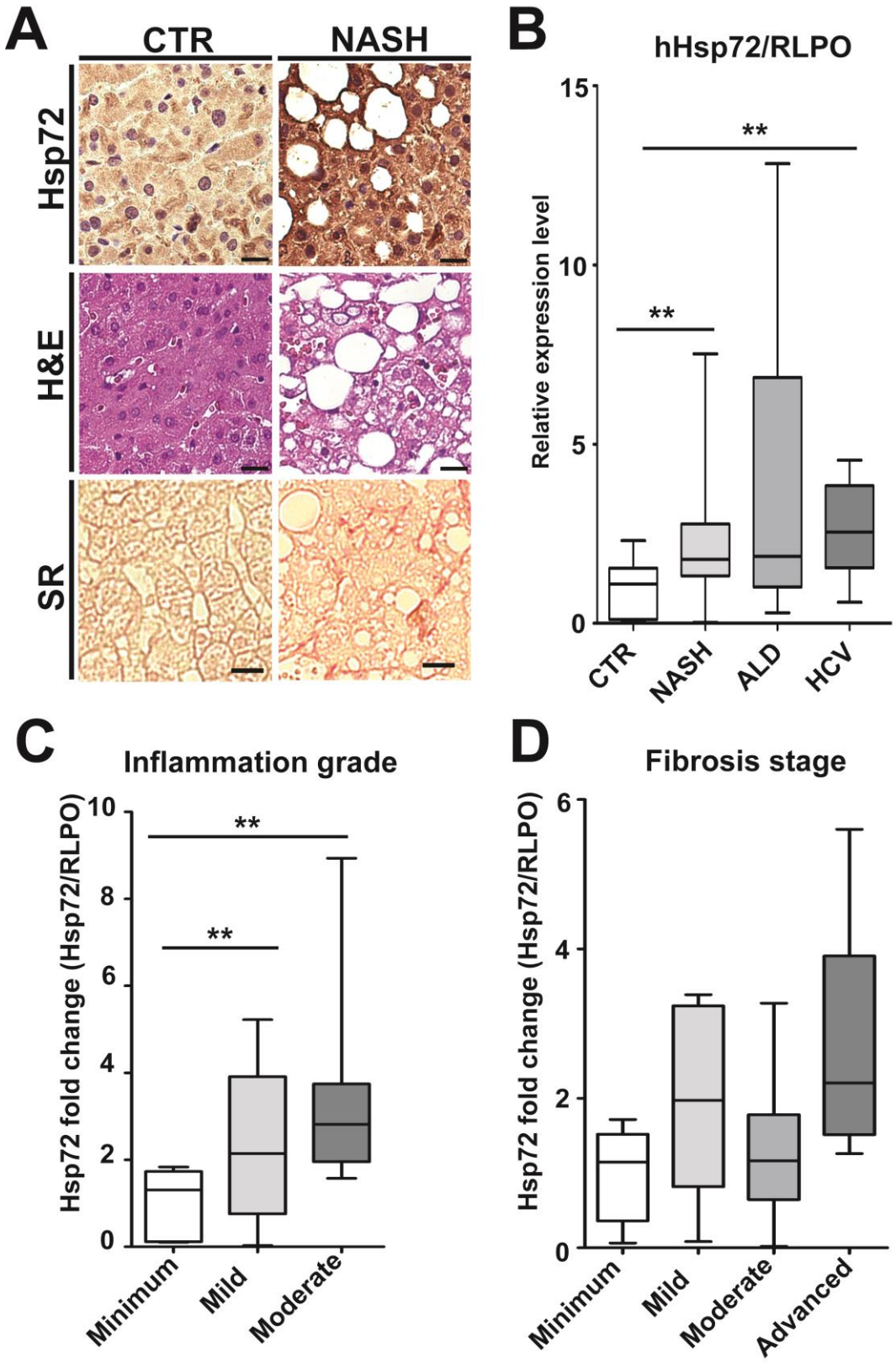

Figure 3.7. Hsp72 expression is increased in patients with chronic hepatitis C and non-alcoholic steatosis. To analyze the expression of Hsp72 in patients with non-alcoholic steatohepatitis (NASH), liver biopsy samples from these subjects as well as histologically normal specimen (CTR) were stained with human Hsp72 (SPA 812) antibody. (A). For determination of inflammation grade and fibrosis stage, livers were stained by H&E

(Hematoxylin and Eosin Stain) and SR (Sirius Red stain), respectively. Human Hsp72 (B) mRNA levels were determined in patients with non-alcoholic steatohepatitis (NASH), alcoholic liver disease (ALD), chronic hepatitis C infection (HCV) and in control samples (CTRL). To study whether hepatic inflammation or hepatic fibrosis affect expression of Hsp72, mRNA levels were compared in patients with minimal, mild and moderate inflammation (C) or with minimal, mild, moderate and advanced fibrosis (D). Human RPLPO (large ribosomal protein) gene was used as an internal control. Data are shown as Whisker box plots. Vertical lines in the box indicate medians, first and third percentile, whiskers depict maximum and minimum non-outlier observations. Double asterisk indicates $p < 0.01$.

3.3. Hsp72 overexpression protects from APAP-induced liver injury

3.3.1. 18h after acetaminophen injection, double transgenic mice displayed lower alanine transaminase levels than non-transgenic animals

To investigate effect of Hsp72 overexpression on acetaminophen toxicity, mice were exposed with an overdose of acetaminophen (800 mg/kg mouse). As expected, both groups of untreated animals (double transgenic and non-transgenic mice) had normal liver enzyme levels under basal condition on the one hand. On the other hand, a moderate elevation of liver enzymes was seen 4h after APAP exposure, but no significant difference was detected between groups. 18h after APAP administration, double transgenic mice showed significantly lower ALT levels compared to non-transgenic animals ($p<0.01$) thereby suggesting that Hsp72 overexpression protects from APAP-induced liver toxicity.

Parameter	Genotype	ALT, U/L	AST, U/L
Control	**WT**	41.00 (± 5.3), N=5	71.00 (± 17.9), N=5
	TG	43.64 (± 5.2), N=11	75.83 (± 14.5), N=6
APAP 4h	**WT**	409 (± 70.1), N=12	1315 (± 129.0), N=14
	TG	353 (± 75.1), N=12	1301 (± 161.7), N=12
APAP 18h	**WT**	1976 (± 499), N=11	1957 (± 293.5), N=11
	TG	933 (± 262)**, N=12	1859 (± 331.4), N=9

Alanine transaminase (ALT), Aspartate transaminase (AST). Acetaminophen treatment for 4h (APAP 4h), Acetaminophen treatment for 18h (APAP 18h). WT and TG refers to non-transgenic animals and double transgenic mice containing both hHsp72 and Lap-tTA constructs. Data are expressed as mean ± SEM, double asterisk indicates $p < 0.01$ (compared to WT mice on the same treatment).

Table 3.1. 18h after acetaminophen injection, double transgenic mice displayed lower alanine transaminase levels than non-transgenic animals.

3.3.2. Hsp72 overexpression protects from APAP-induced liver injury

To investigate the liver injury and tissue damage after APAP exposure; H&E staining was done. Histological examination did not reveal an apparent liver injury or inflammation in untreated animals. Four hours after APAP injection, hepatocyte swelling was seen but no significant differences among genotypes were noted. However, 18h after administration (Figure 3.8), non-transgenic mice exhibited more extended necrotic areas and infiltration of macrophages that leads to higher inflammation level.

These data are in line with liver enzymes and suggest that Hsp72 overexpression protect from APAP-induced liver injury.

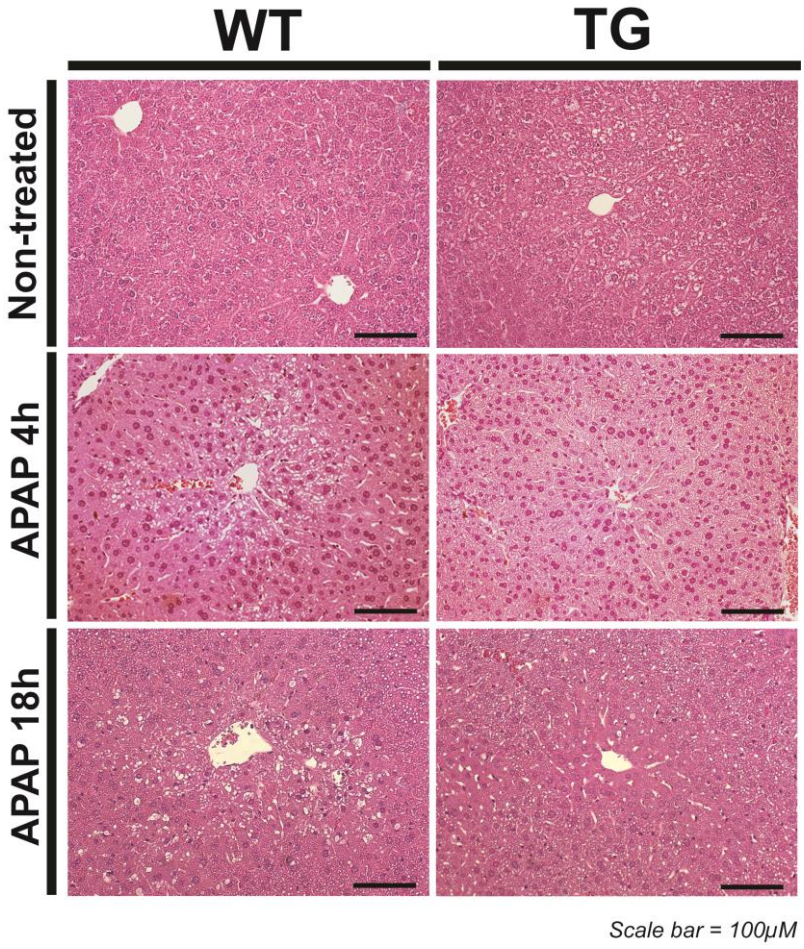

Figure 3.8. Hsp72 overexpression protects from APAP-induced liver injury. HE staining of liver samples showed that double transgenic Hsp72 overexpressing mice (TG) display a decreased inflammation and liver injury than non-transgenic animals (WT) 18h after acetaminophen administration (APAP 18h). No significant differences in liver injury were observed 4 hours after acetaminophen injection (APAP 4h). In non-treated animals regardless their genotype, no obvious liver injury was detected. Scale bar=100μm.

3.3.3. Hsp72 overexpression increases clearance of APAP, but does not affect the levels of APAP-metabolizing enzymes

To test whether Hsp72 overexpression affects the APAP-metabolism we examined mRNA expression of APAP metabolism related genes. The results showed that the genes responsible for APAP metabolism were altered in animals neither under basal condition nor under APAP administration (Table 3.2). 4h after APAP exposure both groups of animals showed depleted GSH level, however no significant difference between them was seen (Figure 3.9, A). Furthermore, as expected, the ratio between GSSG and the reduced GSH was increased after APAP-exposure, however, no significant difference was detected between the groups (Figure 3.9, B).

In order to investigate the impact of Hsp72 overexpression on APAP accumulation, we measured levels of APAP in the serum (Figure 3.10, A). Four hours after APAP administration, double transgenic mice showed significant lower amount of APAP in the serum than non-transgenic animals ($p < 0.05$). To test whether CYP2E1 may have changed after APAP exposure, I performed immunoblotting. The results showed that the level of protein was altered in both groups of animals neither under basal condition nor after APAP treatment (Figure 3.10, B).

In conclusion, my results demonstrate that Hsp72 overexpression increases the clearance of APAP, but does not affect the expression of major APAP-metabolising genes.

Genes	Fold changes, TG/WT		Function of genes
	Basal condition	After APAP 4h treatment	
Cyp2e1	1.01	1.05	Cytochromes catalyzing the transformation of acetaminophen to the reactive metabolite NAPQI.
Cyp1a2	1.10	0.97	
Cyp3a11	1.04	0.90	
Cyp2b10	1.12	0.09	
Ugt1a1	1.25	2.92	Enzymes involved in glucuronidation of acetaminophen that increases its solubility in the water.
Ugt1a6	1.10	0.78	
Sult1a1	0.59	0.73	Enzymes involved in sulfation pathway that make acetaminophen more polar and prone to degradation.
Gst1	1.01	1.05	Enzyme catalyzing conjugation of NAPQI to GSH.

Cytochrome P450 family 2 subfamily E member 1 (Cyp2E1), cytochrome P450 family 1 subfamily A member 2 (Cyp1a2), cytochrome P450, family 3, subfamily a, polypeptide 11 (Cyp3a11), cytochrome P450, family 2, subfamily b, polypeptide 10 (Cyp2b10), UDP glucuronosyltransferase 1 family, polypeptide A1 (Ugt1a1), UDP glucuronosyltransfe-rase 1 family, polypeptide A6 (Ugt1a6), sulfotransferase family 1A member 1 (Sult1a1), glutathione S-transferase (Gst1), N-acetyl-p-benzoquinone imine (NAPQI), Glutathione (GSH). L7 (mouse ribosomal protein) was used as an internal control for all qRT-PCRs.

Table 3.2. Expression of genes involved in APAP metabolism.

No significant difference between double transgenic mice overexpressing hHsp72 (TG) and non-transgenic animals (WT) was observed- neither under basal condition nor after 4h acetaminophen administration (APAP 4h).

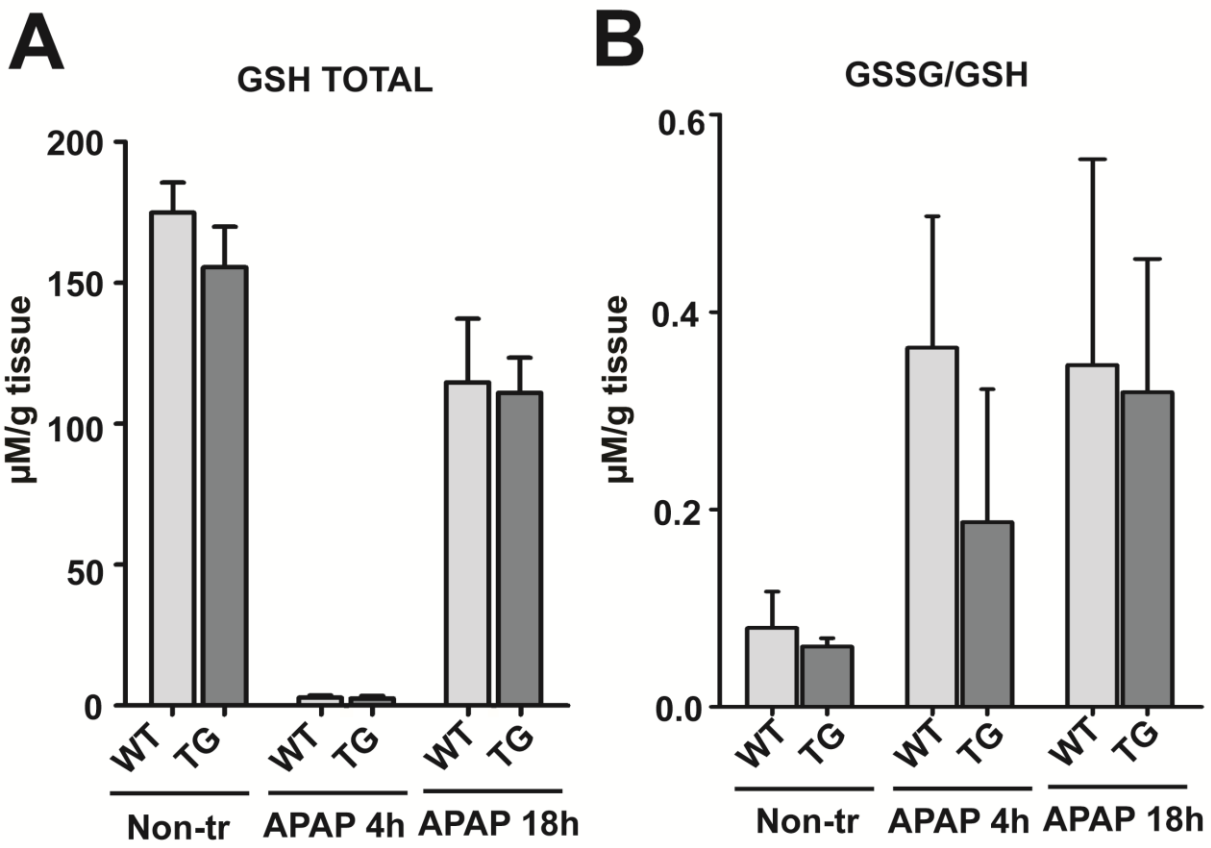

Figure 3.9. Transgenic and non-transgenic mice displayed similar levels of glutathione after APAP treatment. Total glutathione (GSH) was decreased 4 and 18 hours after acetaminophen administration (A). The ratio between oxidized and reduced glutathione (GSSG/GSH) was increased indicating oxidative stress. No significant difference was found between double transgenic Hsp72 overexpressing mice (TG) and non-transgenic mice (WT) in both assays. Results are expressed as mean ± SEM (n = 5).

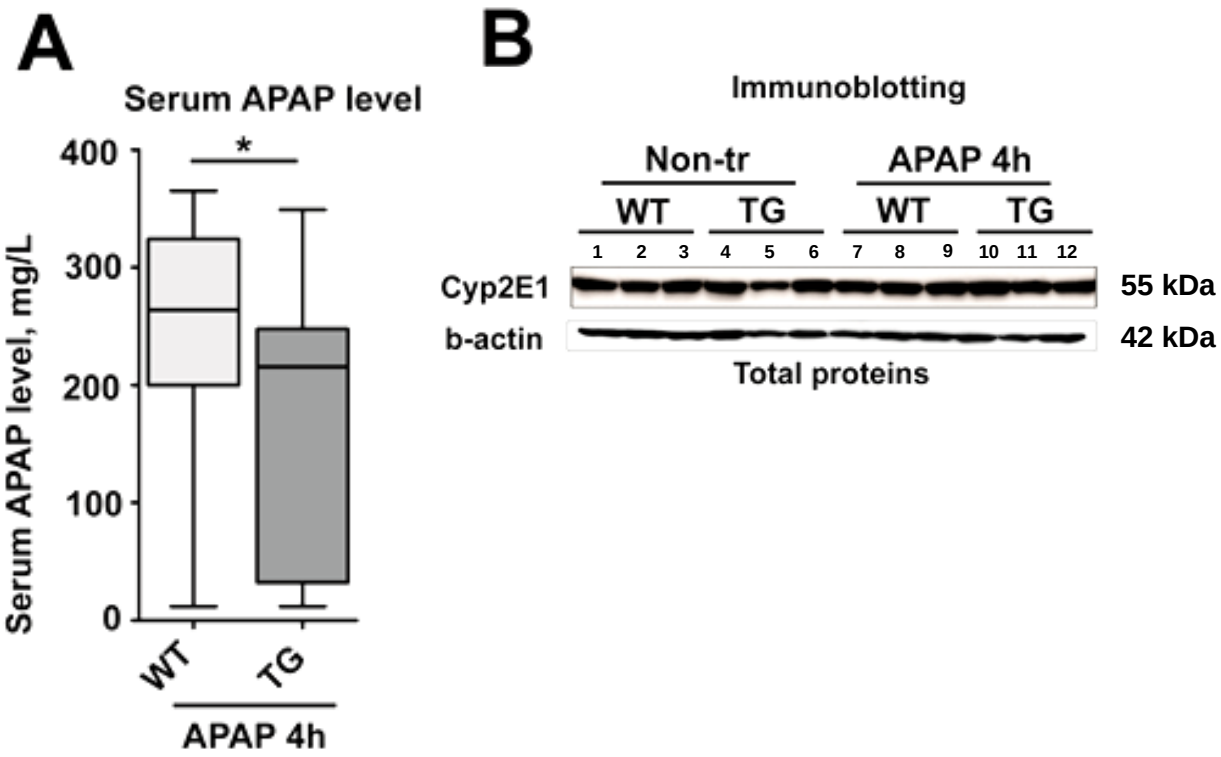

Figure 3.10. Hsp72 overexpression increases clearance of APAP, but does not affect the levels of APAP metabolizing genes. To analyze the effect of Hsp72 overexpression on acetaminophen (APAP) metabolism, APAP serum levels were measured. Double transgenic Hsp72 overexpressing mice (TG) showed lower APAP levels than non-transgenic animals (WT) 4h after acetaminophen administration (APAP 4h) (A). As an important enzyme catalyzing oxidation of acetaminophen, Cytochrome P450 2E1 (Cyp2E1) were quantified by immunoblotting (B, for details of original western blot, see appendix 7.3). The numbers 1 – 3 – numbers of non-treated non-transgenic animals, 4 – 6 – numbers of non-treated double transgenic animals, 7 – 9 – numbers of non-transgenic and 10 – 12 – numbers of double transgenic mice, treated with APAP for 4 hours. Data are showed as Whisker box plots. Vertical lines in the box indicate medians, first and third percentile, whiskers depict maximum and minimum non-outlier observations. At least 5 mice were used per group. b-actin were used as a loading control for immunoblotting. Asterisk highlights $p < 0.05$.

3.3.4. Hsp72 overexpression attenuates APAP-induced hepatic IL6 expression

To study the impact of Hsp72 overexpression on APAP-induced hepatic inflammation, I measured plasma levels of proinflammatory cytokines IL-6 (Figure

3.11, A) and TNF-a (Figure 3.11, B). Plasma levels of both cytokines were elevated in APAP-treated compared to untreated animals, but no significant difference was observed between the treated groups.

To test whether the overexpression of Hsp72 may affect expression IL6 at mRNA level, I performed RT-PCR (Figure 3.11, C). Compared to non-transgenic mice, animals overexpressing Hsp72 showed significantly lower IL6 mRNA level four hours after APAP exposure ($p < 0.05$).

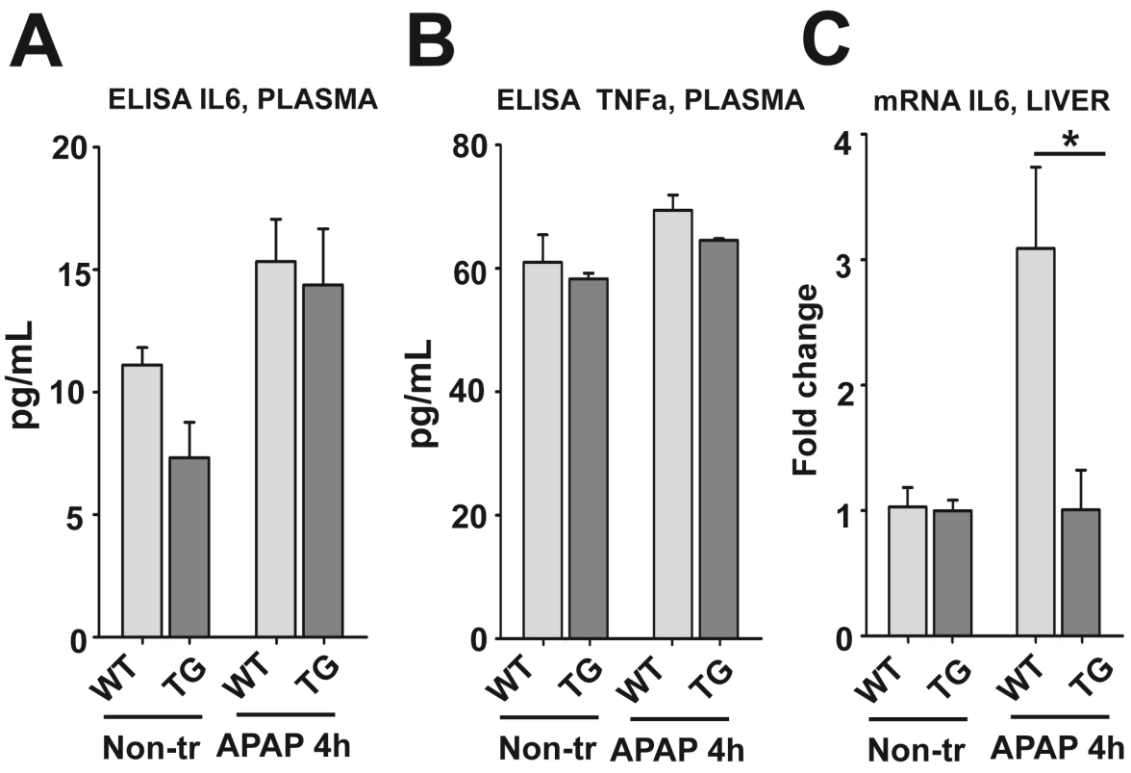

Figure 3.11. Hsp72 overexpression results in lower hepatic IL6 expression after the exposure to acetaminophen. Plasma levels of IL6 (A) and TNF-a (B) were determined in non-treated animals (Non-tr) and in animals treated with acetaminophen for 4 hours (APAP 4h). No significant difference in plasma cytokine levels were seen-neither before and after APAP administration nor between double transgenic Hsp72 overexpressing mice (TG) and non-transgenic mice (WT). IL6 mRNA expression (C) was significantly lower in the liver of APAP-treated double transgenic mice compared to APAP-exposed WT mice. Data are expressed as mean ± SEM, asterisk indicates $p < 0.05$.

3.3.5. Transgenic Hsp72 mice display elevated Hsp72 levels during the entire course of APAP treatment

To investigate whether APAP exposure changes the expression level of Hsp72, immunoblotting was performed (Figure 3.12.). In non-transgenic animals, Hsp72 levels decreased both 4 and 18 hours after APAP exposure, whereas only minimally altered levels were seen in double-transgenic mice. As a result, at all tested time points, double transgenic animals displayed significantly higher Hsp72 levels than non-transgenic mice.

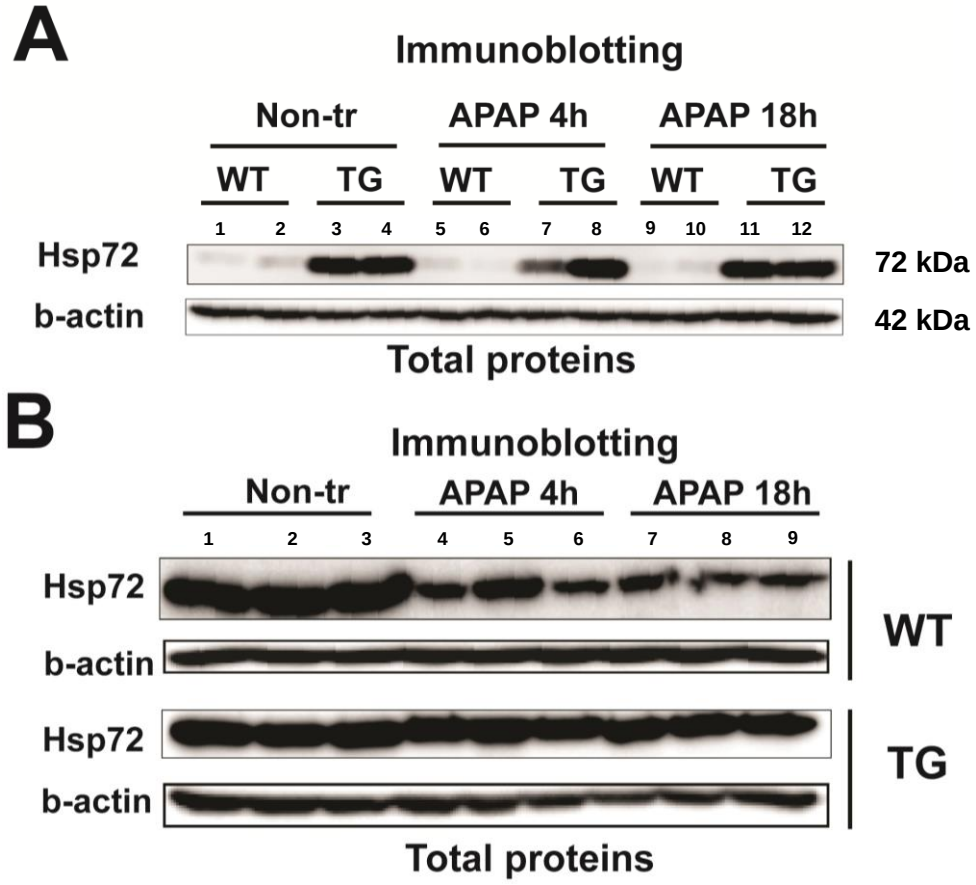

Figure 3.12. Transgenic Hsp72 mice display elevated Hsp72 levels during the entire course of APAP treatment. To test whether expression level of Hsp72 will change during the course of APAP treatment, Hsp72 protein amount was quantified by immunoblotting (A). The numbers 1-2, 5-6, 9-10 – numbers of non-transgenic animals and 3-4, 7-8, 11-12 – numbers of double transgenic animals, non-treated, 4h and 18h after APAP exposure, respectively. Note that Hsp72 amount decreased 4h (APAP 4h) and 18 h (APAP 18h) after acetaminophen administration in both double transgenic (TG) and non-transgenic (WT) animals, compared to non-treated mice (Non-tr). 1-3, 4-6, 7-8 – numbers of animals WT or TG, non-treated, 4h and 18h after APAP administration, respectively. b-actin was used as a loading control for immunoblotting (for details of original western blot, see appendix 7.3).

3.3.6. Overexpression of Hsp72 protects from formation of APAP protein adducts and from JNK hyperphosphorylation

Given that Hsp72 may affect activation of MAPK-kinase pathway [53, 54], JNK activity was quantified by immunoblotting. Total amount of JNK (JNK1 and JNK2) was neither significantly altered between non-transgenic and double-transgenic animals, nor did I see changes after APAP exposure. Among non-treated animals of both genotypes, similar levels of phosphorylated JNK (p-JNK) were detected. However, the APAP-induced JNK hyperphosphorylation seen in non-transgenic animals was significantly attenuated in double transgenic mice (Figure 3.13, A).

Furthermore, to test whether overexpression of Hsp72 affects the formation of APAP-protein adducts, I measured them in the liver tissue after APAP-exposure (Figure 3.13, B). Results showed that double transgenic mice displayed significantly lower amount of the APAP-protein adducts 18h after APAP administration ($p < 0.01$) whereas only a non-significant trend in the same direction was seen after 4 hours.

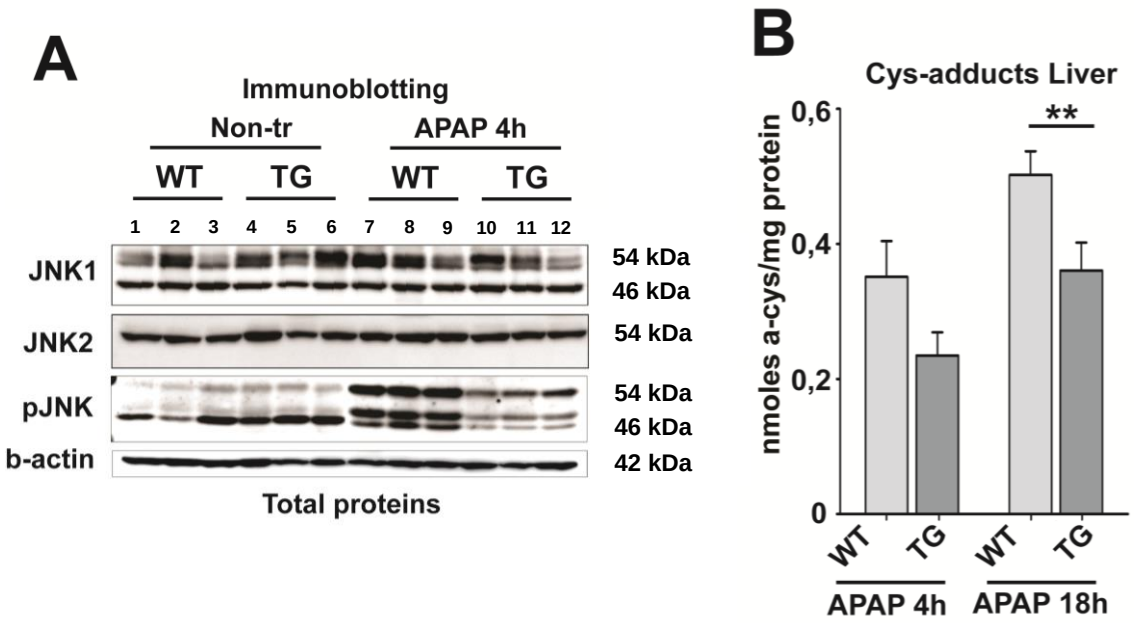

Figure 3.13. Overexpression of Hsp72 protected from formation of APAP protein adducts and from JNK hyperphosphorylation. To analyze the mechanism of protection of double-transgenic Hsp72-overexpressing mice from APAP-induced liver damage, amount of total C-Jun N-Terminal Kinase (JNK1 and JNK2) and its phosphorylated isoform (p-JNK) was examined by immunoblotting prior to (Non-tr) and 4h after acetaminophen exposure (A). A marked pJNK upregulation was seen in non-transgenic (WT) but not double transgenic mice (TG) exposed to APAP. The numbers 1-3, 7-9 – numbers of

WT mice, 4-6, 10-12 – numbers of TG mice, non-treated, or 4h after APAP treatment, respectively. b-actin was used as a loading control (B, for details of original western blot, see appendix 7.3). In addition, amount of APAP-protein adducts (Cys-adducts) was quantified in mouse livers 4h and 18h after acetaminophen exposure (APAP 4h and 18h, respectively). 18h after APAP-administration, APAP-adducts were significantly lower in double transgenic animals compared to non-transgenic mice. The quantification of amount of APAP-adducts was done in Prof. Laura James Lab. (Pediatric Pharmacology and Toxicology, AR-USA). Data are expressed as mean ± SEM, double asterisk indicates $p < 0.01$.

3.4. Hsp72 overexpression protects from MCD-induced liver injury

3.4.1. After 8 weeks of MCD diet, double transgenic mice displayed lower alanine and aspartate transaminase levels than non-transgenic animals

To investigate the effect of Hsp72 overexpression on lipotoxic injury, mice were subjected to a treatment with a methionine choline-deficient (MCD) or were kept on standard diet for 8 weeks. As expected, both double transgenic and non-transgenic mice fed standard diet had normal liver enzyme levels. After 8 weeks of MCD diet, both genotypes displayed elevated AST and ALT levels, however both parameters were significantly lower in double transgenic animals ($p<0.01$ and $p < 0.05$, respectively) thereby suggesting that Hsp72 overexpression protects from MCD-induced liver toxicity.

Parameter	Genotype	ALT, U/L	AST, U/L
Control	**WT**	41.00 (± 5.3), N=5	71.00 (± 17.9), N=5
	TG	43.64 (± 5.12), N=11	75.83 (± 14.5), N=6
MCD 8w	**WT**	283.3 (± 47.2), N=20	293.1 (± 45.52), N=18
	TG	157.9 ± (31.9)*, N=17	206.2 (± 25.85)**, N=17

Alanine transaminase (ALT), Aspartate transaminase (AST), Methionine Choline-Deficient diet (MCD), WT and TG refers to non-transgenic animals and double transgenic mice containing both hHsp72 and Lap-tTA constructs. Data are expressed as mean ± SEM. Asterisk and double asterisk highlight $p < 0.05$ and $p < 0.01$, respectively (compared to WT mice on the same treatment).

Table 3.3. After 8 weeks of MCD diet, double transgenic mice displayed lower alanine and aspartate transaminase levels than non-transgenic animals.

3.4.2. Hsp72 overexpression protects from MCD-induced liver injury

In order to characterize liver injury and tissue damage in double transgenic and non-transgenic mice, H&E staining was performed. Both groups of non-treated animals did not show obvious pathological changes in the liver. After feeding with MCD diet, both genotypes developed steatohepatitis-like changes. Interestingly, non-transgenic mice displayed higher level of lobular inflammation and infiltration with macrophages that, (Figure 3.14, A) was confirmed by morphometric analysis ($p < 0.05$) (Figure 3.14, B).

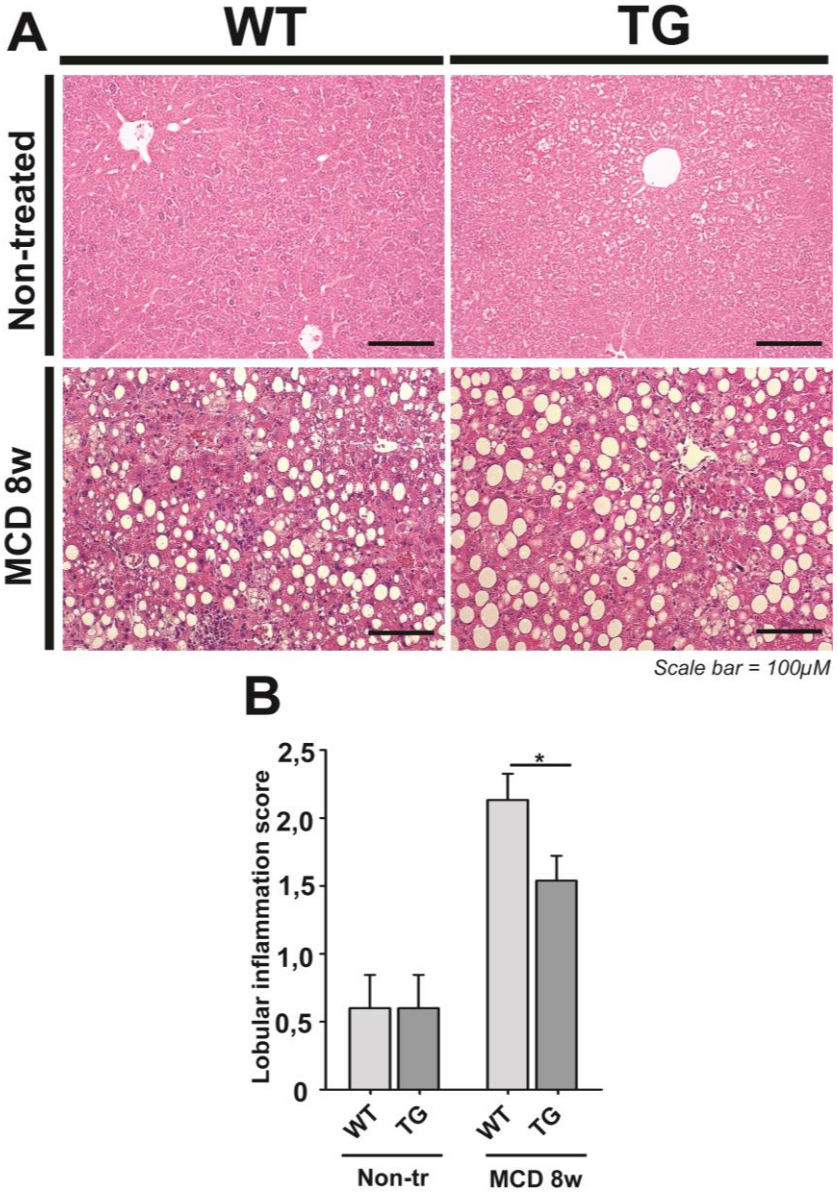

Figure 3.14. Hsp72 overexpression protects from MCD-induced liver injury. HE staining of liver samples showed that double transgenic Hsp72 overexpressing mice (TG)

display a decreased inflammation and liver injury than non-transgenic animals (WT) 8 weeks after feeding with a methionine choline-deficient (MCD) diet (A). In non-treated animals regardless their genotype, no obvious liver injury was detected. Lower level of lobular inflammation was confirmed by morphometric quantification of liver samples (B). The morphological quantification was done by an experienced pathologist (Assoz. Prof. Johannes Haybäck, Institute of Pathology, Medical University Graz, Austria). Results are shown as mean ± SEM. Asterisk highlights $p < 0.05$. Scale bar=100µm.

3.4.3. Hsp72 overexpression does not alter lipid accumulation induced via feeding with MCD diet

To test whether overexpression of Hsp72 affects lipid accumulation induced by MCD diet, I performed Oil-Red staining. Lipid deposition was strongly increased in both genotypes after 8 weeks of MCD diet (Figure 3.15, A). However, morphometric quantification showed no significant differences between the MCD-fed groups (Figure 3.15, B)**.**

To quantify the extent of lipid accumulation in the liver tissue, amount of triglycerides, free fatty acids, ceramides, phosphatidylcholine (PC) and phosphatidylethanolamine (PE) was determined via thin-layer chromatography (TLC). The results showed that both groups of mice experienced an accumulation of triglycerides (Figure 3.16, A), free fatty acids (Figure 3.16, B) and ceramides (Figure 3.16, C) in the liver after feeding with MCD diet, however no significant differences were found between the groups. The ratio between phosphatidylcholine and phosphatidylethanolamine levels was decreased in double transgenic mice as well as non-treated animals fed with MCD diet, but no significant difference was observed between the groups (Figure 3.16, D).

Subsequently, to evaluate whether the overexpression of Hsp72 affects serum concentration of triglycerides or beta-Hydroxybutyric acid (b-HB), serum analysis was performed. As reported previously, feeding with MCD diet decreased amount of triglycerides in the serum, whereas no alterations in b-HB were noted. For both parameters, no significant differences were noted between the genotypes-both prior to and after APAP exposure (Figure 3.16, E, F). Collectively, these data suggest that Hsp72 overexpression does not alter the process of lipid accumulation induced via feeding with MCD diet.

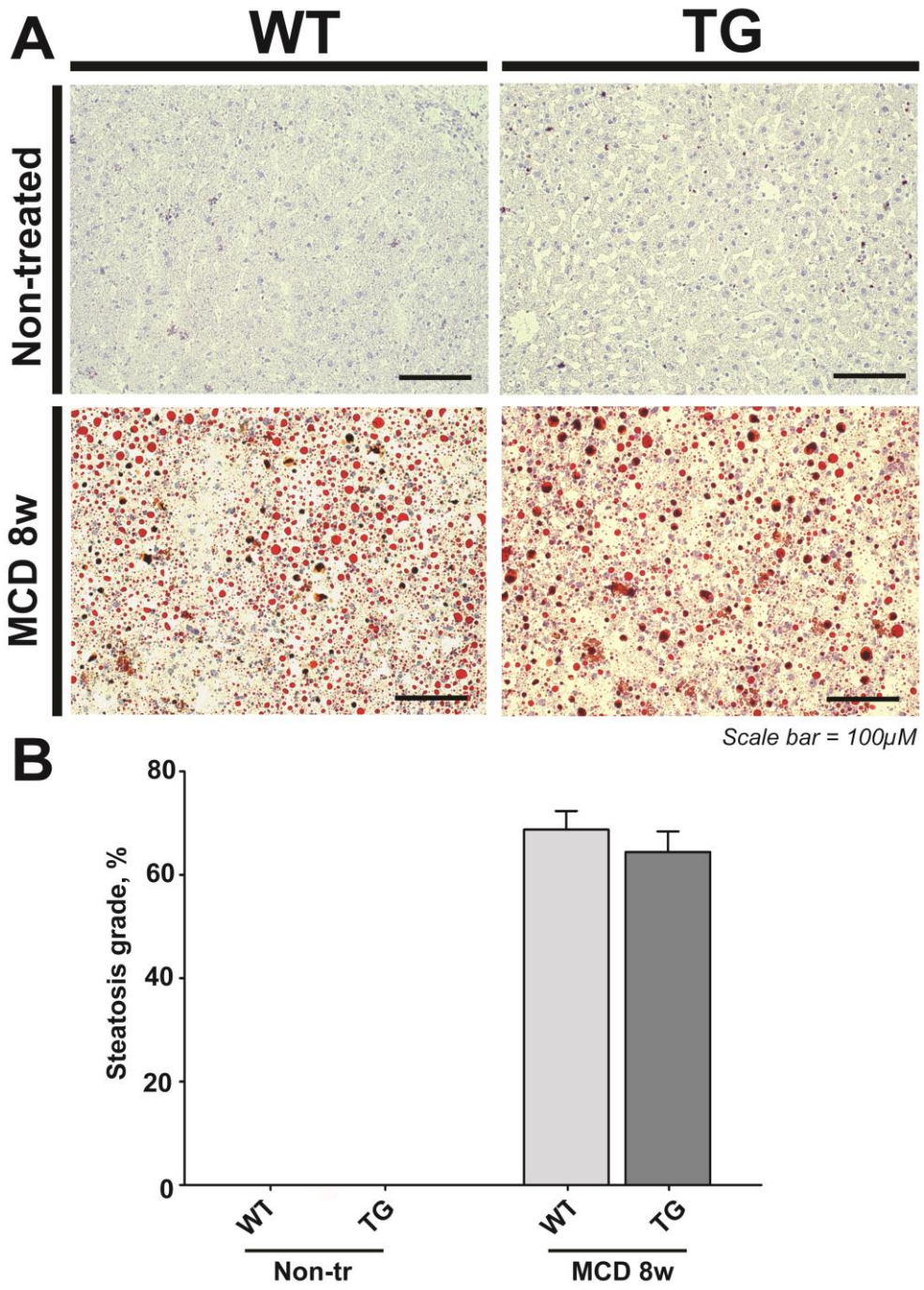

Figure 3.15. Hsp72 overexpression does not alter lipid accumulation induced via feeding with MCD diet. To quantify the extent of liver steatosis, samples from double transgenic overexpressing (TG) as well non-transgenic animals were stained with Oil-Red (A) and subjected to semi-quantitative grading (B). After 8 weeks of feeding with methionine choline-deficient (MCD) diet, an accumulation of lipid droplets was observed. However morphometric analysis showed no significant differences between the MCD-fed groups. Results are expressed as mean ± SEM, at least 7mice per group were analyzed.

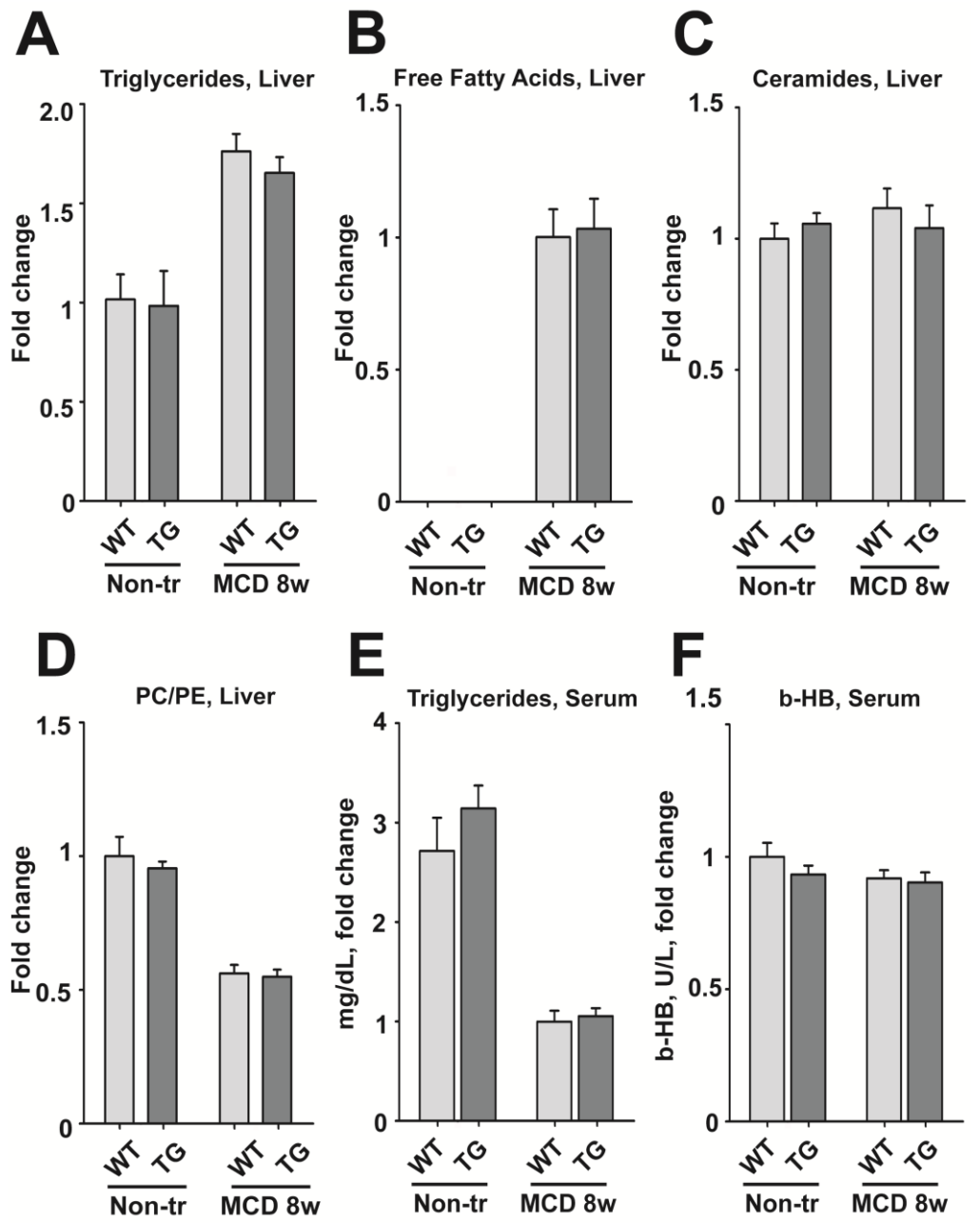

Figure 3.16. Hsp72 overexpression does affect basic parameters of lipid metabolism. The amount of triglycerides (A), free fatty acids (B), ceramides (C), phosphatidylcholine (PC) and phosphatidylethanolamine (PE) in the liver was quantified via thin-layer chromatography (TLC) in the Prof. A. K. Kiemer Lab by Dr. Sonja M. Keßler (Department of Pharmacy, Pharmaceutical Biology, Saarland University, Saarbrücken, Germany). PC/PE (D) refers to a ratio between phosphatidylcholine and phosphatidylethanolamine levels. Serum analysis was performed to test whether Hsp72 overexpression affects concentration of triglycerides (E) or beta-Hydroxybutyric acid (b-HB) (F). No significant difference was found between double transgenic overexpressing Hsp72 mice (TG) and non-transgenic animals (WT) on basal condition or after 8 weeks of MCD diet in all assays. Data are expressed as mean ± SEM, at least 5 mice per group were used.

3.4.4. Transgenic Hsp72 mice display elevated Hsp72 levels both before and after feeding with MCD

To test whether MCD feeding affects the expression level of Hsp72 an immunoblotting was done. After the exposure to MCD, both groups of mice displayed decreased level of Hsp72 compared to non-treated situation (Figure 3.17, A). However, both before and after treatment, double transgenic mice showed elevated expression level of Hsp72 compared to non-transgenic mice (Figure 3.17, B).

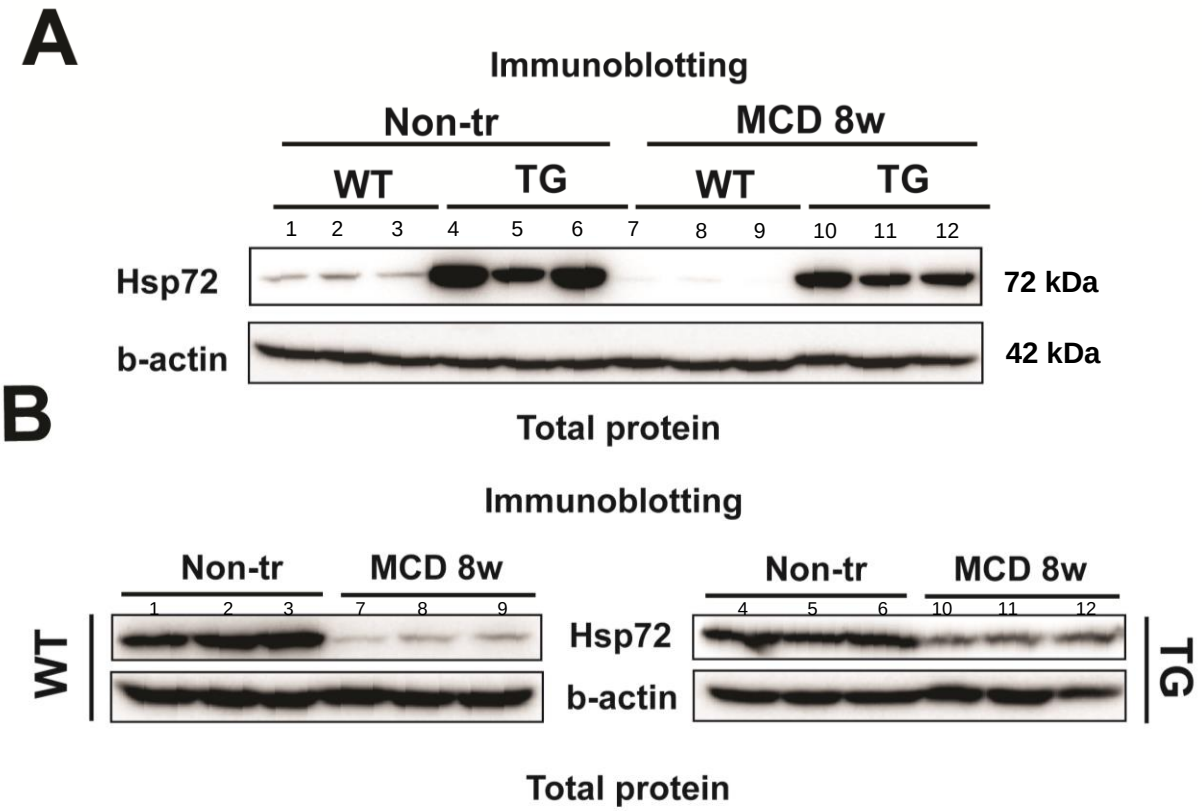

Figure 3.17. Transgenic Hsp72 mice display elevated Hsp72 levels both before and after feeding with MCD. To test whether expression level of Hsp72 changes during the course of MCD diet, Hsp72 protein amount was quantified by immunoblotting (A) of total liver lysates. Note that Hsp72 amount decreased after 8 weeks of feeding with methionine choline-deficient (MCD) diet in both double transgenic (TG) and non-transgenic (WT) animals, compared to non-treated mice (Non-tr). The numbers 1-3, 7-9 – numbers of WT animals; 4–6, 10–12 – numbers of TG mice, prior or after 8 weeks of MCD diet, respectively. b-actin was used as a loading control for immunoblotting (for details of original western blot, see appendix 7.3).

3.4.5. Overexpression of Hsp72 protects from JNK hyperphosphorylation and activation of Rip3 kinase seen after feeding with MCD diet

In order to further evaluate the involvement of Hsp72 overexpression in protection of double transgenic mice from MCD-induced injury, I analyzed expression of major players known to mediate cell death under different stress conditions. Total JNK and phospho-JNK levels were quantified by immunoblotting. The results showed that feeding with MCD-diet decreased JNK2, but not JNK1 levels in both non-transgenic and double transgenic animals. On the other hand, MCD feeding increased both JNK phosphorylation and Rip3 expression in non-transgenic animals and both events were attenuated in double transgenic mice (Figure 3.18).

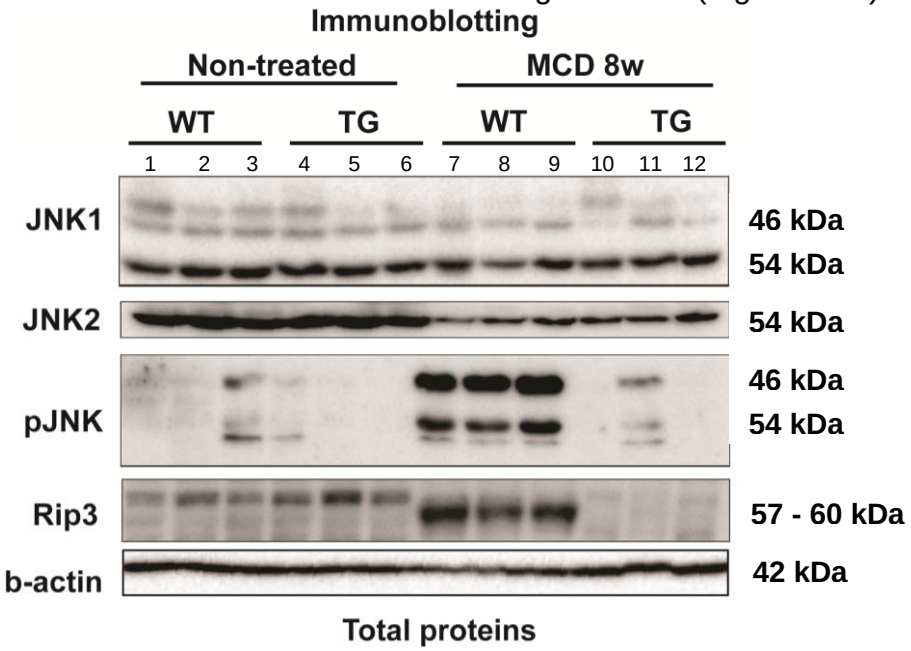

Figure3.18. Overexpression of Hsp72 protected from JNK hyperphosphorylation and activation of Rip3 kinase seen after feeding with MCD diet. To analyze the mechanism of protection of double-transgenic Hsp72-overexpressing mice from MCD-induced liver damage, amount of total C-Jun N-Terminal Kinases (JNK1 and JNK2), their phosphorylated isoforms (p-JNK) and Receptor-Interacting serine/threonine-Protein kinase 3 (Rip3) was examined by immunoblotting prior to (Non-tr) and after 8 weeks of feeding with methionine choline-deficient (MCD) diet. Note that pJNK and Rip3 upregulation was detected in non-transgenic (WT) but not double transgenic mice (TG) exposed to MCD diet. The numbers 1-3, 7-9 – numbers of WT animals; 4-6, 10-12 – numbers of TG mice, prior of after MCD diet, respectively. b-actin was used as a loading control (for details of original western blot, see appendix 7.3).

3.5. Overexpression of Hsp72 protects the hepatocytes from the cell isolation-induced damage

3.5.1. Primary hepatocytes isolated from double transgenic Hsp72 animals are protected from the isolation-induced damage

To better understand the mechanism of Hsp72-mediated cytoprotection, we isolated primary hepatocytes from double transgenic mice as well as non-transgenic animals. Hepatocytes overexpressing Hsp72 showed significantly decreased levels of ALT (Figure 3.19, A) and LDH (Figure 3.19, B) in supernatant under basal condition and after administration of 0,5mM palmitic acid (PA) ($p < 0.05$, $p < 0.01$, $p < 0.005$, respectively).

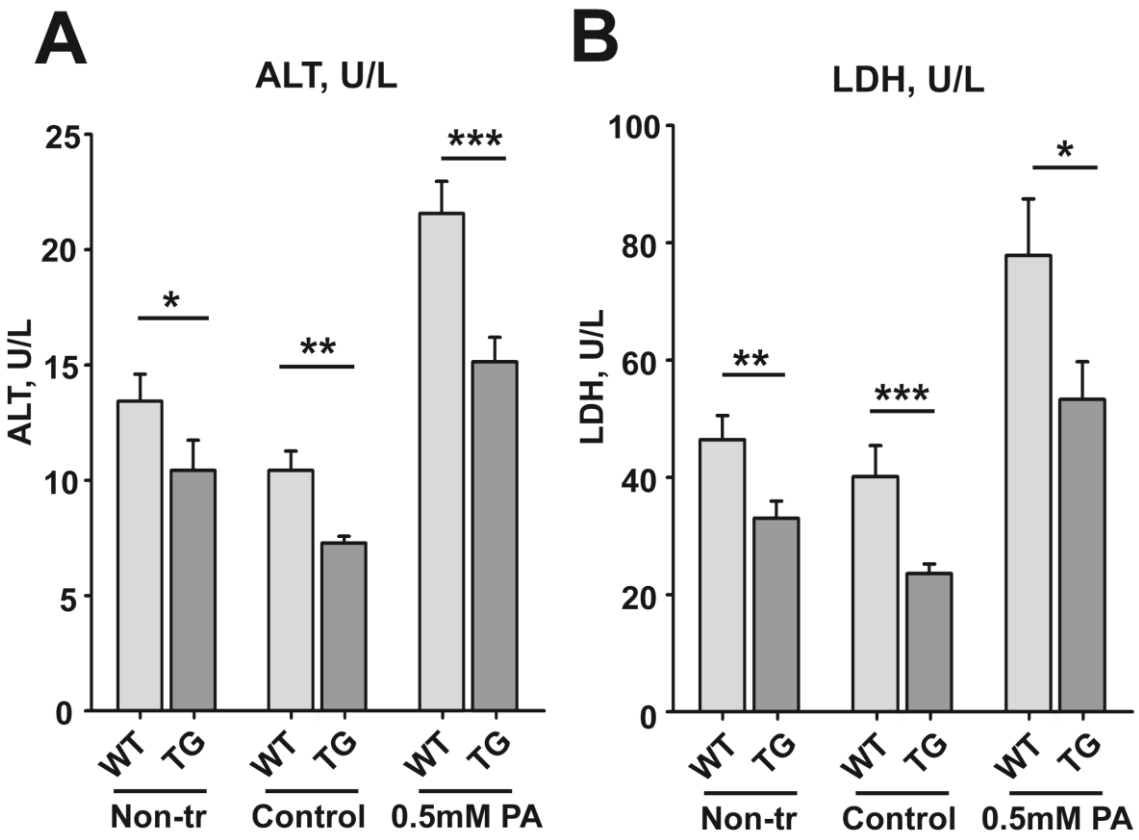

Figure 3.19. Primary hepatocytes isolated from double transgenic Hsp72 animals were protected from the isolation-induced damage. Primary hepatocytes were isolated from non-transgenic (WT) and double transgenic mice (TG) overexpressing Hsp72. Note that transgenic animals showed lower levels of alanine transaminase (ALT) and lactate dehydrogenase (LDH) in the supernatant both under basal condition and after exposure to 0.5 mM palmitic acid (0.5mM PA). Data are expressed as mean ± SEM, at least 5 mice per group were used. Asterisk, double asterisk and triple asterisk highlighted $p < 0.05$, $p < 0.01$, $p < 0.005$, respectively.

3.5.2. Overexpression of Hsp72 does not affect lipid metabolism in primary hepatocytes

To test whether overexpression of Hsp72 affects the amount of triglycerides in primary hepatocytes we stained them with Oil-Red O. Results demonstrated that exposure with palmitic acid increased the amount of lipids similarly in double transgenic and non-transgenic hepatocytes (Figure 3.20). No significant difference was detected between groups. This finding confirmed the results from the *in vitro* experiment and showed that overexpression of Hsp72 does not affect lipid accumulation.

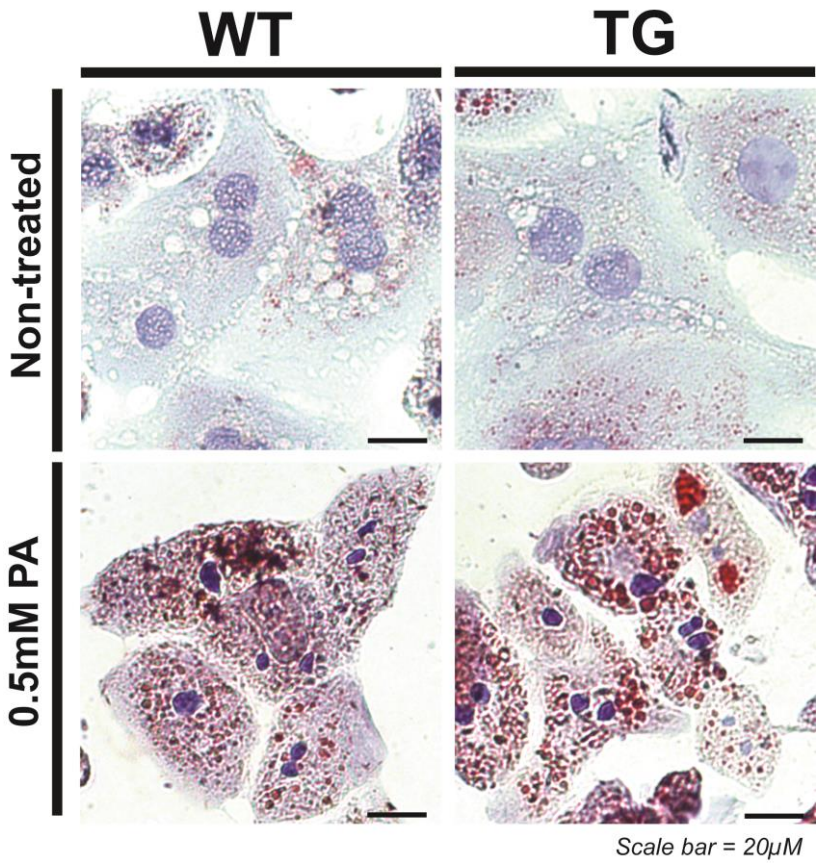

Figure 3.20. Overexpression of Hsp72 does not affect lipid metabolism in primary hepatocytes. Primary hepatocytes that were either untreated or exposed to 0,5 mM palmitic acid (PA) for 24 hours were stained with Oil-Red. Note that administration of palmitic acid increased the amount of lipids similarly in double transgenic (TG) and non-transgenic (WT) hepatocytes. Scale bar=20 μM.

3.5.3. Hsp72 overexpression protects primary hepatocytes from activation of JNK and c-Jun as well as from Rip3 induction

In order to investigate mechanism responsible for protection of primary hepatocytes overexpressing Hsp72 from the isolation-induced damage I quantified total and phosphorylated JNKs, Rip3 and phosphorylated c-JUN by immunoblotting. Hepatocytes overexpressing Hsp72 showed significantly lower amount of phosphorylated c-JUN/JNK as well as Rip3 compared to non-transgenic animals (Figure 3.21).

In summary, the data suggest that overexpression of Hsp72 protects primary hepatocytes from phosphorylation of JNK and c-Jun and from Rip3 activation that is well in lines with previously described results from MCD experiment.

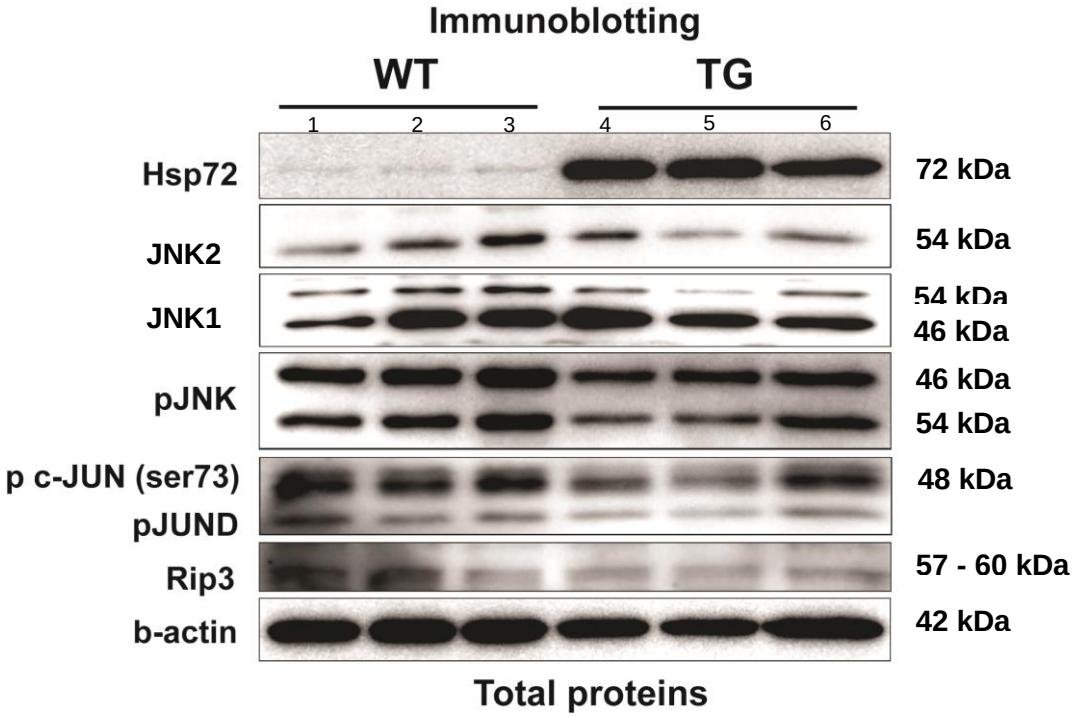

Figure 3.21. Hsp72 overexpression protects primary hepatocytes from activation of JNK and c-Jun as well as from Rip3 induction. The levels of highlighted proteins were quantified by immunoblotting in total protein lysates from isolated primary hepatocytes. Note that hepatocytes overexpressing Hsp72 (TG) display lower levels of Rip3 as well as phosphorylated c-JUN/JNK. The numbers 1-3 – numbers of cell lysates from WT animals, 4-6 – numbers of cell lysates from TG animals. b-actin was used as a loading control (for details of original western blot, see appendix 7.3).

4. Discussion

4.1. Hsp72 overexpressing mice display a robust, liver- specific Hsp72 overexpression and no obvious phenotype under basal condition

To directly address the importance of Hsp72 in the liver, transgenic mice carrying a doxycycline-repressible Hsp72 overexpression construct under control tet-off system have been generated.

The double transgenic Hsp72-Lap animals showed a specific abundant Hsp72 overexpression in the liver, that was not detectable in other tissues that have been analyzed. This is not surprising since previous studies have demonstrated the liver specific expression of other genes under the control of Lap-promoter, i.e. the promoter we employed in our animals [129, 141]. In contrast to our findings, Gallagher with coworkers [142] detected a weak expression of their target protein in the kidney. Further studies are needed to elucidate this discrepancy.

In the generated animals, Hsp72 overexpression did not affect in a major way the expression of other Hsp family members. Nevertheless, a somewhat increased Hsp90 protein levels were seen. This is not surprising since Hsp70 and Hsp90 cooperate as cochaperone complex and this cooperation is facilitated by the chaperone cofactors Hip and Hop [143, 144]. Moreover, the transgenic Hsp72 was detected mainly in cytoplasmic fraction, while nuclear fraction contained substantially lower, but still significant amounts. This is in line with the expected localization of HSPA1A/HSP70 [145] and further demonstrates that the transgenic protein behaves in a similar way as endogenous Hsp72.

Double transgenic Hsp72 mice display no obvious liver phenotype. This meshes well with previous reports showing that animals with constitutive Hsp72 oerexpression tolerated the increased production and demonstrated no obvious phenotype in the liver, heart and pancreas [146-148]. On the other hand, Adachi with coworkers showed that HSP70 overexpression has nondeleterious effects on the neuronal cell morphology and population and on the muscular structure [149].

4.2. Hsp72 overexpression associate with development of chronic hepatitis C and non-alcoholic steatosis

To investigate the potential relevance of our transgenic animal model to human liver disease patients, I have analyzed Hsp72 levels in different human liver diseases. Patients with NASH and chronic hepatitis C infection (HCV) displayed evelated Hsp72 mRNA levels and Hsp72 expression increased with disease activity. This findings match well with the previously published results showing that non-diabetic patients with NAFLD and obesity demonstrate increase expression of Hsp72 in the liver and adipose tissue [128]. On the other hand, Di Naso at al. claimed that obese patients display decreased levels of Hsp72 in the liver and serum, and the reduced levels correlated with insulin resistance and with NAFLD progression [76]. Additionally, it was reported that in the serum of HCV-infected patients the elevated level of Hsp72 was detected [150], but hepatic expression was not analyzed. Thus, further studies are needed to determine the factors regulating Hsp72 production in context of human disease.

4.3. Hsp72 overexpression protects from APAP-induced liver injury and inflammation

While no obvious phenotype was detected under basal condition, double transgenic mice were protected from APAP-induced hepatotoxicity. This is well in line with several previous studies that induced Hsp72 expression by different chemical agents as geranylgeranylacetone (GGA) [103], Schisandrin B [151] or bicyclol [152] and demonstrated that this Hsp72 induction ameliorates the development of APAP-induced injury [103, 151, 152]. However, in contrast to these studies, our paper induced a selective Hsp72 increase and therefore allows a more specific appreciation of Hsp72 function. As another line of evidence, it was reported that liver-specific Hsp72-knockout animals were more susceptible to APAP-hepatotoxicity and cell-death [105].

Although Hsp72 constitutes an established damage-associated molecular pattern (DAMP) known to stimulate inflammation during different type of stresses [153, 154], I did not detect any significant difference in serum TNF-α or IL-6 levels 18 hours after APAP administration. On the other hand, animals overexpressing Hsp72

demonstrated significantly lower IL6 mRNA level in the liver 4h after APAP administration. This is somewhat compatible with previous study that observed decreased levels of proinflammatory cytokines (IL-6, TNFα) in mice that were preconditioned by heat stress, a well-known Hsp72 inducer [155]. On the other hand, knockout of IL6 made the mice more susceptible to APAP-induced hepatotoxicity and decreased expression of Hsp72 [99]. While these data are intriguing, further studies are needed to unequivocally dissect the impact of Hsp72 overexpression on inflammatory pathways.

4.4. Hsp72 overexpression affects the key parameters of APAP metabolism

To better understand the interaction between Hsp72 and APAP, I analyzed the key parameters of APAP metabolism. APAP elimination seems to be more efficient in Hsp72 overexpressing animals that display significantly lower APAP serum levels and likely because of that also lower levels of APAP-protein-adducts. Surprisingly, Hsp72 overexpression did not affect the expression of key genes of APAP metabolism and no significant difference was seen in the APAP-induced glutathione depletion. These results match well with previous studies that did not see obvious differences in APAP metabolism in animals with induced Hsp72 expression [103] nor in Hsp70i KOs [105]. Because of these findings, further studies will be needed to determine how exactly Hsp72 overexpression leads to accelerated Hsp72 clearance from the serum. So far, our data suggest that it stimulates the non-toxic APAP elimination and thereby diminishes the product formation in the toxic pathway. In agreement with that, I demonstrated that Hsp72 animals displayed lower amounts of APAP-protein adducts.

4.5. Hsp72 overexpression protects from MCD-induced liver injury, but does not change the major parameters of lipid metabolism (in vitro and in vivo)

In a second model, I studied the role of Hsp72 in lipotoxic injury using feeding with MCD diet. Hsp72-overexpressing animals showed significantly lower serum levels of hepatic enzymes and less pronounced inflammation. This finding is in the line with previous studies that showed protective effect of Hsp70 from inflammation in several stress-models [51, 52]. In particular, Hsp72 overexpression in the microglial cells decreased TNFα-induced inflammation via attenuation of NF-κB activation [51].

In macrophages, alcohol-induced Hsp72 overexpression resulted in attenuated response to LPS and this effect was abolished by Hsp72 silencing [52].

Although Hsp72 overexpressing animals were protected from hepatic lipotoxicity, I did not see any obviously changes in the major parameters of lipid metabolism *in vitro* or *in vivo* models. These results match well with previous studies that did not see obvious differences in accumulation of triglycerides or ceramides in animals overexpressing Hsp72 in cardiac muscles after HFD diet compared with their non-transgenic littermates [156]. On the other hand, while Hsp72 did not alter the accumulation of fat in the cardiac muscle [156], transgenic Hsp72 overexpression in skeletal muscle prevented an increase in body weight, improved insulin sensitivity and glucose tolerance in mice that were placed on HFD diet [55]. In conclusion, the effect of Hsp72 on fat metabolism seems to differ between tissues and experimental systems.

4.6. Hsp72 overexpression protects from cell death via attenuation of JNK signaling

As the key mechanism likely responsible for the observed cytoprotective effects of Hsp72 overexpression in all employed hepatic stress models, I detected an attenuated JNK signalling. The connection between Hsp72 and JNK activation has also been reported in other experimental models. For example, absence of Hsp70 in cardiomyocytes made them susceptible to both functional and cellular damage by ischemia/reperfusion and resulted in increased levels of JNK phosphorylation [157]. Of note, JNK activation is a halmark of APAP-induced liver injury and it was shown that, absence of JNK in hepatocytes protected mice from APAP-induced liver injury [158]. Similarly, MCD diet was shown to induce JNK activation and this signaling pathway was demonstrated to promote the development of experimental steatohepatitis [159]. In that respect, Jnk1-deficient mice subjected to MCD diet exhibited reduced hepatic triglyceride levels, less pronounced lipid peroxidation, inflammation, liver injury, and apoptosis compared to wild-type [119]. As another line of evidence, Aghazadeh with coworkers showed that inhibition of JNK phosphorylation by teucrium polium ethyl acetate (EtoAc) extract improved MCD-induced steatohepatitis in rats [160]. Furthermore, transgenic animals overexpressing Hsp72 protected from JNK phosphorylation and have decreasing inflammation in skeletal muscles during MCD diet [55].

On a mechanistic level, the link between Hsp72 overexpression and attenuated JNK signalling, that was observed in my thesis, was suggested by several previous studies. In particular, Hsp72 has been shown to prevent activation of JNK [146] via a direct interaction with the peptide-binding domain of JNK [38]. Moreover, using a fibroblast cell line, Park with coworkers demonstrated a direct interaction of Hsp72 with Ask-1, an upstream JNK-activator, as a reason for diminished phosphorylation and activation of JNK [48]. In addition to that, it was found that Hsp72 may indirectly decrease Ask-1 levels via its proteasomal degradation that was mediated by the Hsp72 co-chaperone CHIP [57]. Compatibly with these mechanistic studies, deletion of Hsp72 in mouse embryonic fibroblasts leads to hyperphosphorylation of JNK and activation of caspase-3 during hyperosmolarity-induced apoptosis [161]. Moreover, Bienemann with coworkers reported that virally mediated expression of Hsp72 in the primary sympathetic neuronal culture suppressed the phosphorylation of c-Jun, thereby reducing cytochrome c release and preventing caspase-activated apoptosis [162]. Finally, other study demonstrated that chemically induced Hsp72 expression in striatal cells protects from ROS-induced cell-death via decreasing of JNK/cJun hyperphosphorylation [163].

Given that all stress models displayed attenuated transaminase levels in Hsp72 overexpressing mice, I analyzed the potential modes of hepatocyte cell death but did not find any obvious changes in apoptosis. This is in contrast to several previous studies that described Hsp72 as an anti-apoptotic protein [164]. For example, overexpression of Hsp72 protected from apoptosis induced by metabolic inhibitors via stabilization of the mitochondrial membrane and decreased the activation of caspase 3 [165]. Collectively, these data suggest that the impact of Hsp72 on apoptosis might be cell-type and context-specific.

On the other hand, I observed decreased Rip3 kinase levels in Hsp72 overexpressing MCD-fed mice as a potential hint for attenuated necroptosis signalling. In this respect, previously studies showed that a deletion/knockdown of CHIP, a co-chaperone of Hsp72, leads to hyperactivation of RIPK3 and increased sensitivity to TNF-induced necroptosis [166]. Of note, necroptosis seems to be involved in lipotoxic liver injury since activation of Rip3 was observed in the livers of NASH patients [126, 127]. In line with that, RIP3-deficient mice displayed reduced MCD-induced liver injury [127]. As a potential link to the other described results of my thesis, Gautheron with coworkers recently demonstrated that Rip3-dependent liver

injury in the MCD fed animals is mediated by phosphorylation of JNK [126]. The complex impact of Hsp72 on the JNK and RIP3 signalling pathways suggested in previous studies is highlighted in Figure 4.1.

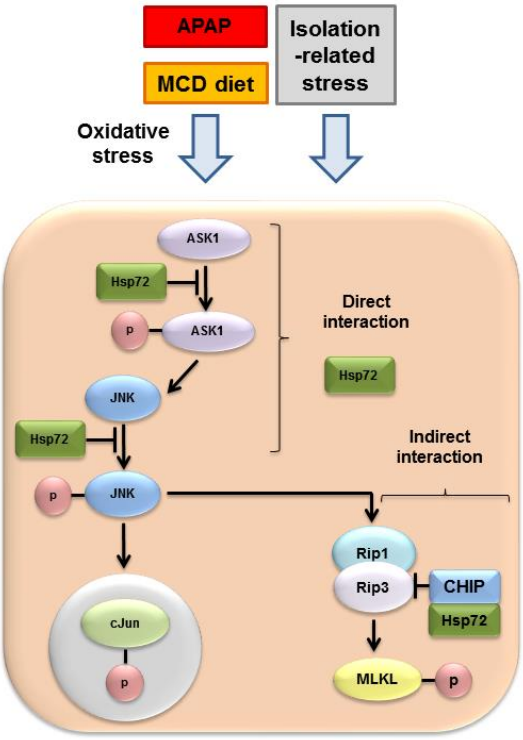

Figure 4.1. Overview of the role of Hsp72 in regulation of JNK/RIP3 signalling.

The surprising finding in my study was the fact that Hsp72 overexpression resulted in only a mild protection effect from the tested stresses. As a potential explanation, modulation of individual Hsps may not be sufficient to improve the function of the entire chaperone machinery [167]. In this respect, a modulation of the master regulations of heat shock response, such as HSF1, is probably more powerful. For example, it was reported that HFS1 knockout animals demonstrated a spontaneous neurodegenerative phenotype [168] and increased prenatal lethality [169], that were not seen in Hsp72-knockout mice [156]. Similarly, Fujimoto and coworkers showed that overexpression of HSF1 constituted a more effective approach to treat proteotoxic insults in mice than overexpression of a single Hsp [170].

In summary, data of my thesis suggested that Hsp72 play a cytoprotective role in different human liver stress situations via attenuation of JNK-signaling pathway. Further analyses are necessary to determine the exact impact of hepatic Hsp72 on this pathway.

5. Summary

Hsp72 is a classic, stress-inducible heat shock protein. It protects the organism from variety of diseases and stress situations. Because of its established cytoprotective function and stress-inducible expression Hsp72 plays an important role in different human disorders. However, its hepatic function remains largely unknown due to a lack of a suitable transgenic model.

To study the hepatic function of Hsp72, I analyzed its expression in patients with liver disease and in newly generated transgenic animals overexpressing Hsp72 under the control of a tissue-specific tetracycline-inducible system. Hsp72 mice were crossbred with animals carrying the tetracycline-responsive transactivator under the control of the liver activator protein promoter (Hsp72-LAP mice). The hepatic phenotype was studied under basal conditions as well as after a single intraperitoneal injection of acetaminophen (APAP, 800mg/kg) or feeding with methionine choline deficient diet (MCD) for 8 weeks. To this end, livers were subjected to histological/immunological staining, real time RT-PCR and immunoblotting.

Patients with non-alcoholic steatohepatitis and chronic hepatitis C infection (HCV) displayed elevated Hsp72 levels and Hsp72 expression increased with disease activity. Hsp72-LAP mice displayed a robust Hsp72 overexpression in hepatocytes, but not in the other tissues or cell types. Under basal conditions, Hsp72-LAP mice did neither show obvious liver phenotype nor altered liver enzymes levels. Primary hepatocytes isolated from Hsp72-overexpressing animals were more resistant towards the isolation-induced stress as determined through lower ALT and LDH levels in the supernatant. 18h after APAP injection, Hsp72-LAP mice demonstrated a significantly lower liver injury, less pronounced histological changes and lower amounts of APAP-protein-adducts. 8 weeks after MCD-diet Hsp72-LAP mice displayed decreased levels of liver enzymes and lower RIP-3 activation. Overexpression of Hsp72 did not affect the extent of steatosis after MCD treatment of mice and palmitic acid treatment-induced injury of primary hepatocytes.

In all three models, the Hsp72-LAP animals/hepatocytes exhibited attenuated JNK signaling as well as lower phosphorylation of c-JUN, a substrate of JNK. In addition, Hsp72-LAP hepatocytes had lower levels of the cell-death kinase RIP3.

In conclusion, the newly generated Hsp72-LAP mice demonstrate a broad, but rather modest cytoprotective function of Hsp72 in the liver that is mediated via attenuation of JNK signaling.

6. References

1. Hartl, F.U., A. Bracher, and M. Hayer-Hartl, *Molecular chaperones in protein folding and proteostasis.* Nature, 2011. **475**(7356): p. 324-332.
2. Ellis, R.J., *Molecular chaperones: assisting assembly in addition to folding.* Trends in biochemical sciences, 2006. **31**(7): p. 395-401.
3. Hartl, F.U., *Molecular chaperones in cellular protein folding.* 1996.
4. Mayer, M. and B. Bukau, *Hsp70 chaperones: cellular functions and molecular mechanism.* Cellular and molecular life sciences, 2005. **62**(6): p. 670-684.
5. Verghese, J., et al., *Biology of the heat shock response and protein chaperones: budding yeast (Saccharomyces cerevisiae) as a model system.* Microbiology and Molecular Biology Reviews, 2012. **76**(2): p. 115-158.
6. Richter, K., M. Haslbeck, and J. Buchner, *The heat shock response: life on the verge of death.* Molecular cell, 2010. **40**(2): p. 253-266.
7. Westerheide, S.D. and R.I. Morimoto, *Heat shock response modulators as therapeutic tools for diseases of protein conformation.* Journal of Biological Chemistry, 2005. **280**(39): p. 33097-33100.
8. Lindquist, S. and E. Craig, *The heat-shock proteins.* Annual review of genetics, 1988. **22**(1): p. 631-677.
9. Kampinga, H.H., et al., *Guidelines for the nomenclature of the human heat shock proteins.* Cell Stress and Chaperones, 2009. **14**(1): p. 105-111.
10. Yu, A., et al., *Roles of Hsp70s in Stress Responses of Microorganisms, Plants, and Animals.* BioMed research international, 2015. **2015**.
11. Morimoto, R.I. and M.G. Santoro, *Stress-inducible responses and heat shock proteins: new pharmacologic targets for cytoprotection.* Nature biotechnology, 1998. **16**(9): p. 833-838.
12. Morimoto, R.I., *Proteotoxic stress and inducible chaperone networks in neurodegenerative disease and aging.* Genes & development, 2008. **22**(11): p. 1427-1438.
13. Szalay, M.S., et al., *Stress-induced rearrangements of cellular networks: consequences for protection and drug design.* FEBS letters, 2007. **581**(19): p. 3675-3680.
14. Toivola, D., et al., *Intermediate filaments take the heat as stress proteins.* Trends in cell biology, 2010. **20**(2): p. 79-91.

15. Gidalevitz, T., V. Prahlad, and R.I. Morimoto, *The stress of protein misfolding: from single cells to multicellular organisms.* Cold Spring Harbor perspectives in biology, 2011. **3**(6): p. a009704.
16. Dai, C. and S.B. Sampson, *HSF1: Guardian of Proteostasis in Cancer.* Trends in cell biology, 2016. **26**(1): p. 17-28.
17. Zügel, U. and S.H. Kaufmann, *Role of heat shock proteins in protection from and pathogenesis of infectious diseases.* Clinical Microbiology Reviews, 1999. **12**(1): p. 19-39.
18. Li, S., et al., *Heat shock protein 72 enhances autophagy as a protective mechanism in lipopolysaccharide-induced peritonitis in rats.* The American journal of pathology, 2011. **179**(6): p. 2822-2834.
19. Qian, J., et al., *Small heat shock protein 20 interacts with protein phosphatase-1 and enhances sarcoplasmic reticulum calcium cycling.* Circulation research, 2011. **108**(12): p. 1429-1438.
20. Pockley, A.G., *Heat shock proteins, inflammation, and cardiovascular disease.* Circulation, 2002. **105**(8): p. 1012-1017.
21. Atalay, M., et al., *Heat shock proteins in diabetes and wound healing.* Current protein & peptide science, 2009. **10**(1): p. 85.
22. Hooper, P.L., *Diabetes, nitric oxide, and heat shock proteins.* Diabetes care, 2003. **26**(3): p. 951-952.
23. Van Molle, W., et al., *HSP70 protects against TNF-induced lethal inflammatory shock.* Immunity, 2002. **16**(5): p. 685-695.
24. Jacquier-Sarlin, M., et al., *Protective effects of hsp70 in inflammation.* Experientia, 1994. **50**(11-12): p. 1031-1038.
25. Wu, B., C. Hunt, and R. Morimoto, *Structure and expression of the human gene encoding major heat shock protein HSP70.* Molecular and Cellular Biology, 1985. **5**(2): p. 330-341.
26. Goate, A.M., et al., *Localization of a human heat-shock HSP 70 gene sequence to chromosome 6 and detection of two other loci by somatic-cell hybrid and restriction fragment length polymorphism analysis.* Human genetics, 1987. **75**(2): p. 123-128.
27. Bonnycastle, L.L., et al., *Cloning, sequencing, and mapping of the human chromosome 14 heat shock protein gene (HSPA2).* Genomics, 1994. **23**(1): p. 85-93.

28. Munro, S. and H.R. Pelham, *An Hsp70-like protein in the ER: identity with the 78 kd glucose-regulated protein and immunoglobulin heavy chain binding protein.* Cell, 1986. **46**(2): p. 291-300.
29. Leung, T., et al., *The human heat-shock protein family. Expression of a novel heat-inducible HSP70 (HSP70B') and isolation of its cDNA and genomic DNA.* Biochemical Journal, 1990. **267**(1): p. 125-132.
30. Parsian, A.J., et al., *The human Hsp70B gene at the HSPA7 locus of chromosome 1 is transcribed but non-functional.* Biochimica et Biophysica Acta (BBA)-Gene Structure and Expression, 2000. **1494**(1): p. 201-205.
31. Dwornczak, B. and M.-E. Mirault, *Structure and expression of a human gene coding for a 71 kd heat shock 'cognate'protein.* Nucleic acids research, 1987. **15**(13): p. 5181-5197.
32. Domanico, S.Z., et al., *Cloning of the gene encoding peptide-binding protein 74 shows that it is a new member of the heat shock protein 70 family.* Molecular and cellular biology, 1993. **13**(6): p. 3598-3610.
33. Bhattacharyya, T., et al., *Cloning and subcellular localization of human mitochondrial hsp70.* Journal of Biological Chemistry, 1995. **270**(4): p. 1705-1710.
34. Han, Z., et al., *Two Hsp70 family members expressed in atherosclerotic lesions.* Proceedings of the National Academy of Sciences, 2003. **100**(3): p. 1256-1261.
35. Daugaard, M., M. Rohde, and M. Jäättelä, *The heat shock protein 70 family: Highly homologous proteins with overlapping and distinct functions.* FEBS letters, 2007. **581**(19): p. 3702-3710.
36. Milarski, K.L. and R.I. Morimoto, *Expression of human HSP70 during the synthetic phase of the cell cycle.* Proceedings of the National Academy of Sciences, 1986. **83**(24): p. 9517-9521.
37. Freeman, B., et al., *Identification of a regulatory motif in Hsp70 that affects ATPase activity, substrate binding and interaction with HDJ-1.* The EMBO journal, 1995. **14**(10): p. 2281.
38. Park, H.S., et al., *Hsp72 functions as a natural inhibitory protein of c-Jun N-terminal kinase.* The EMBO journal, 2001. **20**(3): p. 446-456.
39. Murphy, M.E., *The HSP70 family and cancer.* Carcinogenesis, 2013. **34**(6): p. 1181-1188.

40. Wall, D., M. Zylicz, and C. Georgopoulos, *The NH2-terminal 108 amino acids of the Escherichia coli DnaJ protein stimulate the ATPase activity of DnaK and are sufficient for lambda replication.* Journal of Biological Chemistry, 1994. **269**(7): p. 5446-5451.
41. King, F.W., et al., *Co-chaperones Bag-1, Hop and Hsp40 regulate Hsc70 and Hsp90 interactions with wild-type or mutant p53.* The EMBO Journal, 2001. **20**(22): p. 6297-6305.
42. Allan, R.K. and T. Ratajczak, *Versatile TPR domains accommodate different modes of target protein recognition and function.* Cell stress and chaperones, 2011. **16**(4): p. 353-367.
43. Nollen, E.A. and R.I. Morimoto, *Chaperoning signaling pathways: molecular chaperones as stress-sensingheat shock'proteins.* Journal of cell science, 2002. **115**(14): p. 2809-2816.
44. Kampinga, H.H. and E.A. Craig, *The HSP70 chaperone machinery: J proteins as drivers of functional specificity.* Nature reviews Molecular cell biology, 2010. **11**(8): p. 579-592.
45. Beere, H.M., et al., *Heat-shock protein 70 inhibits apoptosis by preventing recruitment of procaspase-9 to the Apaf-1 apoptosome.* Nature cell biology, 2000. **2**(8): p. 469-475.
46. Saleh, A., et al., *Negative regulation of the Apaf-1 apoptosome by Hsp70.* Nature cell biology, 2000. **2**(8): p. 476-483.
47. Li, C.-Y., et al., *Heat shock protein 70 inhibits apoptosis downstream of cytochrome c release and upstream of caspase-3 activation.* Journal of Biological Chemistry, 2000. **275**(33): p. 25665-25671.
48. Park, H.-S., et al., *Heat shock protein hsp72 is a negative regulator of apoptosis signal-regulating kinase 1.* Molecular and Cellular Biology, 2002. **22**(22): p. 7721-7730.
49. Steel, R., et al., *Hsp72 inhibits apoptosis upstream of the mitochondria and not through interactions with Apaf-1.* Journal of Biological Chemistry, 2004. **279**(49): p. 51490-51499.
50. Ravagnan, L., et al., *Heat-shock protein 70 antagonizes apoptosis-inducing factor.* Nat Cell Biol, 2001. **3**(9): p. 839-43.

51. Sheppard, P.W., et al., *Overexpression of heat shock protein 72 attenuates NF-κB activation using a combination of regulatory mechanisms in microglia.* PLoS Comput Biol, 2014. **10**(2): p. e1003471.
52. Muralidharan, S., et al., *Moderate alcohol induces stress proteins HSF1 and hsp70 and inhibits proinflammatory cytokines resulting in endotoxin tolerance.* The Journal of Immunology, 2014. **193**(4): p. 1975-1987.
53. Adler, V., et al., *UV irradiation and heat shock mediate JNK activation via alternate pathways.* J Biol Chem, 1995. **270**(44): p. 26071-7.
54. Dubois, M.F. and O. Bensaude, *MAP kinase activation during heat shock in quiescent and exponentially growing mammalian cells.* FEBS Lett, 1993. **324**(2): p. 191-5.
55. Chung, J., et al., *HSP72 protects against obesity-induced insulin resistance.* Proceedings of the National Academy of Sciences, 2008. **105**(5): p. 1739-1744.
56. Gabai, V.L., et al., *Hsp70 prevents activation of stress kinases. A novel pathway of cellular thermotolerance.* J Biol Chem, 1997. **272**(29): p. 18033-7.
57. Gao, Y., et al., *Heat shock protein 70 together with its co-chaperone CHIP inhibits TNF-alpha induced apoptosis by promoting proteasomal degradation of apoptosis signal-regulating kinase1.* Apoptosis, 2010. **15**(7): p. 822-33.
58. Klucken, J., et al., *Hsp70 reduces α-synuclein aggregation and toxicity.* Journal of Biological Chemistry, 2004. **279**(24): p. 25497-25502.
59. Petrucelli, L., et al., *CHIP and Hsp70 regulate tau ubiquitination, degradation and aggregation.* Human molecular genetics, 2004. **13**(7): p. 703-714.
60. Henstridge, D.C., et al., *Activating HSP72 in rodent skeletal muscle increases mitochondrial number and oxidative capacity and decreases insulin resistance.* Diabetes, 2014. **63**(6): p. 1881-1894.
61. Drew, B.G., et al., *HSP72 is a mitochondrial stress sensor critical for Parkin action, oxidative metabolism, and insulin sensitivity in skeletal muscle.* Diabetes, 2014. **63**(5): p. 1488-1505.
62. Naka, K., et al., *Hsp70 regulates the doxorubicin-mediated heart failure in Hsp70-transgenic mice.* Cell Stress and Chaperones, 2014. **19**(6): p. 853-864.
63. Henstridge, D.C., M. Whitham, and M.A. Febbraio, *Chaperoning to the metabolic party: the emerging therapeutic role of heat-shock proteins in obesity and type 2 diabetes.* Molecular metabolism, 2014. **3**(8): p. 781-793.

64. Hishiya, A. and S. Takayama, *Molecular chaperones as regulators of cell death.* Oncogene, 2008. **27**(50): p. 6489-6506.
65. Bova, M.P., et al., *Mutation R120G in αB-crystallin, which is linked to a desmin-related myopathy, results in an irregular structure and defective chaperone-like function.* Proceedings of the National Academy of Sciences, 1999. **96**(11): p. 6137-6142.
66. Rohn, T.T., et al., *Caspase-9 activation and caspase cleavage of tau in the Alzheimer's disease brain.* Neurobiology of disease, 2002. **11**(2): p. 341-354.
67. Zhao, M., et al., *The induction of the TNFα death domain signaling pathway in Alzheimer's disease brain.* Neurochemical research, 2003. **28**(2): p. 307-318.
68. Ekegren, T., et al., *Upregulation of Bax protein and increased DNA degradation in ALS spinal cord motor neurons.* Acta neurologica scandinavica, 1999. **100**(5): p. 317-321.
69. Tatton, N.A., *Increased caspase 3 and Bax immunoreactivity accompany nuclear GAPDH translocation and neuronal apoptosis in Parkinson's disease.* Experimental neurology, 2000. **166**(1): p. 29-43.
70. Hartmann, A., et al., *Caspase-8 is an effector in apoptotic death of dopaminergic neurons in Parkinson's disease, but pathway inhibition results in neuronal necrosis.* The Journal of Neuroscience, 2001. **21**(7): p. 2247-2255.
71. Zhou, H., S.-H. Li, and X.-J. Li, *Chaperone suppression of cellular toxicity of huntingtin is independent of polyglutamine aggregation.* Journal of Biological Chemistry, 2001. **276**(51): p. 48417-48424.
72. Magrané, J., et al., *Heat shock protein 70 participates in the neuroprotective response to intracellularly expressed β-amyloid in neurons.* The Journal of neuroscience, 2004. **24**(7): p. 1700-1706.
73. Belter, J.G., H.V. Carey, and T. Garland, *Effects of voluntary exercise and genetic selection for high activity levels on HSP72 expression in house mice.* Journal of Applied Physiology, 2004. **96**(4): p. 1270-1276.
74. Miyabara, E.H., et al., *Overexpression of inducible 70-kDa heat shock protein in mouse attenuates skeletal muscle damage induced by cryolesioning.* American Journal of Physiology-Cell Physiology, 2006. **290**(4): p. C1128-C1138.
75. Miyabara, E.H., et al., *Overexpression of inducible 70-kDa heat shock protein in mouse improves structural and functional recovery of skeletal muscles from*

atrophy. Pflügers Archiv-European Journal of Physiology, 2012. **463**(5): p. 733-741.

76. Cangeri Di Naso, F., et al., *Obesity depresses the anti-inflammatory HSP70 pathway, contributing to NAFLD progression.* Obesity, 2015. **23**(1): p. 120-129.
77. Tsuchiya, D., et al., *Overexpression of rat heat shock protein 70 reduces neuronal injury after transient focal ischemia, transient global ischemia, or kainic acid-induced seizures.* Neurosurgery, 2003. **53**(5): p. 1179-1188.
78. Matsumori, Y., et al., *Hsp70 overexpression sequesters AIF and reduces neonatal hypoxic/ischemic brain injury.* Journal of Cerebral Blood Flow & Metabolism, 2005. **25**(7): p. 899-910.
79. Trost, S.U., et al., *Protection against myocardial dysfunction after a brief ischemic period in transgenic mice expressing inducible heat shock protein 70.* Journal of Clinical Investigation, 1998. **101**(4): p. 855.
80. Suzuki, K., et al., *Heat shock protein 72 enhances manganese superoxide dismutase activity during myocardial ischemia-reperfusion injury, associated with mitochondrial protection and apoptosis reduction.* Circulation, 2002. **106**(12 suppl 1): p. I-270-I-276.
81. Kuboki, S., et al., *Role of heat shock protein 70 in hepatic ischemia-reperfusion injury in mice.* American Journal of Physiology-Gastrointestinal and Liver Physiology, 2007. **292**(4): p. G1141-G1149.
82. Tang, D., et al., *The anti-inflammatory effects of heat shock protein 72 involve inhibition of high-mobility-group box 1 release and proinflammatory function in macrophages.* The Journal of Immunology, 2007. **179**(2): p. 1236-1244.
83. Samborski, P. and M. Grzymisławski, *The Role of HSP70 Heat Shock Proteins in the Pathogenesis and Treatment of Inflammatory Bowel Diseases.* Advances in clinical and experimental medicine: official organ Wroclaw Medical University, 2014. **24**(3): p. 525-530.
84. Kim, J., M. Yenari, and J. Lee, *Regulation of inflammatory transcription factors by heat shock protein 70 in primary cultured astrocytes exposed to oxygen–glucose deprivation.* Neuroscience, 2015. **286**: p. 272-280.
85. Tanaka, T., et al., *HSP70 mediates degradation of the p65 subunit of nuclear factor κB to inhibit inflammatory signaling.* Science signaling, 2014. **7**(356): p. ra119-ra119.

86. Dabeva, M.D. and D.A. Shafritz, *Activation, proliferation, and differentiation of progenitor cells into hepatocytes in the D-galactosamine model of liver regeneration.* The American journal of pathology, 1993. **143**(6): p. 1606.
87. Kmiec, Z., *Cooperation of liver cells in health and disease.* Adv Anat Embryol Cell Biol, 2001. **161**: p. Iii-xiii, 1-151.
88. Takemoto, K., et al., *Necrostatin-1 protects against reactive oxygen species (ROS)-induced hepatotoxicity in acetaminophen-induced acute liver failure.* FEBS Open Bio, 2014. **4**: p. 777-87.
89. Hodgman, M.J. and A.R. Garrard, *A review of acetaminophen poisoning.* Crit Care Clin, 2012. **28**(4): p. 499-516.
90. McGill, M.R. and H. Jaeschke, *Metabolism and disposition of acetaminophen: recent advances in relation to hepatotoxicity and diagnosis.* Pharm Res, 2013. **30**(9): p. 2174-87.
91. Yamamoto, A., et al., *Sulphation of acetaminophen by the human cytosolic sulfotransferases: a systematic analysis.* J Biochem, 2015. **158**(6): p. 497-504.
92. Dahlin, D.C., et al., *N-acetyl-p-benzoquinone imine: a cytochrome P-450-mediated oxidation product of acetaminophen.* Proc Natl Acad Sci U S A, 1984. **81**(5): p. 1327-31.
93. James, L.P., et al., *Detection of acetaminophen protein adducts in children with acute liver failure of indeterminate cause.* Pediatrics, 2006. **118**(3): p. e676-81.
94. Jaeschke, H., C.D. Williams, and A. Farhood, *No evidence for caspase-dependent apoptosis in acetaminophen hepatotoxicity.* Hepatology, 2011. **53**(2): p. 718-9.
95. McGill, M.R., et al., *The mechanism underlying acetaminophen-induced hepatotoxicity in humans and mice involves mitochondrial damage and nuclear DNA fragmentation.* J Clin Invest, 2012. **122**(4): p. 1574-83.
96. Dara, L., et al., *Receptor interacting protein kinase 1 mediates murine acetaminophen toxicity independent of the necrosome and not through necroptosis.* Hepatology, 2015. **62**(6): p. 1847-57.
97. Bajt, M.L., et al., *Nuclear translocation of endonuclease G and apoptosis-inducing factor during acetaminophen-induced liver cell injury.* Toxicol Sci, 2006. **94**(1): p. 217-25.

98. Hinson, J.A., D.W. Roberts, and L.P. James, *Mechanisms of acetaminophen-induced liver necrosis.* Handb Exp Pharmacol, 2010(196): p. 369-405.
99. Masubuchi, Y., et al., *Role of interleukin-6 in hepatic heat shock protein expression and protection against acetaminophen-induced liver disease.* Biochem Biophys Res Commun, 2003. **304**(1): p. 207-12.
100. Salminen, W.F., Jr., R. Voellmy, and S.M. Roberts, *Induction of hsp 70 in HepG2 cells in response to hepatotoxicants.* Toxicol Appl Pharmacol, 1996. **141**(1): p. 117-23.
101. Hosoi, N., et al., *Overexpression of the heat shock protein 70 confers protection against oxidative injury in HEPG2 cells.* Transplant Proc, 2002. **34**(7): p. 2647-9.
102. Salminen, W.F., Jr., R. Voellmy, and S.M. Roberts, *Differential heat shock protein induction by acetaminophen and a nonhepatotoxic regioisomer, 3'-hydroxyacetanilide, in mouse liver.* J Pharmacol Exp Ther, 1997. **282**(3): p. 1533-40.
103. Nishida, T., et al., *Geranylgeranylacetone protects against acetaminophen-induced hepatotoxicity by inducing heat shock protein 70.* Toxicology, 2006. **219**(1-3): p. 187-96.
104. Salminen, W.F., Jr., R. Voellmy, and S.M. Roberts, *Protection against hepatotoxicity by a single dose of amphetamine: the potential role of heat shock protein induction.* Toxicol Appl Pharmacol, 1997. **147**(2): p. 247-58.
105. Tolson, J.K., et al., *Increased hepatotoxicity of acetaminophen in Hsp70i knockout mice.* Toxicol Appl Pharmacol, 2006. **210**(1-2): p. 157-62.
106. Hatting, M., et al., *Hepatocyte caspase-8 is an essential modulator of steatohepatitis in rodents.* Hepatology, 2013. **57**(6): p. 2189-2201.
107. Ramadori, P., et al., *Mouse models of metabolic liver injury.* Lab Anim, 2015. **49**(1 Suppl): p. 47-58.
108. Joshi-Barve, S., et al., *Palmitic acid induces production of proinflammatory cytokine interleukin-8 from hepatocytes.* Hepatology, 2007. **46**(3): p. 823-30.
109. Farrell, G.C., et al., *NASH is an Inflammatory Disorder: Pathogenic, Prognostic and Therapeutic Implications.* Gut Liver, 2012. **6**(2): p. 149-71.
110. Locatelli, I., et al., *Endogenous annexin A1 is a novel protective determinant in nonalcoholic steatohepatitis in mice.* Hepatology, 2014. **60**(2): p. 531-544.

111. Kawai, D., et al., *Hydrogen-rich water prevents progression of nonalcoholic steatohepatitis and accompanying hepatocarcinogenesis in mice.* Hepatology, 2012. **56**(3): p. 912-921.
112. Marra, F., et al., *Molecular basis and mechanisms of progression of non-alcoholic steatohepatitis.* Trends Mol Med, 2008. **14**(2): p. 72-81.
113. Tilg, H. and A.R. Moschen, *Evolution of inflammation in nonalcoholic fatty liver disease: the multiple parallel hits hypothesis.* Hepatology, 2010. **52**(5): p. 1836-46.
114. Takahashi, Y., Y. Soejima, and T. Fukusato, *Animal models of nonalcoholic fatty liver disease/nonalcoholic steatohepatitis.* World J Gastroenterol, 2012. **18**(19): p. 2300-2308.
115. dela Peña, A., et al., *NF-κB activation, rather than TNF, mediates hepatic inflammation in a murine dietary model of steatohepatitis.* Gastroenterology, 2005. **129**(5): p. 1663-1674.
116. Larter, C.Z. and M.M. Yeh, *Animal models of NASH: getting both pathology and metabolic context right.* Journal of gastroenterology and hepatology, 2008. **23**(11): p. 1635-1648.
117. Puri, P., et al., *Activation and dysregulation of the unfolded protein response in nonalcoholic fatty liver disease.* Gastroenterology, 2008. **134**(2): p. 568-576.
118. Malhi, H., et al., *Free fatty acids induce JNK-dependent hepatocyte lipoapoptosis.* Journal of Biological Chemistry, 2006. **281**(17): p. 12093-12101.
119. Schattenberg, J.M. and D. Schuppan, *Nonalcoholic steatohepatitis: the therapeutic challenge of a global epidemic.* Curr Opin Lipidol, 2011. **22**(6): p. 479-88.
120. Tuncman, G., et al., *Functional in vivo interactions between JNK1 and JNK2 isoforms in obesity and insulin resistance.* Proc Natl Acad Sci U S A, 2006. **103**(28): p. 10741-6.
121. Luedde, T., N. Kaplowitz, and R.F. Schwabe, *Cell death and cell death responses in liver disease: mechanisms and clinical relevance.* Gastroenterology, 2014. **147**(4): p. 765-783.e4.
122. Malhi, H. and G.J. Gores, *Molecular mechanisms of lipotoxicity in nonalcoholic fatty liver disease.* Semin Liver Dis, 2008. **28**(4): p. 360-9.

123. Cho, Y.S., et al., *Phosphorylation-driven assembly of the RIP1-RIP3 complex regulates programmed necrosis and virus-induced inflammation.* Cell, 2009. **137**(6): p. 1112-23.
124. Zhang, D.W., et al., *RIP3, an energy metabolism regulator that switches TNF-induced cell death from apoptosis to necrosis.* Science, 2009. **325**(5938): p. 332-6.
125. Sun, L., et al., *Mixed lineage kinase domain-like protein mediates necrosis signaling downstream of RIP3 kinase.* Cell, 2012. **148**(1-2): p. 213-27.
126. Gautheron, J., et al., *A positive feedback loop between RIP3 and JNK controls non-alcoholic steatohepatitis.* EMBO Mol Med, 2014. **6**(8): p. 1062-74.
127. Afonso, M.B., et al., *Necroptosis is a key pathogenic event in human and experimental murine models of non-alcoholic steatohepatitis.* Clin Sci (Lond), 2015. **129**(8): p. 721-39.
128. Tiss, A., et al., *Immunohistochemical profiling of the heat shock response in obese non-diabetic subjects revealed impaired expression of heat shock proteins in the adipose tissue.* Lipids Health Dis, 2014. **13**: p. 106.
129. Sunami, Y., et al., *Hepatic activation of IKK/NFκB signaling induces liver fibrosis via macrophage-mediated chronic inflammation.* Hepatology, 2012. **56**(3): p. 1117-1128.
130. Guldiken, N., et al., *Keratins 8 and 18 are type II acute-phase responsive genes overexpressed in human liver disease.* Liver Int, 2015. **35**(4): p. 1203-12.
131. Lavon, I., et al., *High susceptibility to bacterial infection, but no liver dysfunction, in mice compromised for hepatocyte NF-κB activation.* Nature medicine, 2000. **6**(5): p. 573-577.
132. Bartneck, M., et al., *Liposomal encapsulation of dexamethasone modulates cytotoxicity, inflammatory cytokine response, and migratory properties of primary human macrophages.* Nanomedicine: nanotechnology, biology and medicine, 2014. **10**(6): p. 1209-1220.
133. Fuchs, C.D., et al., *Absence of adipose triglyceride lipase protects from hepatic endoplasmic reticulum stress in mice.* Hepatology, 2012. **56**(1): p. 270-280.
134. Bartneck, M., et al., *Isolation and Time Lapse Microscopy of Highly Pure Hepatic Stellate Cells.* Analytical Cellular Pathology, 2015. **2015**.

135. Bartneck, M., et al., *Molecular response of liver sinusoidal endothelial cells on hydrogels.* Materials Science and Engineering: C, 2015. **51**: p. 64-72.
136. Schefe, J.H., et al., *Quantitative real-time RT-PCR data analysis: current concepts and the novel "gene expression's C T difference" formula.* Journal of molecular medicine, 2006. **84**(11): p. 901-910.
137. Wattiaux, R., et al., *Isolation of rat liver lysosomes by isopycnic centrifugation in a metrizamide gradient.* The Journal of Cell Biology, 1978. **78**(2): p. 349-368.
138. Muldrew, K.L., et al., *Determination of acetaminophen-protein adducts in mouse liver and serum and human serum after hepatotoxic doses of acetaminophen using high-performance liquid chromatography with electrochemical detection.* Drug Metabolism and Disposition, 2002. **30**(4): p. 446-451.
139. Simon, Y., et al., *Elevated free cholesterol in a p62 overexpression model of non-alcoholic steatohepatitis.* World J Gastroenterol, 2014. **20**(47): p. 17839-17850.
140. Kessler, S.M., et al., *Fatty acid elongation in non-alcoholic steatohepatitis and hepatocellular carcinoma.* International journal of molecular sciences, 2014. **15**(4): p. 5762-5773.
141. Du, H., et al., *Hepatocyte-Specific Expression of Human Lysosome Acid Lipase Corrects Liver Inflammation and Tumor Metastasis in lal(-/-) Mice.* Am J Pathol, 2015. **185**(9): p. 2379-89.
142. Gallagher, A.R., et al., *Use of the tetracycline system for inducible protein synthesis in the kidney.* J Am Soc Nephrol, 2003. **14**(8): p. 2042-51.
143. Wegele, H., L. Muller, and J. Buchner, *Hsp70 and Hsp90--a relay team for protein folding.* Rev Physiol Biochem Pharmacol, 2004. **151**: p. 1-44.
144. Genest, O., et al., *Hsp70 and Hsp90 of E. coli Directly Interact for Collaboration in Protein Remodeling.* J Mol Biol, 2015. **427**(24): p. 3877-89.
145. Hageman, J. and H.H. Kampinga, *Computational analysis of the human HSPH/HSPA/DNAJ family and cloning of a human HSPH/HSPA/DNAJ expression library.* Cell Stress Chaperones, 2009. **14**(1): p. 1-21.
146. Gabai, V.L., et al., *Hsp72-mediated suppression of c-Jun N-terminal kinase is implicated in development of tolerance to caspase-independent cell death.* Mol Cell Biol, 2000. **20**(18): p. 6826-36.

147. Lunova, M., et al., *Hsp72 overexpression accelerates the recovery from caerulein-induced pancreatitis.* PLoS One, 2012. **7**(7): p. e39972.
148. Marber, M.S., et al., *Overexpression of the rat inducible 70-kD heat stress protein in a transgenic mouse increases the resistance of the heart to ischemic injury.* J Clin Invest, 1995. **95**(4): p. 1446-56.
149. Adachi, H., et al., *Heat shock protein 70 chaperone overexpression ameliorates phenotypes of the spinal and bulbar muscular atrophy transgenic mouse model by reducing nuclear-localized mutant androgen receptor protein.* J Neurosci, 2003. **23**(6): p. 2203-11.
150. Chumpitazi, B.F., et al., *Biological autoimmunity screening in hepatitis C patients by anti-HepG2 lysate and anti-heat shock protein 70.1 autoantibodies.* Eur J Clin Microbiol Infect Dis, 2009. **28**(2): p. 137-46.
151. Li, L., et al., *Schisandrin B attenuates acetaminophen-induced hepatic injury through heat-shock protein 27 and 70 in mice.* J Gastroenterol Hepatol, 2014. **29**(3): p. 640-7.
152. Bao, X.Q. and G.T. Liu, *Bicyclol: a novel antihepatitis drug with hepatic heat shock protein 27/70-inducing activity and cytoprotective effects in mice.* Cell Stress Chaperones, 2008. **13**(3): p. 347-55.
153. Brenner, C., et al., *Decoding cell death signals in liver inflammation.* J Hepatol, 2013. **59**(3): p. 583-94.
154. Mendonca, R., A.A. Silveira, and N. Conran, *Red cell DAMPs and inflammation.* Inflamm Res, 2016.
155. Oka, Y., et al., *Heat-shock pre-treatment reduces liver injury and aids liver recovery after partial hepatectomy in mice.* Anticancer Res, 2013. **33**(7): p. 2887-94.
156. Henstridge, D.C., et al., *Genetic manipulation of cardiac Hsp72 levels does not alter substrate metabolism but reveals insights into high-fat feeding-induced cardiac insulin resistance.* Cell Stress Chaperones, 2015. **20**(3): p. 461-72.
157. Kim, Y.K., et al., *Deletion of the inducible 70-kDa heat shock protein genes in mice impairs cardiac contractile function and calcium handling associated with hypertrophy.* Circulation, 2006. **113**(22): p. 2589-97.
158. Cubero, F.J., et al., *Combined Activities of JNK1 and JNK2 in Hepatocytes Protect Against Toxic Liver Injury.* Gastroenterology, 2016. **150**(4): p. 968-81.

159. Soon, R.K., Jr., et al., *Stress signaling in the methionine-choline-deficient model of murine fatty liver disease.* Gastroenterology, 2010. **139**(5): p. 1730-9, 1739.e1.
160. Aghazadeh, S. and R. Yazdanparast, *Inhibition of JNK along with activation of ERK1/2 MAPK pathways improve steatohepatitis among the rats.* Clin Nutr, 2010. **29**(3): p. 381-5.
161. Lee, J.S., J.J. Lee, and J.S. Seo, *HSP70 deficiency results in activation of c-Jun N-terminal Kinase, extracellular signal-regulated kinase, and caspase-3 in hyperosmolarity-induced apoptosis.* J Biol Chem, 2005. **280**(8): p. 6634-41.
162. Bienemann, A.S., et al., *Hsp70 suppresses apoptosis in sympathetic neurones by preventing the activation of c-Jun.* J Neurochem, 2008. **104**(1): p. 271-8.
163. Choi, Y.J., et al., *Geldanamycin attenuates 3nitropropionic acidinduced apoptosis and JNK activation through the expression of HSP 70 in striatal cells.* Int J Mol Med, 2014. **34**(1): p. 24-34.
164. Takayama, S., J.C. Reed, and S. Homma, *Heat-shock proteins as regulators of apoptosis.* Oncogene, 2003. **22**(56): p. 9041-7.
165. Mao, H., et al., *hsp72 inhibits focal adhesion kinase degradation in ATP-depleted renal epithelial cells.* J Biol Chem, 2003. **278**(20): p. 18214-20.
166. Seo, J., E.W. Lee, and H. Sung, *CHIP controls necroptosis through ubiquitylation- and lysosome-dependent degradation of RIPK3.* 2016. **18**(3): p. 291-302.
167. Pierce, A., et al., *A Novel mouse model of enhanced proteostasis: Full-length human heat shock factor 1 transgenic mice.* Biochem Biophys Res Commun, 2010. **402**(1): p. 59-65.
168. Homma, S., et al., *Demyelination, astrogliosis, and accumulation of ubiquitinated proteins, hallmarks of CNS disease in hsf1-deficient mice.* J Neurosci, 2007. **27**(30): p. 7974-86.
169. Xiao, X., et al., *HSF1 is required for extra-embryonic development, postnatal growth and protection during inflammatory responses in mice.* The EMBO journal, 1999. **18**(21): p. 5943-5952.
170. Fujimoto, M., et al., *Active HSF1 significantly suppresses polyglutamine aggregate formation in cellular and mouse models.* Journal of Biological Chemistry, 2005. **280**(41): p. 34908-34916.

7. APPENDIX

7.1. List of tables

7.2. List of figures

7.3. Original western blots

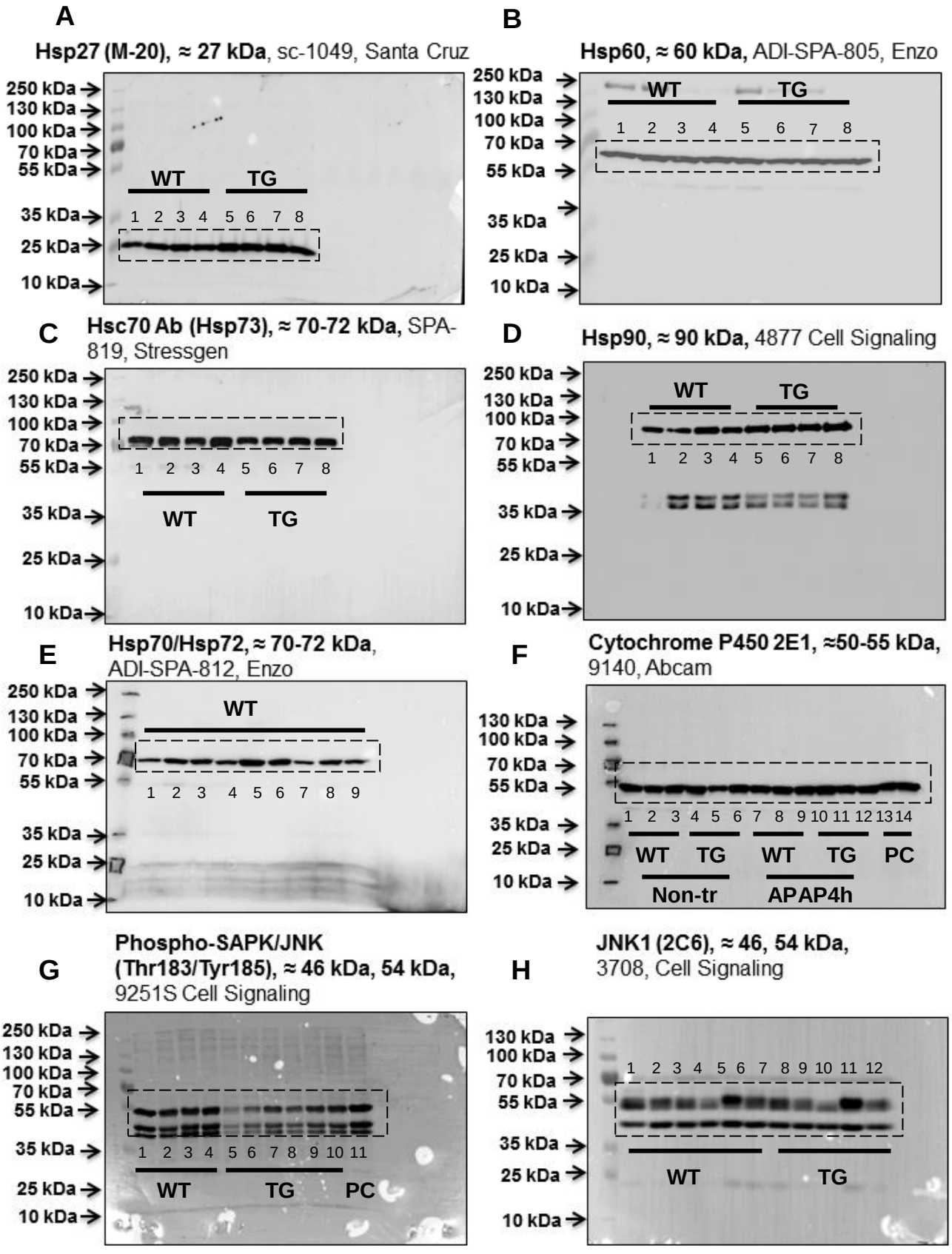

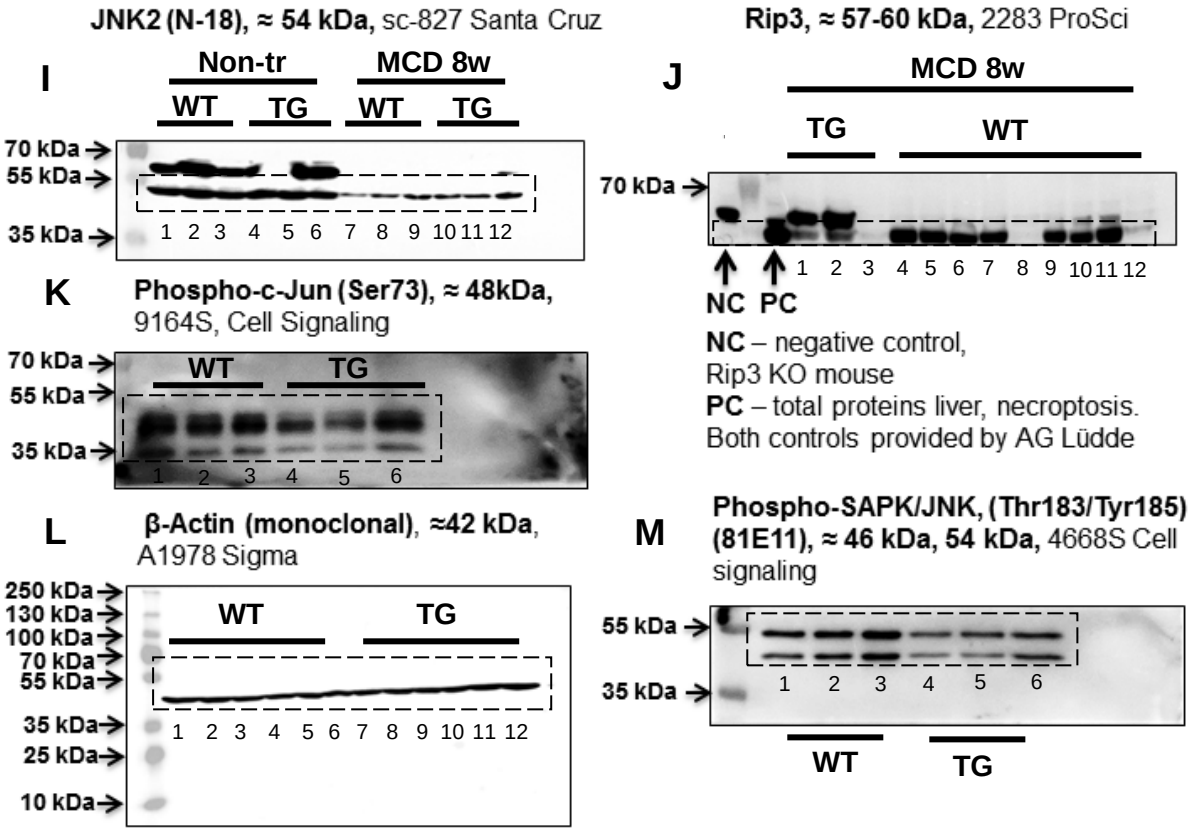

A-D: the numbers 1-4 – numbers of non-transgenic (WT) animals, 5-8 – numbers of double transgenic (TG) mice, under basal condition for both groups; **E:** the numbers 1-9 – numbers of WT mice under basal condition; **F:** the numbers 1-3, 7-9 – numbers of WT mice, 4-6, 10-12 – numbers of TG animals, non-treated or 4h after APAP treatment, respectively; 13-14 – positive control provided by AG Trautwein; **G:** the numbers 1-4 – numbers of WT animals, 5-10 – numbers of TG mice, PC provided by AG Trautwein; **H:** the numbers 1-6 – numbers of WT animals, 7-12 – numbers of transgenic animals, under basal condition for both groups; **I:** the numbers 1-3, 7-9 – numbers of WT mice, 4-6, 10-12 – numbers of TG animals, non-treated or 4h after APAP treatment, respectively; **J:** the numbers 1-3 – numbers of TG animals, 4-12 – number of WT mice; **K:** the numbers 1-3 – numbers of cell lysates from WT mice, 4-6 – numbers of cell lysates from TG mice; **L:** the numbers 1-6 – numbers of WT animals, 7-12 – numbers of TG mice, under basal condition for both groups; **M:** the numbers 1-3 – numbers of cell lysates from WT mice, 4-6 – numbers of cell lysates from TG mice.

7.4. Original western blots of sub-compartmental marker proteins

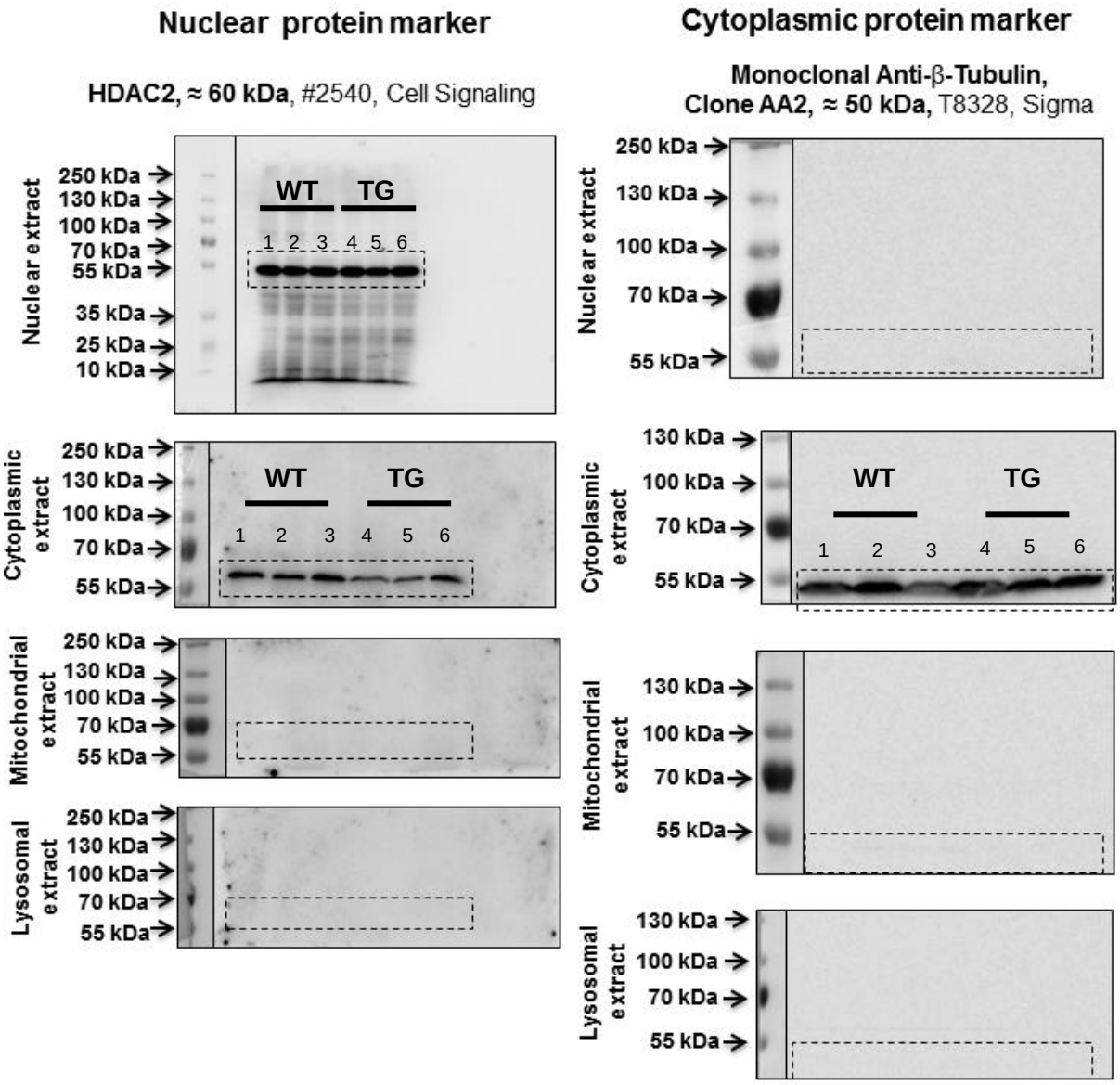

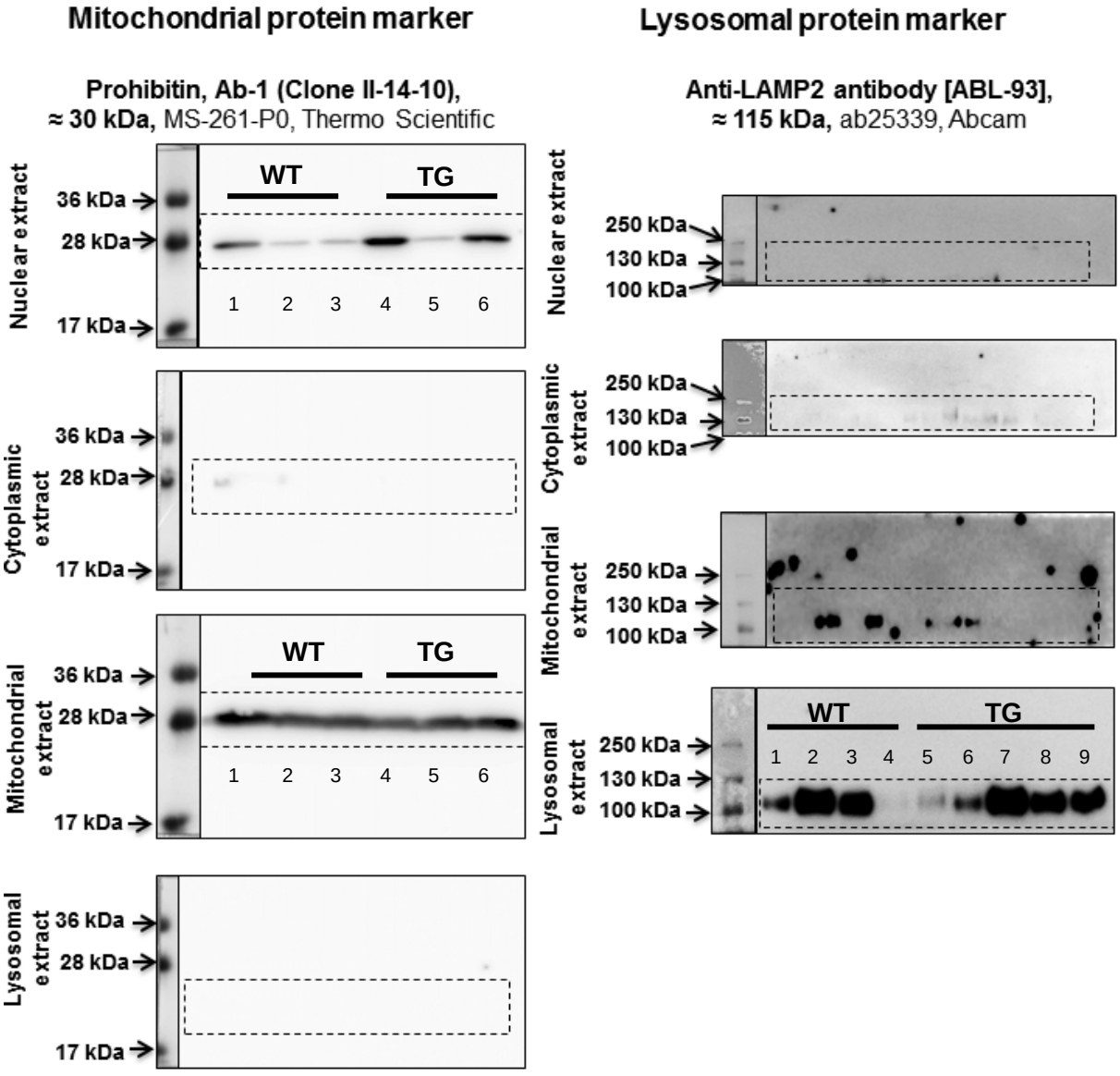

Nuclear protein marker: the numbers 1-3 – numbers of samples of nuclear fractions from non-transgenic animals (WT), 4-6 – numbers of samples of nuclear fractions from double transgenic animals (TG); **Cytoplasmic protein marker**: the numbers 1-3 – numbers of samples of nuclear fractions from WT, 4-6 – numbers of samples of nuclear fractions from TG animals; **Mitochondrial protein marker:** the numbers 1-3 – numbers of samples of nuclear fractions from WT, 4-6 – numbers of samples of nuclear fractions from TG animals; **Lysosomal protein marker:** the numbers 1-4 – numbers of samples of nuclear fractions from WT, 5-9 – numbers of samples of nuclear fractions from TG animals;

7.5. Publications:

Part of this work has been published in advance as scientific abstracts, posters and oral presentations as indicated below:

ORAL PRESENTATIONS:

DGVS 2016 **K. Levada,** N. Guldiken, G. Vella, L. P. James, J. Haybaeck, A. K. Kiemer, S. M. Kessler, C. Trautwein, P. Strnad. Hsp72-Überexpression schützt vor Leberschädigung durch Hemmung der JNK-Aktivierung. DGVS, 2016, CCH Hamburg

EASL 2016 **K. Levada,** N. Guldiken, G. Vella, L. P. James, J. Haybaeck, A. K. Kiemer, S. M. Kessler, C. Trautwein, P. Strnad. Hsp72 overexpression protects from liver injury via attenuation of JNK signaling. EASL 2016, Barcelona, Spain.

AASLD 2015 **K. Levada**, N. Guldiken, F.-R. Mo, C. Trautwein, P. Strnad. Hsp72 overexpression protects from drug-induced- and lipotoxic liver injury. DDW 2015 – Digestive Disease Week – Washington, USA

POSTERS:

GASL 2016 **K. Levada**, N. Guldiken, G. Vella, L. P. James, J. Haybaeck, A. K. Kiemer, S. M. Kessler, C. Trautwein, P. Strnad. Hsp72 overexpression protects from drug-induced- and lipotoxic liver injury. GASL 2016, Düsseldorf, Germany

EASL 2015 **K. Levada**, N. Guldiken, F.R. Mo, C. Trautwein, P. Strnad. Hsp72 overexpression protects from acetaminophen and MCD liver injury. EASL 2015, Vienna, Austria, April 22-26, 2015

GASL 2014 **K. Levada**, N. Güldiken, C. M. Pfaff , F.R. Mo, P. Lahiri, C. Trautwein, P. Strnad. Hsp72 overexpression protects from acetaminophen and DDC-associated liver injury but enhances protein aggregation GASL 2014, Tübingen, Germany

CSHL 2014 **K. Levada**, N. Güldiken, C. M. Pfaff , F.R. Mo, P. Lahiri, C. Trautwein, P. Strnad. Hsp72 overexpression protects from acetaminophen and
DDC-associated liver injury but enhances protein aggregation

"Molecular Chaperones and Stress Responses" CSHL 2014, NY, USA, 2014

EASL 2014 **K. Levada**, N. Güldiken, C. M. Pfaff , F.R. Mo, P. Lahiri, C. Trautwein, P. Strnad. Hsp72 overexpression protects from acetaminophen and DDC-associated liver injury but enhances protein aggregation. EASL 2014, London, UK.

EASL 2013 **K. Levada**, N. Güldiken, C. M. Pfaff, C. Trautwein, P. Strnad. Hsp72 overexpression protects from acetaminophen toxicity, but exacerbates Fas-induced liver injury. EASL 2013, Amsterdam, Netherlands

GASL 2013 **K. Levada,** N. Güldiken, C. M. Pfaff, C. Trautwein, P.Strnad. Die Überexpression von Hsp72 schützt vor Acetaminophen-, aber verstärkt Fas-induzierte Leberschädigung. GASL 2013, Hannover, Germany

7.6. Zusammenfassung

Hsp72 ist ein klassisches, stressinduzierbares, Hitzeschockprotein. Es schützt den Organismus vor einer Vielfalt von Krankheiten und Stresssituationen. Aufgrund seiner etablierten zytoprotektiven Funktion und stressinduzierbaren Expression, spielt Hsp72 eine wichtige Rolle in verschiedenen humanen Erkrankungen. Seine Funktion in der Leber ist jedoch mangels geeigneter transgener Tiermodelle bisher weitgehend unbekannt.

Um seine Funktion in der Leber näher zu erforschen, analysierten wir die Hsp72-Expression in den Lebern von Patienten mit verschiedenen Lebererkrankungen und von mir neu generierten transgenen Mäusen, die, unter Kontrolle eines gewebespezifischen Tetracyclin-induzierbaren Systems, Hsp72 überexprimieren. Hsp72-Mäuse wurden mit Mäusen gekreuzt, die einen auf Tetracyclin reagierenden Transaktivator aufweisen, der durch den leberspezifischen „liver activator protein (LAP)“-Promotor kontrolliert wird (Hsp72-LAP Mäuse). Der Phänotyp der Leber wurde sowohl unter Standardbedingungen, als auch nach einer einmaligen intraperitonealen Injektion von Acetominophen (APAP, 800mg/kg) und einer Methionin- und Cholin-freien Diät über acht Wochen untersucht. Zu diesem Zweck wurden histologische und immunhistologische Färbungen, quantitative RT-PCRs und Immunoblots durchgeführt.

Patienten mit nichtalkoholischer Steatohepatitis oder chronischer Hepatitis-C-Virus-Infektion (HCV) zeigten erhöhte Hsp72-Spiegel, die mit der Krankheitsaktivität korrelierten.

Die Hsp72-LAP-Mäuse wiesen eine stabile Hsp72-Überexpression in Hepatozyten auf, nicht jedoch in anderen Geweben oder Leberzelltypen. Unter Standardbedingungen zeigten Hsp72-Lap-Mäuse weder einen auffälligen Leberphänotyp, noch veränderte Leberenzym-Spiegel.

Primäre Hepatozyten, die aus den Hsp-72-überexprimierenden Tieren gewonnen wurden, waren resistenter gegenüber dem Isolations-bedingten Stress, was durch geringere ALT- und LDH-Spiegeln im Überstand deutlich wurde. 18 Stunden nach der APAP-Injektion, konnte bei den Hsp72-LAP-Mäusen eine signifikant reduzierte Leberschädigung beobachtet werden, ersichtlich durch geringer ausgeprägte histologische Veränderungen und geringere Mengen von APAP-Protein-Addukten.

Acht Wochen nach der Methionin- und Cholin-freien Diät wiesen die Hsp72-LAP-Mäuse niedrigere Leberenzym-Spiegel und eine verminderte Aktivierung von RIP-3 auf.

Die Überexpression von Hsp72 in Mäusen beeinflusste nicht das Ausmaß der Steatose nach Methionin- und Cholin-freier Diät oder nach einer Behandlung der Hepatozyten mit Palmitinsäure.

In allen drei Modellen, wiesen die Hsp72-LAP-Mäuse bzw. deren Hepatozyten eine abgeschwächte Aktivierung des JNK Signalwegs auf, die durch eine verminderte Phosphorylierung von c-JUN, einem Substrat von JNK, bestätigt wurde. Des Weiteren konnten bei den Hsp72-LAP-Hepatozyten geringere Spiegel der Kinase RIP-3 festgestellt werden, die mit Zelltod assoziiert wird. Schlussfolgernd kann man anhand der Hsp-72-LAP-Mäuse eine vielfältige, jedoch eher mäßige zytoprotektive Funktion von Hsp72 in der Leber feststellen, die durch abschwächte Aktivierung des JNK-Signalweges vermittelt wird.

7.7. Eidesstattliche Versicherung

Hiermit erkläre ich, Kateryna Levada dass ich die Dissertation mit dem Titel:

„Hsp72 overexpression protects from APAP and MCD induced liver injury via attenuation of JNK signalling“ selbständig verfasst habe.

Bei der Anfertigung wurden folgende Hilfen Dritter in Anspruch genommen:

In der Abteilung für Gastroenterologie, Stoffwechselerkrankungen und internistische Intensivmedizin (Medizinische Klinik III) im Universitätsklinikum Aachen habe ich die Versuche mit den im Kapitel „Material und Methoden“ aufgeführten Hilfen und Hilfsmitteln durchgeführt.

Die Anfertigung erfolgte unter der Leitung von PD Dr. med. Pavel Strnad, Abteilung für Gastroenterologie, Stoffwechselerkrankungen und internistische Intensivmedizin (Medizinische Klinik III) im Universitätsklinikum Aachen. Die fachliche Betreuung wurde von Univ.-Prof., Dr. rer. nat. Andreas Ludwig, Institut für Pharmakologie und Toxikologie und Univ.-Prof., Dr. phil. nat., Gabriele Pradel, Institut für Zelluläre und Angewandte Infektionsbiologie im Universitätsklinikum Aachen, übernommen.

Ich habe keine entgeltliche Hilfe von Vermittlung- bzw. Beratungsdiensten in Anspruch genommen. Niemand hat von mir unmittelbar oder mittelbar entgeltliche Leistungen für Arbeiten erhalten, die in Zusammenhang mit dem Inhalt der vorgelegten Dissertation stehen. Die Synthese der verwendeten Primer und Antikörper wurden von den jeweils erwähnten Firmen durchgeführt.

Die Dissertation wurde bisher nicht für eine Prüfung oder Promotion oder für einen ähnlichen Zweck der Beurteilung eingereicht.

Ich versichere, dass ich die vorstehenden Angaben nach bestem Wissen vollständig und der Wahrheit entsprechend gemacht habe.

Aachen, den 18.10.2016

7.8. Acknowledgements

The time past so fast and now I can really feel that big and important part of my life will be completed. My research will be never possible without people who helped, supported and kept me motivated during this time.

First of all, I would like to acknowledge my gratitude to my adviser PD Dr. Pavel Strnad, for giving me the opportunity to prepare my thesis in his laboratory, for his excellent guidance, scientific and technical advices, great support, motivation and helpful discussions during all my PhD study. I also would like to thanks for giving me many opportunities to present my work at national and international conferences and for the excellent corrections of this thesis.

I would also like to thank Univ.-Prof. Dr. rer. nat. Andreas Ludwig and Univ.-Prof. Dr. phil. nat. Gabriele Pradel for accepting to be in my PhD defense committee. I appreciate their time to read and comment my thesis and allowing me to accomplish my graduation.

Next, I acknowledge to my collaborators: Prof. Laura P. James from USA, Assoz. Prof. Johannes Haybäck from Graz and Prof. Alexandra K. Kiemer and Dr. Sonja M. Keßler from Saarbrücken for their kind help and contribution in this project.

I would like to thank all members of Department of Medicine III for their help, support and friendly atmosphere. Special thanks I would like to express my friends Dr. rer. nat. Francisco Javier Cubero and Dr. nat. med Yulia Nevzorova for their always helpful advises and kind help.

Last, but not least, I would like to thank to my colleagues from University of Ulm and Aachen (Özlem, Peggy, Elke, Yu, Valentyn, Renwar, Claudia, Suzanne, Anke, Deniz, Annika, Linda, Ingrid, Fa-Rong, Gökce, Kathrin, Igor, Hawraman) for their contribution in this project, nice time together and friendly atmosphere in the Lab. Especially, I would like to thank Dr. Nurdan Guldiken who help me to start to work in this project for her supervising, suggestions and friendship. I would like to thank Giovanna Vella for her great help and contribution. And I would like to thank to my friends Dr. Oleg Lunov and Dr. Mariia Lunova for their support, great advises and nice time together.

Finally, I would like to thank to my family and my friends for love, support and encouragement. My lovely husband, son, parents and sister, this thesis will be never done if all of you did not support and kept me motivated.

CURRICULUM VITAE

PERSONAL PROFILE:

Name: Kateryna Levada

Birth date: 11.06.1981

Citizenship: Ukraine

Home address: 52064 Aachen, Krakaustrasse 11-15

Phone: +4915734740854

E-mail: kateryna.levada@googlemail.com

Family status: married

Child: son, birth date 22.07.2002.

Current position: a PhD student at Department of Internal Medicine III Gastroenterology, Hepatology and Endocrinology University Hospital RWTH Aachen
Pauwelsstr. 30, Aachen, D-52074
(Germany) +49-17680758721

Research Interest: The role of heat shock proteins in the digestive system;
The relationship between human disorders and experimental models of liver diseases;
Lipid metabolism of the liver

EDUCATION:

2011 – 2016: a PhD student at Internal Medicine I / III Department of Universities Clinics Ulm /Aachen at Pavel Strnad research group
Thesis: The role of Hsp72 in the digestive system

2009 – 2011: a volunteer at Human Physiology Department of Donetsk National Medical University at Gaydarova research group.
Theme: Problems of mental activities of foreign students during adaptation for education.

2002 – 2005: Postgraduate student at Department of Psychophysiology at Biological Faculty, Donetsk National University, Ukraine.

2002: Master Degree with in Biology Donetsk National University,

Department of Human and animal Physiology, Donetsk, Ukraine.

1997–2002: a student of Biological faculty of Donetsk National University, Department of Human and Animal Physiology.

1997: graduated Biological Lyceum of Donetsk National University, Donetsk, Ukraine.

EMPLOYMENT:

2013 – 2016: a PhD student at Internal Medicine III Department of Universities Clinic Aachen at Pavel Strnad research group

2011 – 2013: a PhD student at Internal Medicine I Department of Universities Clinic Ulm at Pavel Strnad research group.

2005 – 2011: Teacher of Biology at the International Education Center, Donetsk National Medical University, Ukraine.

GRANTS/AWARDS/HOUNOR:

2016 Young Investigator Bursary (Full Bursary), International Liver Congress 2016 by EASL, Barcelona, Spain, April 13-17, 2016

2015 AASLD Fellow Travel Award, by Washington, DC, May 17-19, 2015

2015 Young Investigator Bursary (Full Bursary), International Liver Congress 2015 by EASL, Vienna, Austria, April 22-26, 2015

2014 Young Investigator Bursary (Full Bursary), International Liver Congress 2014 by EASL, London, UK, April 9-13, 2014

PROFESSIONAL MEMBERSHIPS:

2016 Honored member of EASL society 2016

2015 Honored member of EASL society 2015

2014 Honored member of EASL society 2014

SELECTED PRESENTATIONS:

DGVS 2016 **K. Levada,** N. Guldiken, G. Vella, L. P. James, J. Haybaeck, A. K. Kiemer, S. M. Kessler, C. Trautwein, P. Strnad. Hsp72-Überexpression schützt vor Leberschädigung durch Hemmung der JNK-Aktivierung. DGVS, 2016, CCH Hamburg

EASL 2016 **K. Levada,** N. Guldiken, G. Vella, L. P. James, J. Haybaeck, A. K.

Kiemer, S. M. Kessler, C. Trautwein, P. Strnad. Hsp72 overexpression protects from liver injury via attenuation of JNK signaling. EASL 2016, Barcelona, Spain.

AASLD 2015 **K. Levada**, N. Guldiken, F.-R. Mo, C. Trautwein, P. Strnad. Hsp72 overexpression protects from drug-induced- and lipotoxic liver injury. DDW 2015 – Digestive Disease Week – Washington, USA

SELECTED POSTERS:

GASL 2016 **K. Levada**, N. Guldiken, G. Vella, L. P. James, J. Haybaeck, A. K. Kiemer, S. M. Kessler, C. Trautwein, P. Strnad. Hsp72 overexpression protects from drug-induced- and lipotoxic liver injury. GASL 2016, Düsseldorf, Germany

EASL 2015 **K. Levada**, N. Guldiken, F.R. Mo, C. Trautwein, P. Strnad. Hsp72 overexpression protects from acetaminophen and MCD liver injury. EASL 2015, Vienna, Austria, April 22-26, 2015

GASL 2014 **K. Levada**, N. Güldiken, C. M. Pfaff , F.R. Mo, P. Lahiri, C. Trautwein, P. Strnad. Hsp72 overexpression protects from acetaminophen and DDC-associated liver injury but enhances protein aggregation GASL 2014, Tübingen, Germany

CSHL 2014 **K. Levada**, N. Güldiken, C. M. Pfaff , F.R. Mo, P. Lahiri, C. Trautwein, P. Strnad. Hsp72 overexpression protects from acetaminophen and
DDC-associated liver injury but enhances protein aggregation "Molecular Chaperones and Stress Responses" CSHL 2014, NY, USA, 2014

EASL 2014 **K. Levada**, N. Güldiken, C. M. Pfaff , F.R. Mo, P. Lahiri, C. Trautwein, P. Strnad. Hsp72 overexpression protects from acetaminophen and DDC-associated liver injury but enhances protein aggregation. EASL 2014, London, UK.

EASL 2013 **K. Levada**, N. Güldiken, C. M. Pfaff, C. Trautwein, P. Strnad. Hsp72 overexpression protects from acetaminophen toxicity, but exacerbates Fas-induced liver injury. EASL 2013, Amsterdam, Netherlands

GASL 2013 **K. Levada,** N. Güldiken, C. M. Pfaff, C. Trautwein, P.Strnad. Die

Überexpression von Hsp72 schützt vor Acetaminophen-, aber verstärkt Fas-induzierte Leberschädigung. GASL 2013, Hannover, Germany

PUBLICATIONS:

1. Guldiken N, Zhou Q, Kucukoglu O, Rehm M, **Levada K**, Gross A, Kwan R, James LP, Trautwein C, Omary MB, Strnad P. Human keratin 8 variants promote mouse acetaminophen hepatotoxicity coupled with c-jun amino-terminal kinase activation and protein adduct formation. Hepatology. 2015 Sep; 62(3):876-86.
2. Guldiken N, Usachov V, **Levada K**, Trautwein C, Ziol M, Nahon P, Strnad P. Keratins 8 and 18 are type II acute-phase responsive genes overexpressed in human liver disease. Liver Int. 2015 Apr; 35(4):1203-12.

SKILLS:

1. Extensive expertise in animal models of human gastroenterological diseases (liver, pancreas, colon)
2. Isolation of primary cells, work with cell culture, transfection
3. DNA and RNA based techniques: genotyping PCR and Q-PCR, analyzing of microarray data, primer design
4. Biochemical assays: Western Blot, ELISA, oxidative stress assays, MTT cytotoxicity, in situ hybridization, immunochistochemistry, immunofluorescence, histology staining (H&E, Sirius Red, Prussian Blue, Oil-Red-O), detection of iron, subcellular fractionation, immunoprecipitation, IVIS (in vivo imaging)
5. Computer skills: MathCad, Statistica, Adobe Photoshop, Adobe Illustrator, ImageJ, MS Office (MS-Word, MS- Excel, MS Power- Point etc.). Living Image, Axio Vision, GraphPad Prism, Endnote X7.1, Primer3 Input, The gene bank data.

LANGUAGES:

English (fluently), German (good), Russian (native), Ukrainian (native)